

**INDIRECT PHOTOCHEMICAL FORMATION OF COS AND CS₂ IN
NATURAL WATERS: KINETICS AND REACTION MECHANISMS**

by

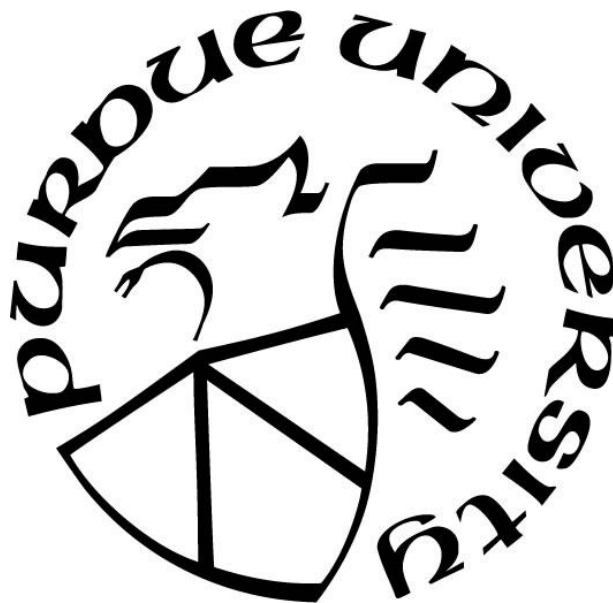
Mahsa Modiri Gharehveran

A Dissertation

Submitted to the Faculty of Purdue University

In Partial Fulfillment of the Requirements for the degree of

Doctor of Philosophy



Lyles School of Civil Engineering

West Lafayette, Indiana

August 2019

**THE PURDUE UNIVERSITY GRADUATE SCHOOL
STATEMENT OF COMMITTEE APPROVAL**

Dr. Amisha Shah, Chair

Lyles School of Civil Engineering

Dr. Chad Jafvert

Lyles School of Civil Engineering

Dr. Ernest Blatchley

Lyles School of Civil Engineering

Dr. Greg Michalski

Department of Earth, Atmospheric, & Planetary Sciences

Approved by:

Dr. Dulcy Abraham

Head of the Graduate Program

*Dedicated to my beloved husband, Ali
my family
for their constant support and unconditional love*

ACKNOWLEDGMENTS

Firstly, I would like to express my sincere gratitude to my advisor Prof. Amisha Shah for the continuous support of my Ph.D study and related research, for his patience, motivation, and immense knowledge. Her guidance helped me in all the time of research, writing papers and specially this dissertation. She was and remains my best role model as a scientist, mentor, and teacher. Besides my advisor, I would like to thank the rest of my Ph.D. committee members: Prof. Chad Javfert, Prof. Ernest Blatchley, and Prof. Greg Michalski for their insightful comments and encouragement during committee meetings and preliminary examination.

I would also like to thank Dr. Nadya Zyaykina for her help and support throughout my Ph.D. study. I thank my fellow lab-mates, Kun Huang and Holly Haflich for the stimulating discussions, for their flexibility in the times we were sharing different instruments in the lab, and for all the fun we have had in the last five years. I would like to acknowledge my best friend, Kun who has always supported me through my academic and personal life. I will never forget all our friendly and inspiring discussions in a small office which we shared for five years. I will always remember her smile, motivation, patience, and knowledge which generously offered to me in this five year. I am also grateful for presence of my dear friend Negar who has been my lovely friend and support for 13 years. From the first day I met her in my first days in college, she has been one of my best friends.

I would like to thank my family: my parents and my brother, Mehrdad, my sister, Parisa and my nephew, Arda. My parents have supported me by their warm words although we were far away and I was not able to see them for 5 years, but I could feel them beside me. My sister and my nephew who supported me every day although through phone calls. I am grateful for my family to support me spiritually throughout writing this dissertation and my life in general.

Last but not the least, for my beloved husband, Ali, which I find it difficult to express my appreciation because it is so boundless. I will not be able to finish this journey without the support of my husband who has lightened my life with his love and wisdom. I am deeply thankful to him for keeping things going and for always showing how proud he is of me. He has showed a continual support of my academic endeavors over the past several years which enabled me to complete this dissertation. He is my most enthusiastic cheerleader; he is my best friend; and he is an amazing husband. I am grateful to him because he has given up so much to make my career a priority in our lives. I feel so lucky since we shared our entire amazing journeys of our Ph.D. periods.

TABLE OF CONTENTS

LIST OF TABLES	9
LIST OF FIGURES	10
ABSTRACT	13
CHAPTER 1. INTRODUCTION	16
1.1 References	20
CHAPTER 2. INDIRECT PHOTOCHEMICAL FORMATION OF COS AND CS ₂ IN NATURAL WATERS	25
2.1 Abstract	25
2.2 Introduction	25
2.3 Material and Methods	26
2.3.1 Description of standards, reagents, and stock preparation	26
2.3.2 Natural water samples	27
2.3.3 Experimental procedure	32
2.3.4 Analytical methods	37
2.3.5 Detailed description of the kintecus modelling data methods	42
2.4 Results and Discussion	44
2.4.1 Effect of sunlight exposure on COS and CS ₂ formation kinetics	44
2.4.2 Effect of temperature	49
2.5 Conclusions	51
2.6 References	52
CHAPTER 3. ROLE OF ORGANIC SULFUR PRECURSORS AND WATER QUALITY CONSTITUENTS ON PHOTOCHEMICAL FORMATION OF COS AND CS ₂	56
3.1 Abstract	56
3.2 Introduction	56
3.3 Material and Methods	57
3.3.1 Description of standards, reagents, and stock preparation	57
3.3.2 Natural water samples	57
3.3.3 Experimental procedure	57
3.3.4 Analytical methods	58

3.4	Results and Discussion	58
3.4.1	Comparison between water types	58
3.4.2	Effect of salinity	63
3.4.3	Role of organic sulfur precursor	64
3.4.4	Role of O ₂	68
3.4.5	Role of CO	69
3.4.6	Proposed mechanisms.....	69
3.5	Conclusions.....	74
3.6	References.....	75
CHAPTER 4. INFLUENCE OF DOM ON COS AND CS ₂ FORMATION FROM CYSTEINE DURING SUNLIGHT PHOTOLYSIS.....		79
4.1	Abstract.....	79
4.2	Introduction.....	80
4.3	Materials and Methods.....	83
4.3.1	Description of standards, reagents, and stock preparation	83
4.3.2	Collection, characterization and modification of different DOM isolates	83
4.3.3	Photochemical reactor setup	86
4.3.4	Experimental procedure.....	86
4.3.5	Analytical methods	87
4.4	Results and Discussion	87
4.4.1	Characterization of DOM	87
4.4.2	COS and CS ₂ formation from different DOM isolates	89
4.4.3	Effect of DOM concentration	93
4.4.4	Effect of cysteine concentration	97
4.4.5	Effect of pH	98
4.4.6	Role of quenching agents.....	99
4.4.7	Role of sodium borohydride treatment	106
4.5	Conclusions.....	108
4.6	References.....	109
CHAPTER 5. INFLUENCE OF DOM ON COS AND CS ₂ FORMATION FROM DIMETHYL SULFIDE (DMS) DURING SUNLIGHT PHOTOLYSIS.....		115

5.1	Abstract.....	115
5.2	Introduction.....	116
5.3	Materials and Methods.....	117
5.3.1	Description of standards, reagents, and stock preparation	117
5.3.2	Collection, characterization and modification of different DOM isolates	118
5.3.3	Photochemical reactor setup	118
5.3.4	Experimental procedure.....	118
5.3.5	Analytical methods	119
5.4	Results and Discussion	119
5.4.1	Characterization of DOM	119
5.4.2	COS and CS ₂ formation from different DOM isolates	119
5.4.3	Effect of DOM concentration	122
5.4.4	Effect of pH	124
5.4.5	Role of quenching agents.....	125
5.4.6	Role of sodium borohydride treatment	132
5.5	Conclusions.....	134
5.6	References.....	135
CHAPTER 6. RESEARCH CONTRIBUTION.....		140
6.1	References.....	141
APPENDIX.....		143

LIST OF TABLES

Table 2-1. Sample location and water quality characteristics of the nine tested natural waters...	31
Table 2-2. A description of the reactions and conditions used to model the kinetics of the COS and CS ₂ hydrolysis at 20°C and pH=8.1. A similar method was used to assess the model kinetics for other temperature and pH values.	43
Table 4-1. The scavenging rates of quenching agents with [•] OH and ³ DOM*	82
Table 4-2. The fluorescence index (FI) and E ₂ /E ₃ values for DOM isolates, calculated based on previously described methods. ^{35,36}	89

LIST OF FIGURES

Figure 2-1. Map locations of the nine natural waters from (a) Florida, (b) Louisiana and (c) Maine.	27
Figure 2-2. The UV-VIS absorbance of the nine natural waters between 200 to 400 nm prior to sunlight exposure.	28
Figure 2-3. Correlation of the waters' UV ₃₆₀ and DOC concentrations with each other.....	29
Figure 2-4. Schematic of the photochemical reactor used in this study. The schematic of the solar simulator was similar to that used by NASA and thus adopted from a picture they provided online ¹⁶	32
Figure 2-5. The photochemical reactor geometry (all dimensions are in cm).	33
Figure 2-6. Relative light spectrum emitted from the OAI TRI-SOL solar simulator which has been compared to the ASTM G173-03 reference spectrum ²⁰ and the sun spectrum captured on August 17, 2015 in West Lafayette, IN, USA (Latitude: 40.430098, Longitude: -86.914392).	34
Figure 2-7. Degradation of 2-NBA following sunlight exposure over time plotted as a zero-order loss ([2-NBA]; y-axis) with time (x-axis)). The three curves reflect values from experiments conducted on different days.	35
Figure 2-8. 2- nitrobenzaldehyde molar absorptivity ($\epsilon \lambda$) values from 300 to 400 nm.	35
Figure 2-9. Experimental data used to measure the reactor pathlength. The data were fitted according to eq. 6.	36
Figure 2-10. The mass balance involved in the sample preparation procedure for GC/MS analysis.	38
Figure 2-11. The effect of a (a) 1:1.5 dilution factor, and a (b) 1:100 dilution factor on the response lost for cysteine caused by the matrix effect in the MA-S, LA-B2, and LA-F waters. DI = deionized water.	40
Figure 2-12. Comparison of COS and CS ₂ hydrolysis rates using the Kintecus modeling software.	43
Figure 2-13. The effect of sunlight exposure on COS and CS ₂ formation for the LA-B1 water when (a,b) spiked or not spiked with cysteine (20±1 °C), (c,d) spiked or not spiked with cysteine or DMS (20±1 °C), and (e,f) varied in temperature (5, 20 and 30 °C) and spiked with cysteine. Cysteine and DMS were measured during diurnal cycling where the DL for cysteine is represented by a horizontal line. Error bars represent the standard error for three replicates. ([cysteine or DMS] ₀ = 14 μM, pH 8.1)	47

- Figure 2-14. The effect of sunlight exposure on COS and CS₂ photoproduction for (a,b) the LA-F and (c,d) the LA-B2 water, spiked or not spiked with cysteine or DMS. Cysteine and DMS were measured during diurnal cycling where the DL for cysteine is represented by a horizontal line. ([cysteine or DMS]₀ = 14 μM, pH: LA-F: 8.0, LA-B2: 8.17). 48
- Figure 2-15. The effect of temperature on COS and CS₂ photoproduction for the LA-B1 water spiked with DMS ([DMS]₀ = 14 μM, pH: LA-B1: 8.1). 49
- Figure 3-1. The effect of different water types on COS and CS₂ photoproduction for (a,c,e,g) based on DOC values and (b,d,f,h) based on [Cl] values when waters spiked or not spiked with cysteine or DMS ([cysteine or DMS]₀ = 14 μM, temperature: 20±1 °C, pH: FL-F: 7.8, FL-B1: 8.0, FL-B2: 8.0, FL-B3: 7.9, FL-S: 8.0, LA-F: 8.0, LA-B1: 8.1, LA-B2: 8.17, MA-S: 7.8). 61
- Figure 3-2. The effect of different water types on COS and CS₂ photoproduction for (a,b) based on carbonate values and (c,d) based on absorbance at 360 nm values when waters spiked or not spiked with cysteine ([cysteine]₀ = 14 μM, temperature: 20±1 °C, pH: FL-F: 7.8, FL-B1: 8.0, FL-B2: 8.0, FL-B3: 7.9, FL-S: 8.0, LA-F: 8.0, LA-B1: 8.1, LA-B2: 8.17, MA-S: 7.8). 62
- Figure 3-3. The effect of different water types on COS and CS₂ photoproduction for (a,b) based on carbonate values and (c,d) based on absorbance at 360 nm values when waters spiked or not spiked with DMS ([DMS]₀ = 14 μM, temperature: 20±1 °C, pH: FL-F: 7.8, FL-B1: 8.0, FL-B2: 8.0, FL-B3: 7.9, FL-S: 8.0, LA-F: 8.0, LA-B1: 8.1, LA-B2: 8.17, MA-S: 7.8). 63
- Figure 3-4. The effect of chloride on COS and CS₂ photoproduction for (a,b) the FL-F water and (c,d) the LA-F water spiked with cysteine ([cysteine]₀ = 14 μM, temperature: 20±1 °C, pH: LA-B1: 8.1, FL-F: 7.8). The error bars represent the standard errors for three replicates. 64
- Figure 3-5. COS and CS₂ formation when exposed to (a,b) different organic sulfur precursors ([cysteine]₀ = [cystine]₀ = [DMS]₀ = [methionine]₀ = 14 μM) with the LA-B1 water, (c,d) when amended with O₂ for the LA-B1 water, and (e,f) when amended with CO for the LA-B1 and synthetic water (temperature: 20±1 °C, pH of LA-B1= 8.1, pH of synthetic water = 8.15), [CO]₀= 6.9 μM, [CO]₀= 11.3 μM, [CO]₀= 20.9 μM. The error bars represent the standard errors for three replicates. 67
- Figure 4-1. The location of sampling sites for: (a) Altamaha and (b) gulf stream isolates (ocean DOM-I and ocean DOM-II)³¹. The right map is similar to the one used by a previous study and thus adopted from a picture provided in it.³¹ 84
- Figure 4-2. Effect of sodium borohydride treatment on DOM absorbance spectra..... 86
- Figure 4-3. Effect of DOM type on COS formation ([CYS]= 14 μM, [DOM]= 5 mg-C/L, pH= 8.3, temperature= 21±1 °C). 90
- Figure 4-4. Effect of DOM concentration on COS formation ([CYS]= 14 μM, pH= 8.3, temperature= 21±1 °C). The grey box shows the general level of dark formation, which was similar for all scenarios. The stock concentration of ocean DOM-I was 12.7 mg-C/L and it was not possible to test 20 mg-C/L. 94
- Figure 4-5. Effect of CYS concentration on COS formation during the sunlight photolysis with ocean DOM-II ([ocean DOM-II]= 5 mg-C/L, pH= 8.3, temperature= 21±1 °C) 98

- Figure 4-6. Effect of pH on COS formation during the sunlight photolysis of cysteine with ocean DOM-II ([ocean DOM-II]= 5 mg-C/L, [CYS]= 14 μ M, temperature= 21 \pm 1 $^{\circ}$ C). 99
- Figure 4-7. Influence of isopropanol on COS formation ([CYS]= 14 μ M, [DOM]= 5 mg-C/L, pH= 8.3, temperature= 21 \pm 1 $^{\circ}$ C). The grey box shows the general level of dark formation, which was similar for all scenarios. 100
- Figure 4-8. Influence of phenol, trimethylphenol (TMP), sorbic acid, and dissolved oxygen on COS formation ([CYS]= 14 μ M, [DOM]= 5 mg-C/L, pH= 8.3, temperature= 21 \pm 1 $^{\circ}$ C). The grey box shows the general level of dark formation, which was similar for both quenched and non-quenched samples. 101
- Figure 4-9. CS₂ formation upon the addition of trimethylphenol (TMP) or sorbic acid to solutions with Altamaha DOM ([CYS]= 14 μ M, [DOM]= 5 mg-C/L, pH= 8.3, temperature= 21 \pm 1 $^{\circ}$ C). The DL for CS₂ is represented by a horizontal line. 105
- Figure 4-10. Role of sodium borohydride treatment on COS formation ([CYS]= 14 μ M, [DOM]= 5 mg-C/L, pH= 8.3, temperature= 21 \pm 1 $^{\circ}$ C). The grey box shows the general level of dark formation, which was similar for all scenarios. 107
- Figure 5-1. Effect of DOM type on COS formation during sunlight photolysis when not spiked or spiked with DMS ([DMS]₀= 14 μ M, [DOM]₀= 5 mg-C/L, pH= 8.3, temperature= 21 \pm 1 $^{\circ}$ C). The grey box shows the dark formation which was similar for all scenarios. 120
- Figure 5-2. Effect of DOM concentration on COS formation ([DMS]= 14 μ M, [DOM]= 5 mg-C/L, pH= 8.3, temperature= 21 \pm 1 $^{\circ}$ C). The grey box shows the general level of dark formation, which was similar for all scenarios. The stock concentration of ocean DOM-I was 12.7 mg-C/L and it was not possible to test 20 mg-C/L. 123
- Figure 5-3. Effect of pH on COS formation ([DOM]= 5 mg-C/L, [DMS]= 14 μ M, temperature= 21 \pm 1 $^{\circ}$ C) 125
- Figure 5-4. Influence of isopropanol on COS formation ([DMS]= 14 μ M, [DOM]= 5 mg-C/L, pH= 8.3, temperature= 21 \pm 1 $^{\circ}$ C). The grey box shows the general level of dark formation, which was similar for all scenarios. 126
- Figure 5-5. Influence of phenol, trimethylphenol (TMP), sorbic acid, and dissolved oxygen (O₂) on COS formation ([DMS]= 14 μ M, [DOM]= 5 mg-C/L, pH= 8.3, temperature= 21 \pm 1 $^{\circ}$ C). The grey box shows the general level of dark formation, which was similar for all scenarios. 129
- Figure 5-6. Comparison of net formation from \bullet OH and ³DOM* to the total formation with humic acid. The loss in COS formation due to the removing of each specific RI was considered as net formation with that specific RI. 132
- Figure 5-7. Effect of sodium borohydride treatment on COS formation ([DMS]= 14 μ M, [DOM]= 5 mg-C/L, pH= 8.3, temperature= 21 \pm 1 $^{\circ}$ C). The grey box shows the general level of dark formation, which was similar for all scenarios. 133

ABSTRACT

Author: Modiri Gharehveran, Mahsa. PhD

Institution: Purdue University

Degree Received: August 2019

Title: Indirect Photochemical Formation of COS and CS₂ in Natural Waters: Kinetics and Reaction Mechanisms

Committee Chair: Amisha Shah

COS and CS₂ are sulfur compounds that are formed in natural waters. These compounds are also volatile, which leads them move into the atmosphere and serve as critical precursors to sulfate aerosols. Sulfate aerosols are known to counteract global warming by reflecting solar radiation. One major source of COS and CS₂ stems from the ocean. While previous studies have linked COS and CS₂ formation in these waters to the indirect photolysis of organic sulfur compounds, much of the chemistry behind how this occurs remains unclear. This study examined this chemistry by evaluating how different organic sulfur precursors, water quality constituents, and temperature affected COS and CS₂ formation in natural waters.

In the first part of this thesis (chapters 2 and 3), nine natural waters ranging in salinity were spiked with various organic sulfur precursors (e.g. cysteine, cystine, dimethylsulfide (DMS) and methionine) exposed to simulated sunlight over varying exposures. Other water quality conditions including the presence of O₂, CO and temperature were also varied. Results indicated that COS and CS₂ formation increased up to 11× and 4×, respectively, after 12 h of sunlight while diurnal cycling exhibited varied effects. COS and CS₂ formation were also strongly affected by the DOC concentration, organic sulfur precursor type, O₂ concentration, and temperature while salinity differences and CO addition did not play a significant role.

To then specifically evaluate the role of DOM in cleaner matrices, COS and CS₂ formation was examined in synthetic waters (see chapters 4 and 5). In this case, synthetic waters were spiked

with different types of DOM isolates ranging from freshwater to ocean water along with either cysteine or DMS and exposed to simulated sunlight for up to 4 h. Surprisingly, CS₂ was not formed under any of the tested conditions, indicating that other water quality constituents, aside from DOM, were responsible for its formation. However, COS formation was observed. Interestingly, COS formation with cysteine was fairly similar for all DOM types, but increasing DOM concentration actually decreased formation. This is likely due to the dual role of DOM on simultaneously forming and quenching the reactive intermediates (RIs). Additional experiments with quenching agents to RIs (e.g. ³DOM* and •OH) further indicated that •OH was not involved in COS formation with cysteine but ³DOM* was involved. This result differed with DMS in that •OH and ³DOM* were both found to be involved. In addition, treating DOM isolates with sodium borohydride (NaBH₄) to reduce ketone/aldehydes to their corresponding alcohols increased COS formation, which implied that the RIs formed by these functional groups in DOM were not involved. The alcohols formed by this process were not likely to act as quenching agents since they have been shown to low in reactivity. Since ketones are known to form high-energy-triplet-states of DOM while quinones are known to form low-energy-triplet-states of DOM, removing ketones from the system further supported the role of low-energy-triplet-states on COS formation. This was initially hypothesized by findings from the testes on DOM types. In the end there are several major research contributions from this thesis. First, cysteine and DMS have different mechanisms for forming COS. Second, adding O₂ decreased COS formation, but it did not stop it completely, which suggests that further research is required to evaluate the role of RI in the presence of O₂. Lastly, considering the low formation yields of COS and CS₂ formation from the organic sulfur precursors tested in this study, it is believed that some other organic sulfur

precursors are missing which are likely to generate these compounds to higher levels and this needs to be investigated in future research.

CHAPTER 1. INTRODUCTION

COS and CS₂ are important atmospheric gases because of their potential to form sulfate aerosols in the stratosphere that are known to counteract global warming¹ and impact ozone chemistry². Sulfate aerosols can affect Earth's radiation balance, directly through scattering radiation or indirectly through participating in cloud condensation nuclei.³ They can also influence nitrogen oxides concentrations which can catalytically destroy ozone.³ COS can reach the stratosphere due to its > 1 year tropospheric lifetime¹, where it is photo-oxidized by ultraviolet light (100-300 nm). Additionally, CS₂ can also form COS in the stratosphere by reacting with hydroxyl radicals.⁴ Previously, it has been shown that COS is the principal source of sulfate aerosols in the stratosphere.⁵ The ocean is one major source of COS and CS₂, but previous models have varied in accurately predicting their flux from the ocean. COS fluxes have varied from 39-639 Gg as S/year,^{5,6} while CS₂ fluxes have varied from 0.09-0.7 TG CS₂/year.^{7,8} Recently,⁶ a new model was proposed by implementing more details of COS uptake by soils and leaves, which improved the ability of model to predict the seasonal variations and vertical gradients of COS. However, there were still differences between predicted concentrations and values collected from the field, thus an additional photochemical source of 600 Gg as S/year was added in order to offset the errors.⁶ Consequently, such inconsistencies provide convincing evidence that a more comprehensive understanding is still needed towards evaluating how COS and CS₂ are formed in natural waters.

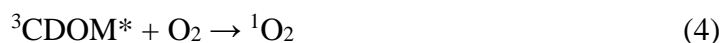
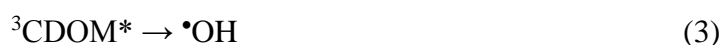
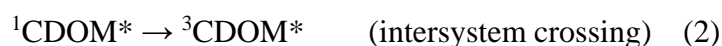
Therefore, the major focus of this thesis is aimed at exploring the chemistry of how COS and CS₂ are formed in natural waters. COS and CS₂ are typically found at picomolar (pM) to nanomolar (nM) concentrations in ocean waters where their formation has been found to enhance with sunlight exposure⁹⁻¹² and decrease with increasing the ocean depth. For example, decreasing

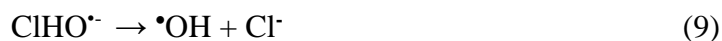
sunlight intensity and increasing ocean depth of 1 to 3 m and 0 to 10 m, has caused 50 and 20% decrease in COS and CS₂ formation, respectively.^{13,12} Additionally, COS formation has been found to follow a diurnal cycle and its concentration was found to increase by 2× in early afternoon.¹⁰ While these findings show the importance of sunlight in COS and CS₂ formation, most of the organic sulfur precursors typically present in natural waters (e.g. cysteine and DMS) do not absorb sunlight. Therefore, COS and CS₂ formation should occur through indirect photolysis from sunlight. Currently, the COS flux models use a two parameter modeling framework to assess COS production, the ocean surface sunlight intensity and the seawater absorbance at 360 nm (UV₃₆₀), which serves as a surrogate for the chromophoric dissolved organic matter (CDOM) content.

This approach though underscores the fact that much remains unknown about the photochemical processes that govern COS and CS₂ formation in such waters and what specific precursors, reactive intermediates, and reaction mechanisms are involved. This is especially evident given that nearshore waters exhibit up to 40× higher COS concentrations than open ocean waters.^{9,10,14} While this may be due to the higher CDOM concentrations found in the nearshore waters,¹⁵ the influence of other factors remains unclear which will be investigated in this study. There are some factors which could affect COS and CS₂ photochemical formation in natural waters. One factor may be the organic sulfur content which has mostly been quantified for individual compound (e.g. cysteine and dimethylsulfide (DMS)) concentrations, which range from pM to nM for freshwater and seawater.^{1,16} Alternatively, total dissolved organic sulfur (DOS) content has been challenging to measure due to analytical constraints, but one study indicated that it ranged in the low (<0.4) μmol-DOS/L in open ocean waters.¹⁷ Further variations in water quality constituents include: (i) DOM concentration/type where seawaters contain 0.4-1 mg-C/L of more aliphatic-type moieties¹⁸ whereas freshwaters contain 1-20 mg-C/L¹⁹ of more aromatic-type

moieties²⁰ with photosensitive chromophores,²⁰ and (ii) halide concentrations where seawater contains 1811× and 670× higher mean Cl⁻ and Br⁻ concentrations than freshwater, respectively²¹.

These water quality constituents are important since they can react with sunlight to produce a broad range of reactive intermediates (RIs), including: (i) ³DOM* which is an electronically excited form of DOM. In this case, CDOM is excited by the absorption of a photon to form the excited singlet state of CDOM, ¹CDOM* (eq. 1), which then converts to ³CDOM* through intersystem crossing (eq. 2). The lifetimes of ³CDOM* (i.e. triplets) have been estimated to be around 20 and 2 μs, respectively, for O₂-independent and -dependent relaxation pathways,^{22,23} which means that the O₂-dependent quenching rate constant of ³CDOM* ($K_{O_2}[O_2]=2\times 10^5 \text{ s}^{-1}$)²³ is significantly higher than that of the O₂-independent ($K_d\sim 2\times 10^4 \text{ s}^{-1}$)²², (ii) reactive oxygen species (ROS; e.g. •OH (eq. 3) and ¹O₂ (eq. 4))^{24,25}, •OH is an important environmental oxidant with a short lifetime of 5-10 μs²⁶. While there is an incomplete understanding of the pathways through formation of •OH, direct CDOM path to •OH has been reported to be dominant source (eq. 3).²⁶ CDOM has been shown to photochemically form •OH through O₂-dependent and -independent mechanisms (eq. 3).²⁶ It has been reported that the O₂-dependent pathway only accounts for ~50% of •OH production, while the mechanism for the O₂-independent pathway remains unclear,²⁶ (iii) reactive halide species (RHS; e.g. Br• and Cl•),^{14,27,28} which can form through the reaction of •OH with halides (eq. 5 and 6),²⁹ while Cl• can also participate in reactions to form •OH (eqs. 7-9) and (iv) the carbonate radical (CO₃•⁻),²⁴ which is produced from the reaction of •OH with either carbonate or bicarbonate ions (eq. 10).





Organic sulfur compounds like thiols (e.g., cysteine^{14,27,30}) or thioethers (DMS and methionine)^{27,28,30-33} can react with such RIs. However, the previous research has been inconsistent in terms of COS and CS₂ formation with these organic sulfur precursors. For example, COS and CS₂ formation for these reactions has been difficult to evaluate from prior research given the varied experimental conditions (water type, sunlight dose, organic sulfur precursors type and dose) used. Results varied such that COS either decreased by 0.6× or increased by 6-8×^{14,34,35} whereas CS₂ increased by 15-25×^{12,35}. Furthermore, the reaction mechanisms proposed to form COS or CS₂ with RIs have been limited. Thiols have been proposed to react with RIs (e.g. $\bullet\text{OH}$, $\text{CO}_3\bullet^-$, $\text{Br}\bullet$, and $\bullet\text{OOR}$) through hydrogen abstraction to first form a thiyl radical ($\text{R-S}\bullet$)³⁶ (eq. 11) which can then react with CO ³⁶ (generated from DOM during sunlight photolysis^{37,38}) (eq. 12) or react with $\text{R-C}\bullet(\text{O})$ (acyl radical)³⁴ (eq. 13) to form COS.



CS₂ is proposed to form from thiols by initially forming either a $\text{R-S}\bullet$ or a carbon centered radical ($\text{R-H}_2\text{C}\bullet\text{-SH}$) by hydrogen abstraction with $\bullet\text{OH}$.³⁵ However, no known studies have proposed mechanisms for other reduced organic sulfur compounds (e.g. thioethers).

Overall, this information clearly demonstrates that considerable knowledge gaps still exist to better understand the fundamental processes that govern COS and CS₂ formation. This thesis was aimed to close these gaps by providing a comprehensive experimental framework. In chapters 2 and 3, nine different natural waters ranging from freshwater to seawater were exposed to sunlight photolysis. These waters were amended with various organic sulfur precursors (cysteine, DMS, cystine and methionine), water quality constituents, and altered in temperature. From this work, reaction mechanisms for each organic sulfur precursor were also proposed and was discussed in chapter 3. This part of study has already been published in *Environmental Science and Technology*.³⁹ In chapters 4 and 5, COS and CS₂ formation was explored in synthetic waters where five different DOM isolates ranging from freshwater to seawater were assessed. Two different types of organic sulfur precursors were evaluated including cysteine (chapter 4) and DMS (chapter 5). The effects of DOM type/concentration, the organic sulfur precursor concentration and pH were also investigated. Additionally, in order to better elucidate the role of RIs, different quenching agents including isopropanol,^{26,40–42} phenol,⁴³ trimethylphenol,^{43–45} sorbic acid^{46,47} and O₂²⁵ were tested. More specifically, the role of RIs formed by specific functional groups of DOM such as ketones was also assessed. DOM isolates were treated with sodium borohydride (NaBH₄) which is well-known to selectively reduce ketones/aldehydes to their corresponding alcohols.

1.1 References

- (1) Mopper, K.; Kieber, D.; Stubbins, A. Chapter 8 - Marine Photochemistry of Organic Matter: Processes and Impacts. In *Biogeochemistry of Marine Dissolved Organic Matter (Second Edition)*; Academic Press: Burlington, 2015; pp 389–450.
- (2) Hofmann, D. .; Solomon, S. Ozone Destruction through Heterogeneous Chemistry Following the Eruption of El Chichón. *J. Geophys. Res.* **1989**, *94*, 5029–5041.

- (3) Tie, X.; Emmons, L.; Horowitz, L.; Brasseur, G.; Ridley, B.; Atlas, E.; Stround, C.; Hess, P.; Klonecki, A.; Madronich, S.; et al. Effect of Sulfate Aerosol on Tropospheric NO_x and Ozone Budgets: Model Simulations and TOPSE Evidence. *J. Geophys. Res. Atmos.* **2003**, *108* (D4).
- (4) Logan, J. A.; McElroy, M. B.; Wofsy, S. C.; Prather, M. J. Oxidation of CS₂ and COS: Sources for Atmospheric SO₂. *Nature* **1979**, *281* (5728), 185–188.
- (5) Kettle, A. J.; Kuhn, U.; von Hobe, M.; Kesselmeier, J.; Liss, P. S.; Andreae, M. O. Comparing Forward and Inverse Models to Estimate the Seasonal Variation of Hemisphere-Integrated Fluxes of Carbonyl Sulfide. *Atmos. Chem. Phys. Discuss.* **2002**, *2* (3), 577–621.
- (6) Berry, J.; Wolf, A.; Campbell, J. E.; Baker, I.; Blake, N.; Blake, D.; Denning, a. S.; Kawa, S. R.; Montzka, S. a.; Seibt, U.; et al. A Coupled Model of the Global Cycles of Carbonyl Sulfide and CO₂: A Possible New Window on the Carbon Cycle. *J. Geophys. Res. Biogeosciences* **2013**, *118* (2), 842–852.
- (7) Chin, M.; Davis, D. D. Global Sources and Sinks of COS and CS₂ and Their Distribution. *Global Biogeochem. Cycles* **1993**, *7* (2), 321–337.
- (8) Kim, K.-H.; Andreae, M. O. Carbon Disulfide in Seawater and the Marine Atmosphere over the North Atlantic. *J. Geophys. Res. Atmos.* **1987**, *92* (D12), 14733–14738.
- (9) Andreae, M. O. Ocean-Atmosphere Interactions in the Global Biogeochemical Sulfur Cycle. *Mar. Chem.* **1990**, *30*, 1–29.
- (10) Andreae, M.; Ferek, R. J. Photochemical Production of Carbonyl Sulfide in Sea Water and Its Emmision to the Atmosphere. *Global Biogeochem. Cycles* **1992**, *6*, 175–183.
- (11) Kim, K.-H.; Andreae, M. O. Carbon Disulfide in the Estuarine, Coastal, and Oceanic Environments. *Mar. Chem.* **1992**, *40* (3), 179–197.
- (12) Xie, H.; Moore, R. M.; Miller, W. L. Photochemical Production of Carbon Disulphide in Seawater. *J. Geophys. Res. Ocean.* **1998**, *103* (C3), 5635–5644.
- (13) Ferek, R.; Andreae, M. Photochemical Production of Carbonyl Sulphide in Marine Surface Waters. *Nature* **1984**, *370*, 148–150.
- (14) Zepp, R. G.; Andreae, M. O. Factors Affecting the Photochemical Production of Carbonyl Sulfide in Seawater. *Geophys. Res. Lett.* **1994**, *21* (25), 2813–2816.
- (15) Guéguen, C.; Guo, L.; Tanaka, N. Distributions and Characteristics of Colored Dissolved Organic Matter in the Western Arctic Ocean. *Cont. Shelf Res.* **2005**, *25* (10), 1195–1207.

- (16) Hu, H.; Mylon, S. E.; Benoit, G. Distribution of the Thiols Glutathione and 3-Mercaptopropionic Acid in Connecticut Lakes. **2006**, *51* (6), 2763–2774.
- (17) Ksionzek, K. B.; Lechtenfeld, O. J.; Mccallister, S. L.; Schmitt-kopplin, P.; Geuer, J. K.; Geibert, W.; Koch, B. P. Dissolved Organic Sulfur in the Ocean: Biogeochemistry of a Petagram Inventory. *Science*. **2016**, *354* (6311), 456–460.
- (18) Dennis A. Hansell; Carlson, C. A. *Biogeochemistry of Marine Dissolved Organic Matter*; Academic Press: amsterdam, 2002.
- (19) Brezonik, P.; Arnold, W. *Water Chemistry-An Introduction to the Chemistry of Natural and Engineered Aquatic Systems*; Osford University Press: New York, USA, 2011.
- (20) McKnight, D. M.; Boyer, E. W.; Westerhoff, P. K.; Doran, P. T.; Kulbe, T.; Andersen, D. T. Spectrofluorometric Characterization of Dissolved Organic Matter for Indication of Precursor Organic Material and Aromaticity. *Limnol. Oceanogr.* **2001**, *46* (1), 38–48.
- (21) Holland, H. D. *The Chemistry of the Atmosphere and Oceans*; New York, USA, 1978.
- (22) Zepp, R. G.; Schlotzhauer, P. F.; Sink, R. M. Photosensitized Transformations Involving Electronic Energy Transfer in Natural Waters: Role of Humic Substances. *Environ. Sci. Technol.* **1985**, *19* (1), 74–81.
- (23) Sharpless, C. M. Lifetimes of Triplet Dissolved Natural Organic Matter (DOM) and the Effect of NaBH₄ Reduction on Singlet Oxygen Quantum Yields: Implications for DOM Photophysics. *Environ. Sci. Technol.* **2012**, *46* (8), 4466–4473.
- (24) Vione, D.; Minella, M.; Maurino, V.; Minero, C. Indirect Photochemistry in Sunlit Surface Waters: Photoinduced Production of Reactive Transient Species. *Chem. – A Eur. J.* **2014**, *20* (34), 10590–10606.
- (25) McNeill, K.; Canonica, S. Triplet State Dissolved Organic Matter in Aquatic Photochemistry: Reaction Mechanisms, Substrate Scope, and Photophysical Properties. *Environ. Sci. Process. Impacts* **2016**, *18* (11), 1381–1399.
- (26) Rosario-Ortiz, F. L.; Canonica, S. Probe Compounds to Assess the Photochemical Activity of Dissolved Organic Matter. *Environ. Sci. Technol.* **2016**, *50* (23), 12532.
- (27) Chu, C.; Erickson, P. R.; Lundeen, R. A.; Stamatelatos, D.; Alaimo, P. J.; Latch, D. E.; McNeill, K. Photochemical and Nonphotochemical Transformations of Cysteine with Dissolved Organic Matter. *Environ. Sci. Technol.* **2016**, *50* (12), 6363–6373.

- (28) Huang, J.; Mabury, S. A. Steady-State Concentrations of Carbonate Radicals in Field Waters. *Environ. Toxicol. Chem.* **2009**, *19* (9), 2181–2188.
- (29) Parker, K. M.; Mitch, W. A. Halogen Radicals Contribute to Photooxidation in Coastal and Estuarine Waters. *Proc. Natl. Acad. Sci.* **2016**, *113* (21), 5868–5873.
- (30) Adams, G. E.; Aldrich, J. E.; Bisby, R. H.; Cundall, R. B.; Redpath, J. L.; Willson, R. L. Selective Free Radical Reactions with Proteins and Enzymes: Reactions of Inorganic Radical Anions with Amino Acids. *Radiat. Res.* **1972**, *49* (2), 278–289.
- (31) Cutter, G. A.; Cutter, L. S.; Filippino, K. C. Sources and Cycling of Carbonyl Sulfide in the Sargasso Sea. *Limnol. Oceanogr.* **2004**, *49* (2), 555–565.
- (32) Toole, D. A.; Kieber, D. J.; Kiene, R. P.; White, E. M.; Bisgrove, J.; del Valle, D. A.; Slezak, D. High Dimethylsulfide Photolysis Rates in Nitrate-Rich Antarctic Waters. *Geophys. Res. Lett.* **2004**, *31* (11).
- (33) Kieber, D. J.; Jiao, J.; Kiene, R. P.; Bates, T. S. Impact of Dimethylsulfide Photochemistry on Methyl Sulfur Cycling in the Equatorial Pacific Ocean. *J. Geophys. Res. Ocean.* **1996**, *101* (C2), 3715–3722.
- (34) Pos, W. H.; Riemer, D. D.; Zika, R. G. Carbonyl Sulfide (OCS) and Carbon Monoxide (CO) in Natural Waters: Evidence of a Coupled Production Pathway. *Mar. Chem.* **1998**, *62* (1–2), 89–101.
- (35) Du, Q.; Mu, Y.; Zhang, C.; Liu, J.; Zhang, Y.; Liu, C. Photochemical Production of Carbonyl Sulfide, Carbon Disulfide and Dimethyl Sulfide in a Lake Water. *J. Environ. Sci.* **2016**, *51* (September), 1–11.
- (36) Flöck, O. R.; Andreae, M. O.; Dräger, M. Environmentally Relevant Precursors of Carbonyl Sulfide in Aquatic Systems. *Mar. Chem.* **1997**, *59* (1–2), 71–85.
- (37) Valentine, R. L.; Zepp, R. G. Formation of Carbon Monoxide from the Photodegradation of Terrestrial Dissolved Organic Carbon in Natural Waters. *Environ. Sci. Technol.* **1993**, *27* (2), 409–412.
- (38) Miller, W. L.; Zepp, R. G. Photochemical Production of Dissolved Inorganic Carbon from Terrestrial Organic Matter: Significance to the Oceanic Organic Carbon Cycle. *Geophys. Res. Lett.* **1995**, *22* (4), 417–420.

- (39) Modiri Gharehveran, M.; Shah, A. D. Indirect Photochemical Formation of Carbonyl Sulfide and Carbon Disulfide in Natural Waters: Role of Organic Sulfur Precursors, Water Quality Constituents, and Temperature. *Environ. Sci. Technol.* **2018**, *52* (16), 9108–9117.
- (40) Guerard, J. J.; Miller, P. L.; Trouts, T. D.; Chin, Y.-P. The Role of Fulvic Acid Composition in the Photosensitized Degradation of Aquatic Contaminants. *Aquat. Sci.* **2009**, *71* (2), 160–169.
- (41) Bahnmüller, S.; Von Gunten, U.; Canonica, S. Sunlight-Induced Transformation of Sulfadiazine and Sulfamethoxazole in Surface Waters and Wastewater Effluents. *Water Res.* **2014**, *57*, 183–192.
- (42) Zeng, T.; Arnold, W. A. Pesticide Photolysis in Prairie Potholes: Probing Photosensitized Processes. *Environ. Sci. Technol.* **2013**, *47* (13), 6735.
- (43) Canonica, S.; Jans, U.; Stemmler, K.; Hoigne, J. Transformation Kinetics of Phenols in Water: Photosensitization by Dissolved Natural Organic Material and Aromatic Ketones. *Environ. Sci. Technol.* **1995**, *29* (7), 1822–1831.
- (44) Boreen, A. L.; Edhlund, B. L.; Cotner, J. B.; McNeill, K. Indirect Photodegradation of Dissolved Free Amino Acids: The Contribution of Singlet Oxygen and the Differential Reactivity of DOM from Various Sources. *Environ. Sci. Technol.* **2008**, *42* (15), 5492–5498.
- (45) Guerard, J. J.; Chin, Y.-P. Photodegradation of Ormetoprim in Aquaculture and Stream-Derived Dissolved Organic Matter. *J. Agric. Food Chem.* **2012**, *60* (39), 9801–9806.
- (46) Morrison, J.; Osthoff, H.; Wan, P. Photoredox, Photodecarboxylation, and Photo-Retro-Aldol Chemistry of p-Nitrobiphenyls. *Photochem. Photobiol. Sci.* **2002**, *1* (6), 384–394.
- (47) Zepp, R. G.; Gumz, M. M.; Miller, W. L.; Gao, H. Photoreaction of Valerophenone in Aqueous Solution. *J. Phys. Chem. A* **1998**, *102* (28), 5716–5723.

CHAPTER 2. INDIRECT PHOTOCHEMICAL FORMATION OF COS AND CS₂ IN NATURAL WATERS

A version of this chapter has been previously published in Environmental Science and Technology Journal.

Modiri Gharehveran, M.; Shah, A. D. Indirect Photochemical Formation of Carbonyl Sulfide and Carbon Disulfide in Natural Waters: Role of Organic Sulfur Precursors, Water Quality Constituents, and Temperature. *Environ. Sci. Technol.* **2018**, 52 (16), 9108–9117.

DOI: 10.1021/acs.est.8b01618

2.1 Abstract

This chapter evaluated how sunlight, simulated diurnal cycling and temperature affected COS and CS₂ formation. Three natural waters ranging in salinity were spiked with cysteine and dimethylsulfide (DMS) and exposed to simulated sunlight over varying times and water quality conditions. Results indicated that COS and CS₂ formation increased up to 11× and 4× with cysteine, respectively, after 12 h of sunlight while diurnal cycling exhibited varied effects. DMS formed COS and CS₂ by 0.5× lower than cysteine. COS and CS₂ formation were also strongly affected by temperature where the effect was different for COS and CS₂.

2.2 Introduction

Photochemical production of COS and CS₂ is an important source for these compounds in natural surface waters,^{1–4} where COS formation also follows a diurnal cycle⁵. In addition, the temperature of these waters can vary from a warm 30°C in the tropics to a very cold -2°C near the poles.⁶ This variation in temperature is expected to affect COS and CS₂ formation. Therefore, this study evaluated the role of sunlight, diurnal cycling and temperature on COS and CS₂ formation kinetics. Three natural waters ranging from freshwater to seawater were evaluated. Selected waters

were spiked with 14 μM cysteine (thiol) and DMS (thioether) and then were exposed to sunlight under simulated diurnal cycling. It should be noted that, the majority of these experiments were also purged with N_2 to remove dissolved O_2 , which is known to quench RIs such as $^3\text{DOM}^*$,^{7,8} carbon-centered radicals,⁹ and alkyl radicals¹⁰ as well as sulfur-centered radicals¹¹. The fact that O_2 was absent is notably different than the conditions encountered in the environment, but O_2 was removed in order to better elucidate the reaction mechanisms involved, which was a major focus of this thesis. The effect of O_2 was then later evaluated in chapter 3, where the dissolved oxygen was not directly measured but it was expected to be $[\text{O}_2]_0 \approx 8.9 \text{ mg/L}$ at 20°C since these waters were left in equilibrium with the atmosphere during storage. Overall, this study helped identify the role of sunlight, diurnal cycling, two organic sulfur precursors (cysteine and DMS), and temperature on forming COS and CS_2 in natural waters.

2.3 Material and Methods

2.3.1 Description of standards, reagents, and stock preparation

CS_2 , cysteine, dimethylsulfide (DMS), bromobimane or monobromobimane (mBbr), MES sodium salt, methanesulfonic acid, sodium perchlorate, and 2-nitrobenzaldehyde (2-NBA) were purchased at $\geq 97\%$ purity from Sigma Aldrich. Sodium chloride (NaCl) was purchased from Acros Organics. Stock solutions for cysteine was prepared in N_2 -purged purified water in order to prevent its ability to reaction with O_2 over time. The stock solutions were prepared immediately prior to use ($< 30 \text{ min}$) and were stable over the time of storing ($< 30 \text{ min}$) under oxygen free conditions. COS was purchased as calibration gas standards at 1 ppm (mol/mol), in N_2 from Gasco. Overall, these and other chemicals such as methanol (MeOH), acetonitrile (ACN), and NaOH were purchased at reagent grade or higher. Purified water ($\geq 18.2 \text{ M}\Omega \text{ cm}$) was obtained from a Nanopure

(Thermo Scientific) water purification system. All glassware was acid washed to clean any trace metal contamination which may catalyze organic sulfur compound oxidation¹².

2.3.2 Natural water samples

Nine water samples were collected off the coast of Florida (FL), Louisiana (LA) and Maine (MA) (Fig. 2-1). These waters were defined as freshwater (F), brackish water (B), or seawater (S) based on their salinity and labeled as: (i) FL-F, (ii) FL-B1, (iii) FL-B2, (iv) FL-B3, (v) FL-S, (vi) LA-F, (vii) LA-B1, (viii) LA-B2, and (ix) MA-S. The raw waters were filtered (0.7 μm glass-fiber filter) prior to shipping and held at 4°C before use. Notably, this 0.7 μm filtration range cannot remove bacteria, but additional evidence indicated that it likely has a negligible effect on COS and CS₂ formation (see later discussions). Moreover, the waters were stored for up to 12 months but were confirmed to be stable towards forming COS and CS₂ as their concentrations from different aged

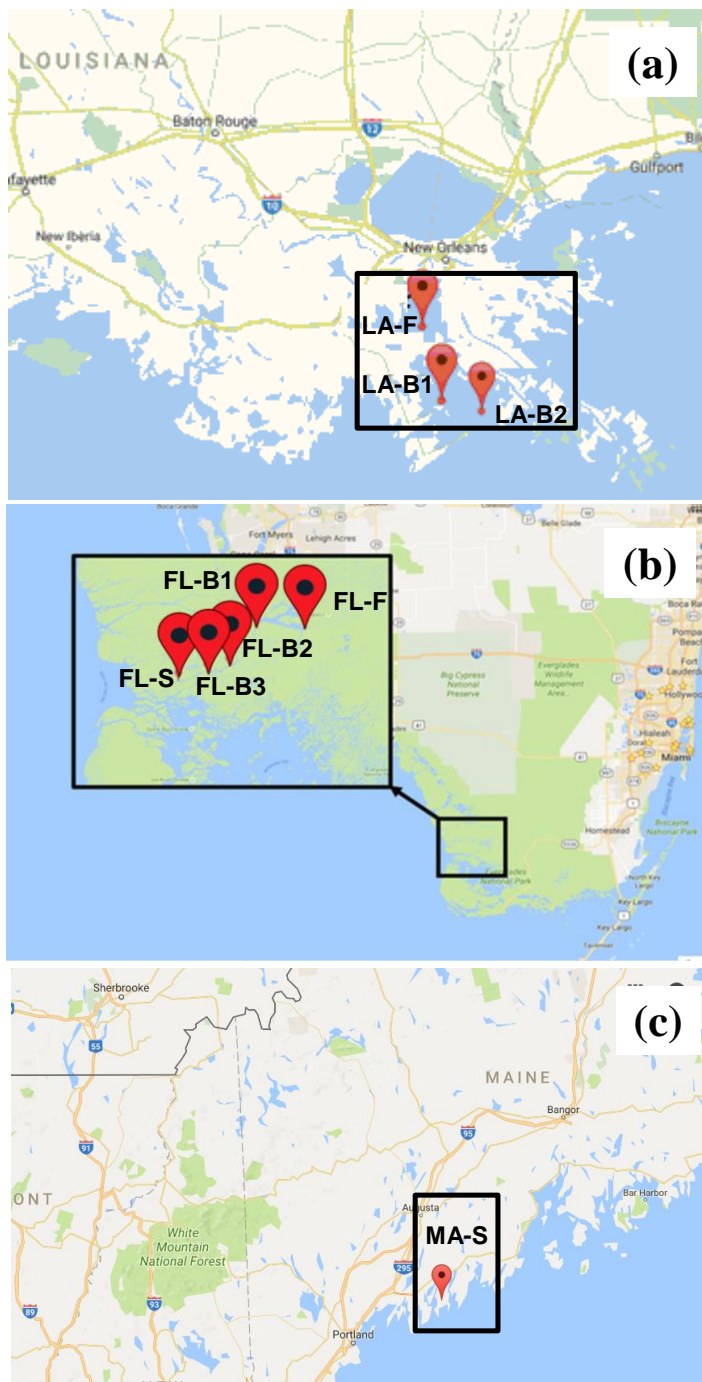


Figure 2-1. Map locations of the nine natural waters from (a) Florida, (b) Louisiana and (c) Maine.

waters only differed by a standard deviation of 0.05 ($<$ detection limit (DL) = 0.06 nM) and 0.02 nM ($<$ DL = 0.1 nM), respectively, over this time. This was confirmed by routinely (3 weeks after collection to up to 12 months) measuring COS and CS₂ from dark no-spike and irradiated (4 h) no-spike or cysteine-spiked waters. Various water quality parameters including [DOC], UV₃₆₀, pH, [Cl⁻], carbonate ([HCO₃⁻] + [CO₃⁻²]), and various metals were also measured.

Various water quality parameters in these waters were measured including the dissolved organic carbon (DOC) concentration, absorbance at 360 nm (UV₃₆₀), pH, Cl⁻ concentration, carbonate ([HCO₃⁻] + [CO₃⁻²]) concentration, and concentrations of various metals (Cu, Hg, and Pb). The DOC concentrations for all of these waters were either measured based on the SERC SOP-007 method¹³ (FL waters), a previously described method (LA waters)¹⁴, or by a TOC-V Shimadzu Total Organic Carbon Analyzer (MA water). The UV absorbance of these waters were also measured from 200 to 400 nm prior to sunlight exposure, including 360 nm, using a Shimadzu UV-VIS spectrophotometer (Fig. 2-2). The high absorbance at low

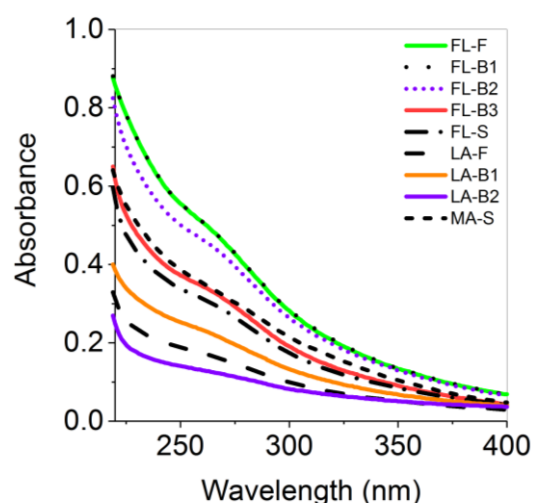


Figure 2-2. The UV-VIS absorbance of the nine natural waters between 200 to 400 nm prior to sunlight exposure.

wavelengths ($<$ 250nm) is mostly attributed the NO₃⁻ content of these waters.

The UV₃₆₀ values were then plotted versus the DOC values to determine whether or not they are correlated with each other (Fig. 2-3). A fairly low linear correlation ($R^2 = 0.776$) was observed between the DOC concentration and the UV₃₆₀ value of these waters. Therefore, each parameter, (DOC concentration or UV₃₆₀ values) was evaluated separately when relating it to COS and CS₂ formation.

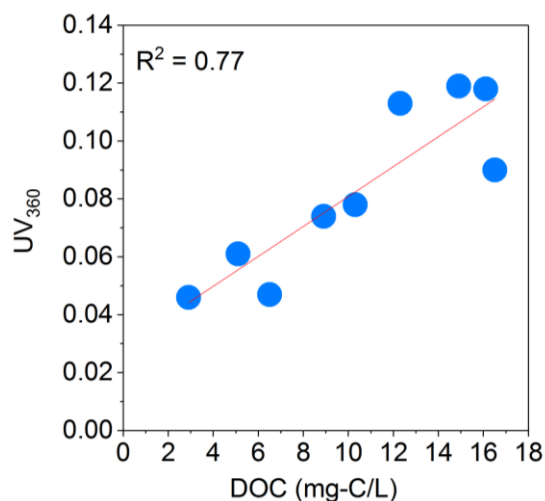


Figure 2-3. Correlation of the waters' UV₃₆₀ and DOC concentrations with each other.

The Cl⁻ concentration in these waters was measured using a 940 Metrohm IC with a conductivity detector. The eluent contained 1.0 mM Na₂CO₃ and 4.0 mM NaHCO₃ with a flow rate of 0.7 ml/min, and the samples were separated using an A Supp 5-100/4.0 column. The carbonate concentration in these waters was measured by acidifying the waters, reducing the pH to 2 – 4 with sulfuric acid and converting all the of the carbonate to CO₂. The total CO₂ concentration after acidification was then measured by placing the water samples in 20 mL headspace-free screw-top vials. A small volume (50 μL) of these acidified waters were transferred to pre-N₂-purged GC vials and injected onto a GC-FID for CO₂ analysis. The details for the analytical methods of GC-FID are described in later sections. The total CO₂ concentration after acidification (C_T) was then equivalent to the sum of CO₂, HCO₃⁻ and CO₃²⁻ before acidification (eq. 4).

$$[\text{CO}_2]_{(\text{after acid.})} = C_T = [\text{HCO}_3^-]_{(\text{before acid.})} + [\text{CO}_3^{2-}]_{(\text{before acid.})} + [\text{CO}_2]_{(\text{before acid.})} \quad (4)$$

in which $[\text{CO}_2]_{(\text{before acid.})} = 14.4 \mu\text{M}$ (CO_2 concentration prior to acidification in equilibrium with atmospheric CO_2). Metal concentrations (Pb, Cu, and Hg) were analyzed using an inductively coupled plasma emission spectrometer (ICPE-9820). The method detection limits (MDL) for each of these metals varied with water type since the presence of other salts created a matrix effect where it was necessary that the waters be diluted to reach a salinity of 5 ppt before analysis. All of these values are reported in Table 2-1.

The storage of natural waters and microbial effect

The raw waters were filtered ($0.7 \mu\text{m}$ glass-fiber filter) prior to shipping and held at 4°C before use. Notably, this $0.7 \mu\text{m}$ filtration range cannot remove bacteria, but additional evidence indicated that it likely has a negligible effect on COS and CS_2 formation. First, the decrease in COS in the phase II data fit well to the hydrolysis models (details in later discussions), indicating that microbial effects were not involved. Alternatively, CS_2 did form in the dark but only for cysteine-spiked samples (details in later discussions). However, a previous study indicated that the cysteine biotic removal rate was very slow when compared to its abiotic photochemical and nonphotochemical rates.¹² Additional studies similarly reported that COS and CS_2 formation were likely not linked to microbial activity.^{1,15}

Table 2-1. Sample location and water quality characteristics of the nine tested natural waters.

Water Type	GPS Coordinates (Lat, Long)	pH	DOC (mg-C/L)	UV ₃₆₀	Chloride (M)	Carbonate (μ M/kg seawater)	Cu (ppb)	Hg (ppb)	Pb (ppb)
FL-F	25.411, -80.968	7.8	14.9	0.119	0.09	2160	<20	<20	<20
FL-B1	25.416, -81.007	8.0	16.1	0.118	0.12	1954	7.2	<26	<26
FL-B2	25.375, -81.036	8.0	12.3	0.113	0.27	2159	<60	<60	<60
FL-B3	25.372, -81.054	7.9	10.3	0.078	0.28	2122	<60	<60	<60
FL-S	25.363, -81.082	8.0	8.9	0.074	0.42	2548	<100	<100	<100
LA-F	29.295, -90.085	8.0	6.5	0.047	0.12	1282	<26	<26	<26
LA-B1	29.260, -90.055	8.1	5.1	0.061	0.25	1256	<60	<60	<60
LA-B2	29.338, -89.905	8.1	2.9	0.046	0.27	1625	<60	<60	<60
MA-S	43.876, -69.693	7.8	16.5	0.09	0.18	1630	<40	<40	<40

2.3.3 Experimental procedure

Photochemical reactor setup

A solar simulator (OAI Tri-Sol; AM 1.5G filter) was used to simulate collimated sunlight (Fig. 2-4). Small custom-designed reactors (~ 11 mL) containing selected waters with no headspace were placed below the sunlight beam under constant mixing and temperature conditions (5 to 30°C) using a water bath (Fig. 2-4). The reactors were made of quartz glass since it has better ultraviolet light transmission than most other glasses. These reactors were made with a flat top (surface area of 2 cm²) while the bottom contained a threaded opening with a septum-capped screw top for gas-tight sampling (Fig. 2-5). This geometry was not chosen, but the quartz on top of the reactors were preferred. Also, the vials attached to the quartz were purchased commercially and were only available at the sizes smaller than the quartz.

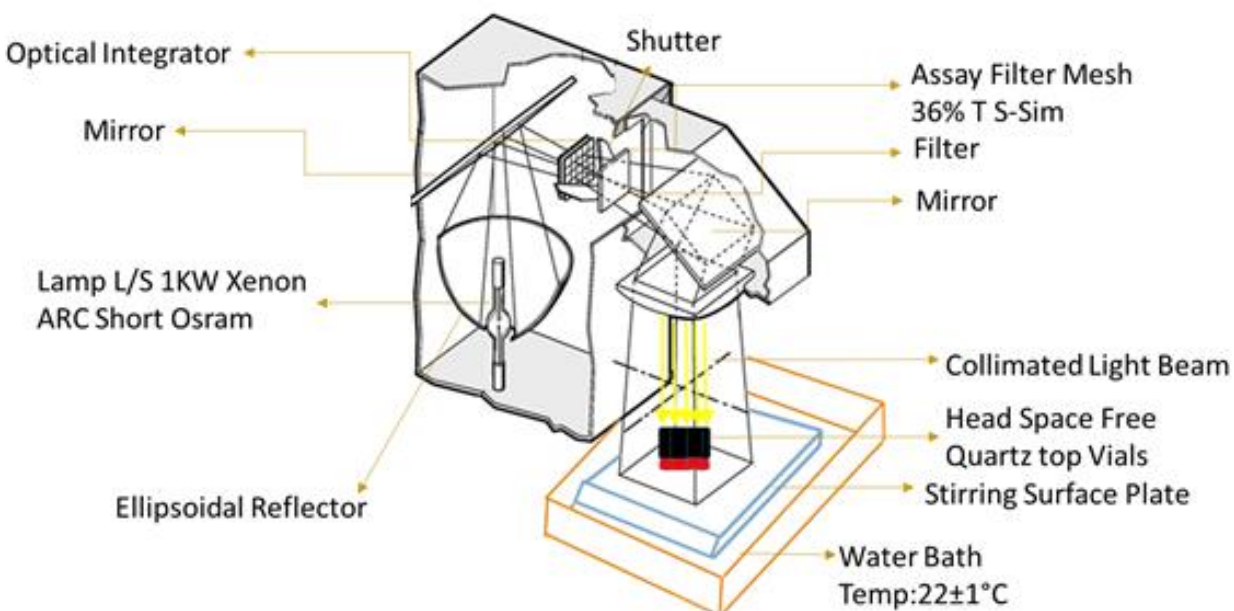


Figure 2-4. Schematic of the photochemical reactor used in this study. The schematic of the solar simulator was similar to that used by NASA and thus adopted from a picture they provided online¹⁶.

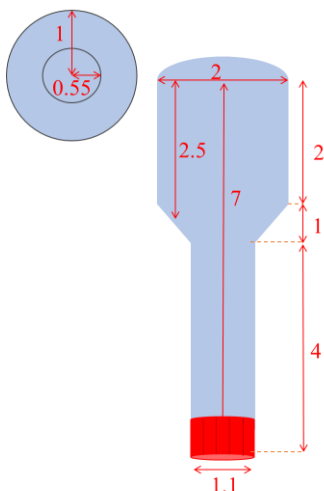


Figure 2-5. The photochemical reactor geometry (all dimensions are in cm).

The sunlight intensity measurement and pathlength determination

The sunlight intensity from the solar simulator (OAI Tri-Sol) was measured from 300 to 400 nm. This range was selected since many compounds (e.g., DOM)¹⁷ in natural waters absorb light over this wavelength range, and COS and CS₂ are known to increase in formation with decreasing wavelength from 400 to 300 nm.^{1,18} The light intensity was measured in units of mJ/ cm²/s by coupling the solar spectrum obtained from an Optics 2000+ spectrophotometer (Fig. 2-6) with the photon flux (moles of photons /cm²/s) measured using 2-NBA as a chemical actinometer.¹⁹

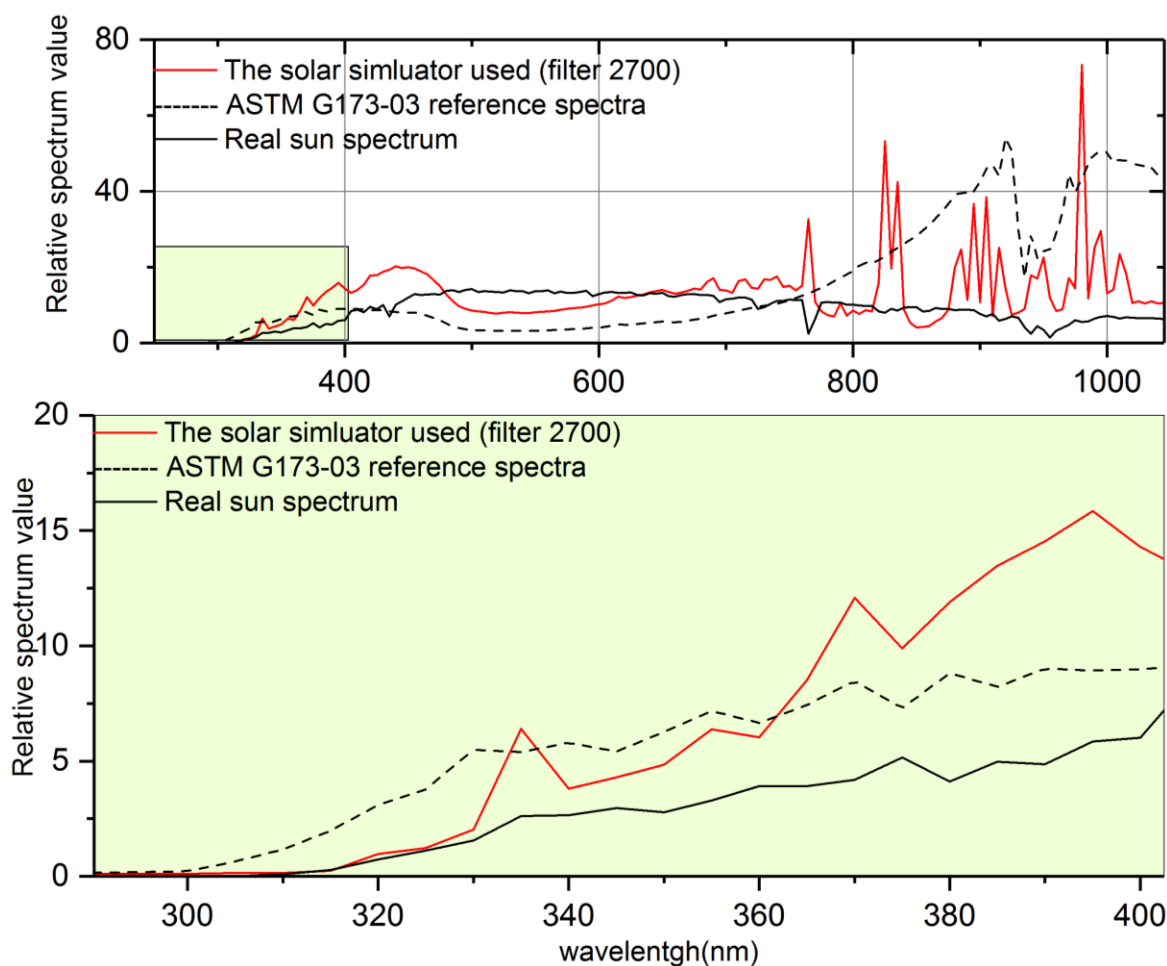


Figure 2-6. Relative light spectrum emitted from the OAI TRI-SOL solar simulator which has been compared to the ASTM G173-03 reference spectrum²⁰ and the sun spectrum captured on August 17, 2015 in West Lafayette, IN, USA (Latitude: 40.430098, Longitude: -86.914392).

2-NBA was exposed to sunlight following a procedure modified from previous literature^{19,21} where 2 mM 2-NBA solutions (20/80 % ACN/water) were exposed to sunlight over 30 min. Samples were periodically collected and analyzed by HPLC. Values were then plotted according to zero-order photodecay where the slope of the line was equivalent to the photodecay rate (k) which ranged from $1.0\text{-}1.4 \times 10^{-5} \text{ Ms}^{-1}$ ($R^2 = 0.99$) (Fig. 2-7). It should also be noted that the whole fraction of light was absorbed by 2-NBA which was added at high concentrations to make the solution opaque at the relevant wavelengths.

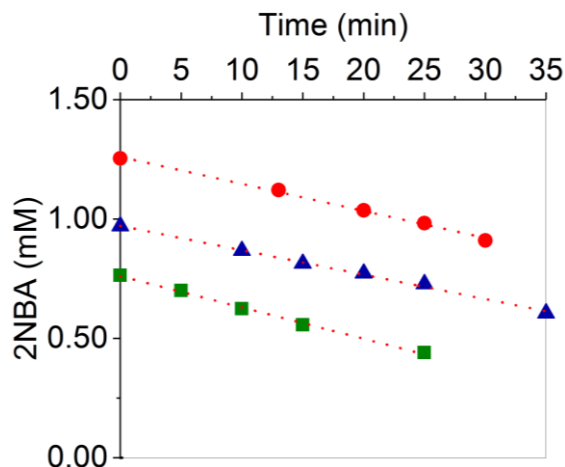


Figure 2-7. Degradation of 2-NBA following sunlight exposure over time plotted as a zero-order loss ([2-NBA]; y-axis) with time (x-axis)). The three curves reflect values from experiments conducted on different days.

This k value was then used to calculate the light intensity (I_λ) ($\text{mJ}/\text{cm}^2/\text{s}$) in eq. 5:¹⁹

$$I_\lambda = -k \cdot \frac{1}{\Phi_\lambda} \cdot \frac{1}{1 \cdot 10^{-\epsilon_\lambda l C}} \cdot \frac{V}{S} \cdot E_\lambda \quad (5)$$

where Φ_λ (quantum yield) = 0.4 (moles of 2-NBA/moles of photons) from 300 to 400 nm for solutions containing mixtures of water and organic solvents,²¹ ϵ_λ = molar absorptivity ($\text{M}^{-1}\text{cm}^{-1}$),

l = path length (cm), C = initial 2-NBA concentration of 2.0×10^3 M which was considered constant given its high concentration (M), V = sample volume (cm^3), S = surface area of reactor (cm^2), and E_λ = energy of photons ($\text{mJ}/\text{moles of photons}$). The ϵ_λ values were found to range from $1590 \pm 19 \text{ M}^{-1}\text{cm}^{-1}$ to $224 \pm 12 \text{ M}^{-1}\text{cm}^{-1}$ from 300 to 400 nm, respectively,

by measuring its absorbance using various standards (50-200 μM in 20/80 % ACN/water) (Fig. 2-8).

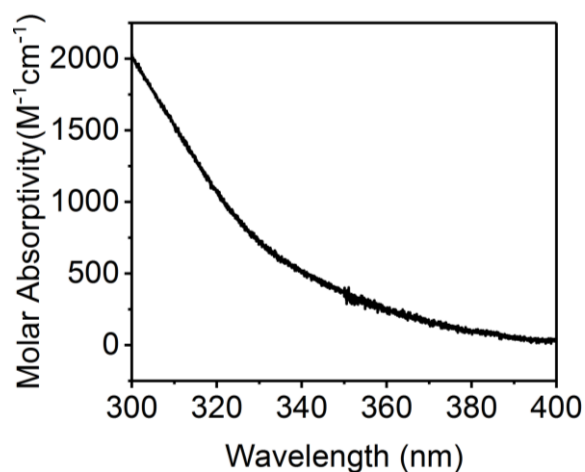


Figure 2-8. 2- Nitrobenzaldehyde molar absorptivity (ϵ_λ) values from 300 to 400 nm.

In addition, the average path length (l) was determined based on a previously described method.²² Briefly, the initial degradation of 2-NBA was assessed over a short time period (5 min) at varying initial concentrations (10 μ M to 1 mM). The slopes of these lines represented the change in concentration over time (i.e. dC/dt). The maximum dC/dt values were found to occur at the higher initial 2-NBA concentrations and were subsequently defined as $(dC/dt)_{max}$. X then was defined based on eq. 6:

$$\frac{dC/dt}{(dC/dt)_{max}} = X = 1 - 10^{-\epsilon_{\lambda} C l} \quad (6)$$

where X is the ratio of 2-NBA degradation at concentration C to that at a concentration in which all the light was absorbed. Each of these values were then used in eq. 7:

$$-\log \left(1 - \frac{dC/dt}{(dC/dt)_{max}} \right) = a \cdot l \cdot [2\text{-NBA}]_i \quad (7)$$

where $[2\text{-NBA}]_i$ = the initial 2-NBA concentration (M) and a = the weighted average of the ϵ_{λ} values from 300 to 400 nm which were calculated based on the relative solar spectrum values ($M^{-1}cm^{-1}$). These data were then plotted according to eq. 7 which is a linearized function where the path length (l) equaled the slope of the line (Fig. 2-9). The path length (l) was found to be 3.97 cm. This value matched the average path length of the reactor when calculating the value from eq. 8 using the dimensions provided from Fig. 2-5.

$$\text{average path length } (l) = \frac{7 \times \pi \times 0.55^2 + 2.5 \times \pi \times (1^2 - 0.55^2)}{\pi \times 0.55^2 + \pi \times (1^2 - 0.55^2)} = 3.86 \text{ cm} \quad (8)$$

In this case, the average path length equaled 3.86 cm which was close to the 3.97 cm value measured experimentally.

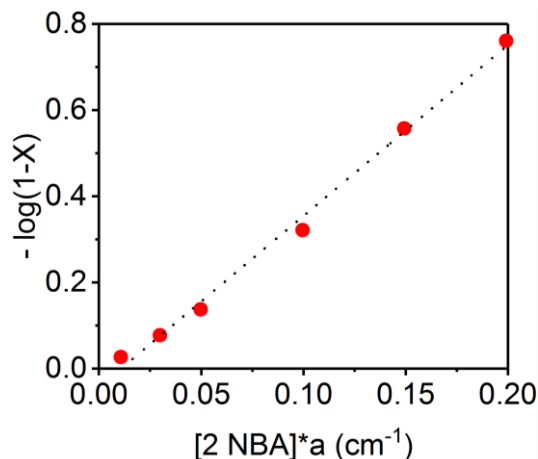


Figure 2-9. Experimental data used to measure the reactor pathlength. The data were fitted according to eq. 7.

Kinetic Experiments

Kinetic experiments were performed with the LA-F, LA-B1, and LA-B2 waters which were initially purged with N₂ for 10 min to remove dissolved O₂ and either used as is or spiked with 14 μM cysteine or DMS. The concentrations of μM were chosen in order to: (i) see the effect on COS and CS₂ formation and (ii) monitor the degradation of organic S precursors. The waters were then (i) left in the dark over 12 h, (ii) exposed to sunlight over 12 h or (iii) exposed to diurnal cycling which included 4 h of sunlight (phase I), 4 h of dark (phase II), and 4 h of sunlight (phase III). This 4 h cycling period was shortened from the natural diurnal cycling period (~ 9-14 h) in order to make the sampling time frame more reasonable for the experimentalist. Additional kinetic experiments with the LA-B2 water assessed the effect of temperature (5 to 30°C).

2.3.4 Analytical methods

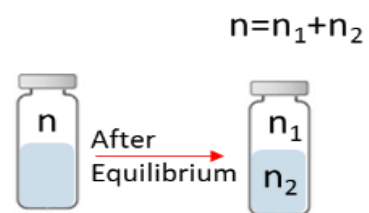
COS, CS₂, and DMS

A method to measure COS, CS₂ and DMS in the gas phase was developed using headspace GC-MS (Agilent 6420) and was then used to measure their aqueous phase concentrations from samples taken from the photochemical experiments. This procedure included transferring 5 mL of sample liquid to sealed gastight vials that were exposed to N₂ gas. The gas phase in these samples were measured by first placing them in an agitator for 5 min at 35°C to reach equilibrium conditions. A syringe was used to collect 1 mL of this headspace which was immediately injected into the GC-MS. The value obtained from this analysis was then cross-compared against standards to obtain the gas phase concentration after equilibrium in these two phase samples. Standards were prepared under N₂ within a glove box from neat solutions provided commercially in both the gas (COS) and liquid (CS₂ and DMS) phases. Gas phase standards were then diluted directly into septum-capped vials. For the liquid phase standards, 2.5-5 μL of the neat solution was placed in

septum-capped vials and stored in the oven at 120°C to convert the liquid to the gas phase (boiling points for CS₂ and DMS are 46.3 and 37°C, respectively), following a similar procedure done previously.²³ Additional dilutions were prepared in the gas phase in septum-capped vials. The standards were used to create a calibration curve for COS, CS₂, and DMS as a function of partial pressure which was determined after the GC/MS headspace syringe was injected and raised up to 1 mL since the new equilibrium was established at this point.

The aqueous phase concentrations in the samples were then determined in two steps from the gas phase concentration. First, the aqueous phase concentration from the gas phase concentration was determined using Henry's Law (eq. 9)). It should be noted that an equilibrium was established by incubating the samples for 10 min in the incubator of the auto-sampler in GC system. To then ensure the equilibrium condition, a set of experiments were conducted, where the Henry's Law constant of COS was calculated which was found to match the

previously reported values. The aqueous phase concentrations were then used to calculate the total number of moles in the system, according to the mass balance shown in the eq. 10 (Fig. 2-10):



$$C_{w\text{-after eq.}} = H \times P_{\text{after eq.}} \quad (9)$$

$$n_{T\text{-after eq.}} = n_{T\text{-before eq.}} = \frac{P_{\text{after eq.}} \times V_{\text{HP}}}{R \times T} + C_{w\text{-after eq.}} \times V_w \quad (10)$$

Figure 2-10. The mass balance involved in the sample preparation procedure

in which $C_{w\text{-after eq.}}$ = liquid phase concentration after equilibrium (M), H = Henry's law constant ($H_{\text{COS}} = 0.022$, $H_{\text{CS}_2} = 0.055$, $H_{\text{DMS}} = 0.35 \text{ M kg}^{-1}\text{bar}^{-1}$, temperature = 308.15 °K),²⁴ $P_{\text{after eq.}}$ = the partial pressure after equilibrium (bar), $n_{\text{total-after eq.}}$ = the total number of moles in the system (moles), V_{HP} = volume of head space including syringe volume (6+1 mL), R = ideal gas law constant ($\text{m}^3 \text{ bar K}^{-1} \text{ M}^{-1}$), T = temperature (K), and V_w = volume of liquid phase (5 mL). These

total number of moles were then used in the second step to obtain the liquid concentrations prior to equilibrium (i.e., the concentrations in the photochemical reactors = $C_{w\text{-before eq.}}$) by using eq. 11:

$$C_{w\text{-before eq.}} = \frac{n_{w\text{-after eq.}}}{V_w} \quad (11)$$

Following injection, samples were split with a ratio of 1:10 at an injection port temperature of 250°C and separated using a GC GS-GasPro (30 m × 320 μm × 0 μm) column. The oven program started at 60°C for 2 min, was increased up to 160°C at a rate of 20°C /min, was held at this temperature for 4 min, and was followed by a 2 min post-run. The carrier gas (He) velocity was maintained at 24 cm/s. The transfer line and MS source temperatures were held at 250 and 320°C, respectively. The mass spectrometer was operated in EI mode (70 eV). The compounds were measured in SIM mode at m/z values of 60, 76, and 62 for COS, CS₂, and DMS, respectively. The method detection limits (DL) were 0.060 and 0.10 nM for COS and CS₂, respectively. The DL values were measured according to the method described by the Environmental Protection Agency (EPA) and defined as the minimum concentration that could be measured with 99% confidence to be greater than zero.²⁵

Cysteine and methionine

The analytical method for cysteine was developed using pre-column derivitization with high-performance liquid chromatography (HPLC; Shimadzu) equipped with a fluorescence detector (RF-10AXL). Cysteine was derivatized following a modified method described previously²⁶ using the fluorescence probe, mBbr. All experimental conditions matched the previous method except that HEPPS buffer was replaced by 1.0 mM methanesulfonic acid sodium salt (MES) to achieve a pH of 8.1. Briefly, samples were diluted by 1.5 ml of MES buffer to reach a final concentration of 30-300 nM cysteine. To this mixture, 10 μl of 30 mM mBbr was added, and the solution was incubated at 40 °C for 30 min to derivatize the samples. After this, the reaction was quenched by

dropping the pH to 2 with excess methanesulfonic acid ($\text{CH}_3\text{SO}_3\text{H}$) and stored at $-20\text{ }^\circ\text{C}$ for up to 5 days before HPLC analysis.

Standards were derivatized directly in deionized water, but when they were derived from the cysteine-spiked various natural waters including both freshwater and seawater, a large response was lost, indicating that there was a matrix effect from these waters. To further assess this problem, three selected natural waters (MA-S, LA-F, and LA-B2) were diluted by deionized water at various ratios of 1:1.5 (natural water: deionized water), 1:10, and 1:100 (Fig. 2-11). They were then derivatized under buffered conditions, similar to that of the original procedure. The results from these dilutions indicated that the responses for the 1:1.5 and 1:10 dilutions were 130 \times and 20 \times lower than the deionized water response, indicating that the matrix effect still remained. However, the 1:100 dilution results led to the same response as the deionized water sample (Fig. 2-11), and thus this dilution ratio was used when derivatizing all of the natural waters tested when measuring residual cysteine.

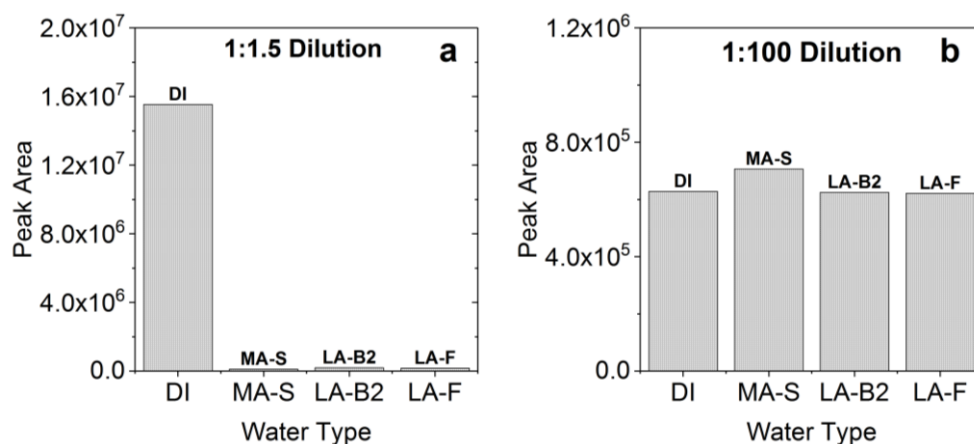


Figure 2-11. The effect of a (a) 1:1.5 dilution factor, and a (b) 1:100 dilution factor on the response lost for cysteine caused by the matrix effect in the MA-S, LA-B2, and LA-F waters. DI = deionized water.

After derivatization, samples were separated using an Agilent C18 Eclipse Plus reverse phase column (150 mm × 2.1 mm × 3.5 μm). The eluents were run at 0.4 ml/min in gradient mode. The two eluents included of 0.1 % trifluoroacetic acid (TFA) in water (solution A) and 0.1 % TFA in ACN (solution B). The gradient program was set at 95/5% A/B for 10 min., switched to 73/27% A/B at 17 min., switched to 0/100% A/B at 23 min., and finally switched to 95/5% A/B at 38 min. where it was left at this ratio for 7 min. The excitation and emission wavelengths for fluorescence detection were fixed at 380 and 470 nm, respectively. Overall, the method detection limit when using the 1:100 dilution procedure was 7.3 μM.

Methionine was measured via LC-MS (Agilent 1200 Infinity-6420 MS) with electrospray ionization (ESI). Samples were separated using an Agilent C18 Eclipse Plus reverse phase column (150 mm × 2.1 mm × 3.5 μm). The eluents including water (solution A) and ACN (solution B) were run at 0.4 ml/min in gradient mode. The gradient program switched from 90/10% A/B to 70/30% A/B at 1 min., 30/70% A/B at 3 min., 5/95% A/B at 4 min., left at this ratio for 6 min., and was followed by a 5 min post-run. The MS was run with ESI using a source temperature of 300 °C. The MS was operated in positive ion multiple reaction monitoring (MRM) mode. The precursor ion was m/z 150, and the product ions (m/z) were 132.8, 103.8, 101.8, and 55.9.

CO and CO₂

CO was measured by headspace GC-FID (3800 Varian GC). Samples were separated using a Molesieve 5Å (80/100 MESH, 6', 1/8" SS) column. The oven program was run in isocratic mode at 50°C for 15 min. The carrier gas (He) flow rate was 5 ml/min. The CO concentration in the samples were calculated in two steps from the gas phase concentration using eqs. 5-7 but using a different Henry's Law constant ($H_{CO} = 0.00099 \text{ M kg}^{-1}\text{bar}^{-1}$) different gas/liquid volumes for the headspace vials ($V_{HP} = 16+1 = 17 \text{ mL}$, $V_w = 5 \text{ mL}$). CO₂ was measured by GC-FID which was

separated by a HayeSep N micro-packed column ($4' \times 1/16''$) with a carrier gas (He) flow rate of 5 ml/min.

2-NBA

2-NBA was measured using an HPLC (Agilent 1200 Infinity) with diode array detection (DAD). Samples were separated using an Agilent C18 Eclipse Plus reverse phase column (150 mm \times 2.1 mm \times 3.5 μ m). The eluents included water (solution A) and methanol (solution B) and were run at 0.12 ml/min in gradient mode. The gradient program started at 90/10% A/B, switched to 60/40% A/B at 2 min, 20/80% A/B at 4 min, 100/0% A/B at 7 min, 90/10% A/B at 10.1 min., and left at this ratio for up to 14 min. The UV wavelength was fixed at 210 nm.

2.3.5 Detailed description of the kintecus modelling data methods

Kintecus software was used to model the chemical kinetics of COS and CS₂ hydrolysis. The software was downloaded from the website, www.kintecus.com.²⁷ This software is based on a Microsoft Excel platform in which a VBA macros has been embedded so that a system of reactions to be modeled simultaneously over time. The details and reaction rates used in the model are described in the table below:

Table 2-2. A description of the reactions and conditions used to model the kinetics of the COS and CS₂ hydrolysis at 20°C (the temperature at which most of the experiments were conducted) and pH=8.1. A similar method was used to assess the model kinetics for other temperature (i.e., 5 and 30°C) and pH values.

k ₁	Reaction	Comments
6.90E-04 (s ⁻¹)	H ₂ O ==> H ⁺ + OH ⁻	Acid dissociation reactions for water
1.00E+11 (M ⁻¹ s ⁻¹)	H ⁺ + OH ⁻ ==> H ₂ O	Acid dissociation reactions for water
2.23E-05 (s ⁻¹) ^a	OCS ==> H ₂ S + CO ₂	COS hydrolysis
1.29E+01 (M ⁻¹ s ⁻¹) ^a	OCS + OH ⁻ ==> HS ⁻ + CO ₂	COS hydrolysis
<<1.00E-05 (s ⁻¹) ^a	CS ₂ ==> Products	CS ₂ hydrolysis
1E-03 (M ⁻¹ s ⁻¹) ^a	CS ₂ + OH ⁻ ==> Products	CS ₂ hydrolysis

^a These reaction rates were estimated by combining the Arrhenius expressions at two temperatures (i.e., 5 and 30°C) (equation equals $\ln\left(\frac{k_2}{k_1}\right) = \frac{E_a}{R} \left(\frac{1}{T_2} - \frac{1}{T_1}\right)$). The E_a values included: 20-23 kcal for the COS reaction with H₂O,²⁸ 12-14 kcal for the COS reaction with OH⁻,²⁸ and 20-23 kcal for the CS₂ reaction with H₂O.²⁹

The CS₂ hydrolysis was further investigated by using Kintecus, where COS and CS₂ hydrolysis was modeled under similar conditions at 20°C. Both COS and CS₂ hydrolysis rates were compared to each other when first considering an initial COS and CS₂ concentrations of 1.0 nM (a mid-range experimental value) at 20°C and pH 8.1 over a reaction time of 4 h (see Fig. 2-12). In this case though, the upper limit value

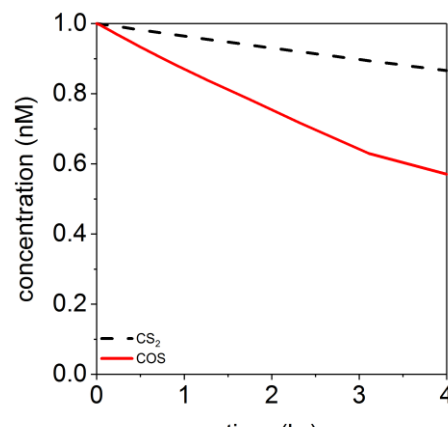


Figure 2-12. Comparison of COS and CS₂ hydrolysis rates using the Kintecus modeling software.

for the CS₂ hydrolysis rate ($= 1 \times 10^{-5}$ value in Table 2-2) was used. Thus, while the model curve seems to suggest that approximately 13% of CS₂ is lost over 4 h, this loss is likely considerably lower than this since the rate constant is in fact $\ll 1 \times 10^{-5}$ (Table 2-2). Additional modeling efforts further indicated the CS₂ hydrolysis with H₂O rather than with OH⁻ was the only reaction that controlled the overall hydrolysis at the relevant pH conditions. Given this information, the effect of temperature on CS₂ hydrolysis was evaluated by only focusing the CS₂ reaction with H₂O in

which different rate constants were estimated using the activation energies provided in Table 2-2. The role of temperature was found to have a negligible effect on altering the loss of CS₂ by hydrolysis. Thus, in the end, CS₂ hydrolysis was considered to have a negligible effect for the experimental conditions used in this study. This effect was further confirmed by a previous study which found that CS₂ hydrolysis in the sea does not occur rapidly enough to be considered as a sink.²⁹

2.4 Results and Discussion

2.4.1 Effect of sunlight exposure on COS and CS₂ formation kinetics.

Cysteine-spiked waters

With the LA-F, LA-B1, and LA-B2 waters, COS and CS₂ increased in formation in the presence of sunlight to up to low (< 11) nM concentrations, a range consistent with previous studies.^{15,18,30} It is worth mentioning though, that these COS and CS₂ concentrations were generated without O₂ present and therefore were at higher levels than would be formed in natural waters at typical O₂ levels (see later discussions for the role of O₂). However, the absence of O₂ aided in better elucidating the mechanisms involved in forming these compounds which are hypothesized to similarly occur within natural waters containing O₂. Given this, COS and CS₂ data were presented separately within Fig. 2-13 (LA-B1) and Fig. 2-14 (LA-F and LA-B2). For the LA-B1 water, COS did not form above the detection limit (DL) in the dark with no cysteine, but increased up to 0.89 nM with cysteine after 12 h (Fig. 2-13a). The ability for cysteine to form COS in the dark has been observed previously³ and several reaction mechanisms have been proposed (see mechanistic section for further details and other later discussed reactions). COS formation then increased with light to a greater degree over 12 h with no cysteine while increasing even

further with cysteine (Fig. 2-13a). These results suggested that the inherent organic or inorganic sulfur precursors present were able to form some degree of COS, but COS increased further once cysteine was added. In addition, a considerable portion of cysteine (~ 50% within 4 h (Fig. 2-13a)), when added, was lost over time. This loss was not attributed to COS formation (<0.015 % yield), but rather to forming other known by-products (e.g. RSSR, RSOH, RSO₂H, and RSO₃H).¹² These increased COS levels also matched prior results where COS increased by 1.8-7×,^{3,18,31} with sunlight (here and in the remainder of the section, 1× corresponds to equality while >1× and <1× correspond for an increase and decrease, respectively). Similarly, CS₂ did not form above the DL with no cysteine after 12 h in the dark, as observed previously¹, but increased to a greater degree with cysteine (Fig. 2-13b). While cysteine did not form CS₂ previously in the dark¹, this result is not surprising since it is unstable in the dark¹², which may induce CS₂-generating pathways. With light, CS₂ did not form above the DL after 4 h but increased again after 12 h with no cysteine, again due to the inherent sulfur precursors present, but increased even further with cysteine (Fig. 2-13b).

During diurnal cycling, COS formation followed a different trend where its concentration increased, decreased, and then increased during phase I (light), II (dark), and III (light), respectively (Fig. 2-13b). These trends were similar for both the no spike and cysteine-spiked LA-B1 waters, although as expected, the cysteine-spiked water formed ~ 4.6-5.2× higher COS concentrations than the non-spiked water for all three phases (Fig. 2-13a). These similar trends further suggested that the different organic sulfur precursors involved (inherent DOS vs. cysteine) induced similar photochemical pathways. A similar comparison with CS₂ could not be made since it did not form above the DL for the no spike water (Fig. 2-13b). However, differences due to diurnal cycling between COS and CS₂ formation trends were especially noticeable within phase II

and the end of phase III (Fig. 2-13 and Fig. 2-14). Within phase II, their kinetics differed since COS decreased in concentration due to significant COS hydrolysis while CS₂ increased fairly linearly (Fig. 2-13), due to negligible CS₂ hydrolysis. The role of COS and CS₂ hydrolysis was modeled using Kintecus (see lines in Fig. 2-13 for COS hydrolysis; model details for both COS and CS₂ hydrolysis in Section 2.3.5). For COS, the experimental data validated the modeling results well for both the no spike and cysteine-spiked experimental results (Fig. 2-13a). Similar effects of COS hydrolysis were observed in the open ocean during diurnal cycling events.^{5,32,33} This pattern differed for CS₂ that interestingly increased over this dark period, suggesting that light was not required to continue forming CS₂ (Fig. 2-13b). Instead, an initial period of light within phase I was necessary to reach these phase II concentrations since similar levels were not reached for the dark controls (Fig. 2-13b). These data suggested that a long-lived intermediate was likely involved that still remained during the dark phase. This long-lived intermediate also led CS₂ after phase III to only differ from the 12 h irradiated sample by 0.87× with cysteine (Fig. 2-13b).

Similar results were observed for the LA-F and LA-B2 waters (Fig. 2-14). These waters did result in different endpoint COS and CS₂ concentrations for the same condition tested, which is attributed to the varied quality parameters of these waters (more details in later discussions).

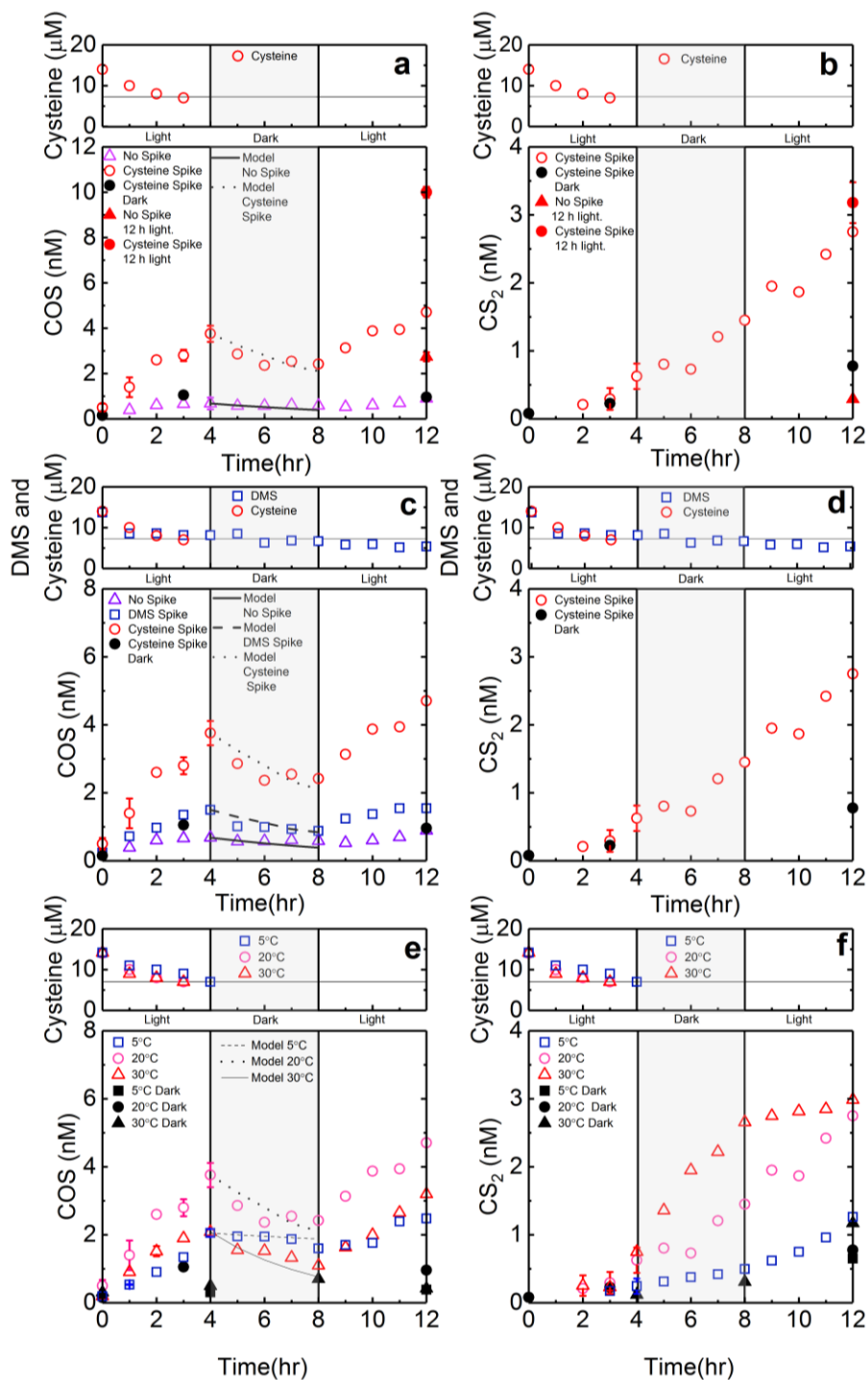


Figure 2-13. The effect of sunlight exposure on COS and CS_2 formation for the LA-B1 water when (a,b) spiked or not spiked with cysteine ($20 \pm 1^\circ\text{C}$), (c,d) spiked or not spiked with cysteine or DMS ($20 \pm 1^\circ\text{C}$), and (e,f) varied in temperature (5, 20 and 30°C) and spiked with cysteine. Cysteine and DMS were measured during diurnal cycling where the DL for cysteine is represented by a horizontal line. Error bars represent the standard error for three replicates. ($[\text{cysteine or DMS}]_0 = 14 \mu\text{M}$, pH 8.1)

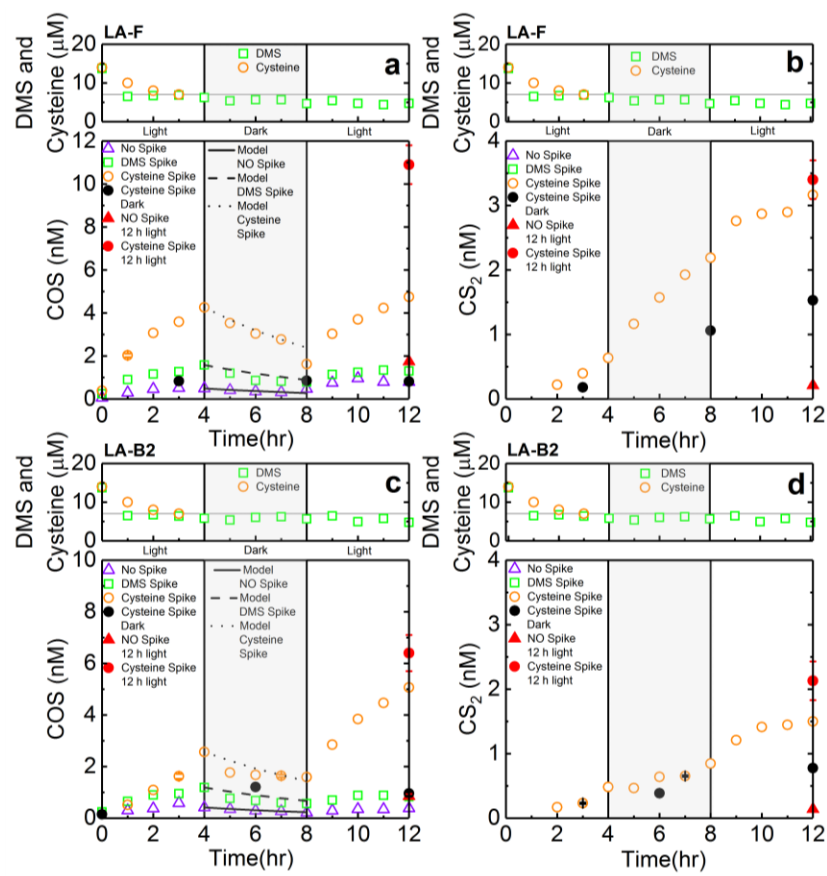


Figure 2-14. The effect of sunlight exposure on COS and CS₂ photoproduction for (a,b) the LA-F and (c,d) the LA-B2 water, spiked or not spiked with cysteine or DMS. Cysteine and DMS were measured during diurnal cycling where the DL for cysteine is represented by a horizontal line. ([cysteine or DMS]₀ = 14 μM, pH: LA-F: 8.0, LA-B2: 8.17).

DMS-spiked waters

To further evaluate the role of diurnal cycling, additional experiments of this type were conducted with DMS-spiked waters which were found to be similar to the cysteine-spiked results. For all three waters, COS did not form at concentrations above the DL in the dark. The formation increased up to 0.56-1.6 nM after all three phases occurred within the diurnal cycle. The trends in each phase were similar for all three waters (LA-B1 in Fig. 2-13c, LA-F in Fig. 2-14a and LA-B2 in Fig. 2-14c). By comparison, the COS formed for all three DMS-spiked waters was 2× higher

than with no DMS but was $< 0.5\times$ lower than with cysteine when averaging over the entire diurnal cycle (LA-B1 in Fig. 2-13c, LA-F in Fig. 2-14a and LA-B2 in Fig. 2-14c). Therefore, DMS was a precursor for COS but at a lower extent than cysteine, indicating that thioethers form less COS and CS_2 than thiols. Previously, COS formation was also lower by $0.3\times$ with DMS than cysteine in two different natural waters ($[\text{cysteine or DMS}]_0 = 10 \mu\text{M}$).¹⁸ CS_2 was also lower with DMS for all three waters in the dark as well as during diurnal cycling since it did not form above the DL. Similar to cysteine, DMS also degraded rapidly by $\sim 50\%$ within 4 h (Fig. 2-13), which indicated that other dominant pathways (e.g. DMSO formation)^{34,35} controlled its loss rather than those associated with COS and CS_2 .

2.4.2 Effect of temperature

Temperature was also varied from 5 and 30 °C following diurnal cycling (cysteine- (Fig. 2-13) and DMS- spiked (Fig. 2-15) LA-B1 water) where different trends between COS and CS_2 formation were observed. For example, COS concentrations were greatest at 20°C whereas CS_2 concentrations were greatest at 30°C. This temperature effect was true for both dark and diurnal cycling conditions with cysteine (Fig. 2-13) and DMS (Fig. 2-15) (exceptions included cases where there was no formation above the DL). More specifically, COS formation with cysteine following diurnal cycling was greater at 20°C than 5 and

30°C by 1.4-1.9 \times within all three phases (Fig. 2-13e). Within phases I and III, it is possible that the temperature incurred this pattern due to its dual effect on increasing COS formation with higher

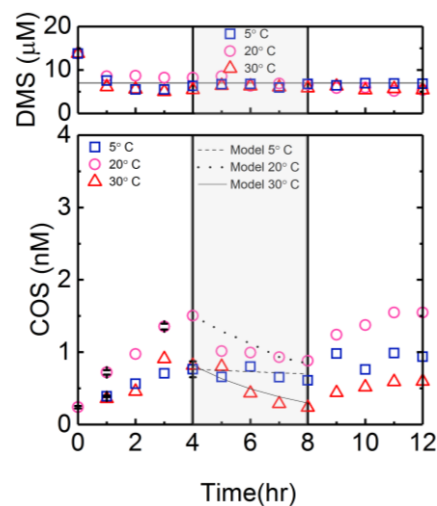


Figure 2-15. The effect of temperature on COS and CS_2 photoproduction for the LA-B1 water spiked with DMS ($[\text{DMS}]_0 = 14 \mu\text{M}$, pH: LA-B1: 8.1).

temperatures (in parallel, cysteine also decreased faster with greater temperature (Fig. 2-13e)), but also increasing COS hydrolysis with higher temperatures^{28,36-38}. In fact, both the hydrolysis and base-catalyzed hydrolysis rate constants for COS^{28,36,38} and CS₂²⁹ are well established in literature. Thus for COS, the hydrolysis and base-catalyzed hydrolysis rate constants over this temperature range were assessed based on the reaction rate constants and activation energies provided in Section 2.3.5. The hydrolysis rate constants with H₂O increased from 1.48×10^{-6} , 2.23×10^{-5} , and 4.75×10^{-5} (s⁻¹), and the pseudo first-order hydrolysis rate constants with OH⁻ at pH 8.1 (pH of most natural waters) increased from 4.26×10^{-6} , 1.66×10^{-5} , and 3.4×10^{-5} (s⁻¹) when temperatures increased from 5, 20, and 30 °C, respectively. So, the highest COS levels formed at 20°C potentially because these two effects were balanced. Alternatively, at 5°C, the lowered COS formation rate appeared to outcompete the lowered hydrolysis rate while at 30°C an elevated hydrolysis rate appeared to outcompete the formation rate (Fig. 2-13e). The situation differed in phase II because hydrolysis only played a role, where modeling results matched the experimental data for all three temperatures (Fig. 2-13e). Varying temperatures incurred similar effects with DMS (Fig. 2-15).

Interestingly, temperature exhibited different results with CS₂ where its formation with cysteine increased with increasing temperature (maximum observed at 30°C), under both dark and diurnal cycling conditions, since hydrolysis was not a factor (Fig. 2-13f). This was further confirmed by modeling CS₂ hydrolysis at 5, 20, and 30°C (see Section. 2.3.5. for modeling details) which did not affect CS₂ loss. However, the extent of CS₂ formation varied after each diurnal cycling phase and is hypothesized to lead to two important points. First, the data between 30 and 20°C began to converge in phase III (Fig. 2-13f). This trend seemed to indicate that at 30°C, CS₂ formation began to reach a maximum level where all available precursors were consumed due to

high formation rates. Within phase II, the CS₂ concentrations at 5 and especially 30°C also increased (Fig. 2-13f), again seeming to indicate that light was only needed in phase I to trigger CS₂ formation.

2.5 Conclusions

The aim of this study was to investigate how the presence of sunlight, simulated diurnal cycling (light-dark-light) and temperature affected the formation of COS and CS₂ in natural waters. These effects were assessed with three different natural waters ranging from freshwater to seawater. The results indicated that COS and CS₂ formation increased up to 11× and 4× with cysteine, respectively, after 12 h of sunlight while diurnal cycling exhibited varied effects. Also, COS and CS₂ formed at lower degree with DMS than cysteine. During diurnal cycling, COS formation followed an interesting trend where its concentration increased, decreased, and then increased during phase I (light), II (dark), and III (light), respectively. The kinetics of COS and CS₂ formation were found to be substantially different during phase II (dark), where COS formation dramatically decreased while CS₂ formation kept increasing. This difference was attributed to the strong effect of hydrolysis on COS loss in the dark which outcompeted its dark formation. However, the effect of hydrolysis on the loss of CS₂ in the dark was negligible.

Additionally, COS and CS₂ formation were highly influenced by temperature. Specifically, the COS formation with cysteine following diurnal cycling was greater at 20°C than 5 and 30°C by 1.4-1.9× within all three phases. Interestingly, temperature exhibited different results with CS₂ where its formation with cysteine increased with increasing temperature. This difference can be attributed to the dual role of temperature which simultaneously affected the rates of COS formation and hydrolysis. It is noteworthy that the CS₂ hydrolysis was not affected by temperature.

2.6 References

- (1) Xie, H.; Moore, R. M.; Miller, W. L. Photochemical Production of Carbon Disulphide in Seawater. *J. Geophys. Res. Ocean.* **1998**, *103* (C3), 5635–5644.
- (2) Cutter, G. A.; Cutter, L. S.; Filippino, K. C. Sources and Cycling of Carbonyl Sulfide in the Sargasso Sea. *Limnol. Oceanogr.* **2004**, *49* (2), 555–565.
- (3) Flöck, O. R.; Andreae, M. O.; Dräger, M. Environmentally Relevant Precursors of Carbonyl Sulfide in Aquatic Systems. *Mar. Chem.* **1997**, *59* (1–2), 71–85.
- (4) Flöck, O. R.; Andreae, M. O. Photochemical and Non-Photochemical Formation and Destruction of Carbonyl Sulfide and Methyl Mercaptan in Ocean Waters. *Mar. Chem.* **1996**, *54* (1), 11–26.
- (5) Andreae, M.; Ferek, R. J. Photochemical Production of Carbonyl Sulfide in Sea Water and Its Emission to the Atmosphere. *Global Biogeochem. Cycles* **1992**, *6*, 175–183.
- (6) National Oceanic and Atmospheric Administration, the temperature of ocean water varies by location – both in terms of latitude and from top to bottom, due to variations in solar radiation and the physical properties of water. <https://oceanexplorer.noaa.gov/facts/temp-vary.html> (accessed Mar 9, 2019).
- (7) McNeill, K.; Canonica, S. Triplet State Dissolved Organic Matter in Aquatic Photochemistry: Reaction Mechanisms, Substrate Scope, and Photophysical Properties. *Environ. Sci. Process. Impacts* **2016**, *18* (11), 1381–1399.
- (8) Parker, K. M.; Pignatello, J. J.; Mitch, W. A. Influence of Ionic Strength on Triplet-State Natural Organic Matter Loss by Energy Transfer and Electron Transfer Pathways. *Environ. Sci. Technol.* **2013**, *47* (19), 10987–10994.
- (9) Wright, J.; Hooman, S.; L., C. L. Stability of Carbon-centered Radicals: Effect of Functional Groups on the Energetics of Addition of Molecular Oxygen. *J. Comput. Chem.* **2008**, *30* (7), 1016–1026.
- (10) Marchaj, A.; Kelley, D. G.; Bakac, A.; Espenson, J. H. Kinetics of the Reactions between Alkyl Radicals and Molecular Oxygen in Aqueous Solution. *J. Phys. Chem.* **1991**, *95* (11), 4440–4441.
- (11) Du, Q.; Mu, Y.; Zhang, C.; Liu, J.; Zhang, Y.; Liu, C. Photochemical Production of Carbonyl Sulfide, Carbon Disulfide and Dimethyl Sulfide in a Lake Water. *J. Environ. Sci.* **2016**, *51* (September), 1–11.

- (12) Chu, C.; Erickson, P. R.; Lundeen, R. A.; Stamatelatos, D.; Alaimo, P. J.; Latch, D. E.; McNeill, K. Photochemical and Nonphotochemical Transformations of Cysteine with Dissolved Organic Matter. *Environ. Sci. Technol.* **2016**, *50* (12), 6363–6373.
- (13) *Standard Operating Procedure (SERC-007) Determination of Total Organic Carbon In Water Samples*; Southeast Environmental Research Center-Nutrient Analysis Laboratory OE-148, Florida International University, Miami, 2016.
- (14) Osburn, C. L.; St-Jean, G. The Use of Wet Chemical Oxidation with High-Amplification Isotope Ratio Mass Spectrometry (WCO-IRMS) to Measure Stable Isotope Values of Dissolved Organic Carbon in Seawater. *Limnol. Oceanogr. Methods* **2007**, *5* (10), 296–308.
- (15) Ferek, R.; Andreae, M. Photochemical Production of Carbonyl Sulphide in Marine Surface Waters. *Nature* **1984**, *370*, 148–150.
- (16) NASA solar simulator <http://pics-about-space.com/nasa-solar-simulator?p=1#img76125632372949276> (accessed Jan 1, 2016).
- (17) Schwarzenbach, R. P.; Gschwend, Philip M. Imboden, D. M. *Environmental Organic Chemistry, 3rd Edition*; Wiley: New Jersey, 2017.
- (18) Zepp, R. G.; Andreae, M. O. Factors Affecting the Photochemical Production of Carbonyl Sulfide in Seawater. *Geophys. Res. Lett.* **1994**, *21* (25), 2813–2816.
- (19) Willett, K. L.; Hites, R. A. Chemical Actinometry: Using o-Nitrobenzaldehyde to Measure Lamp Intensity in Photochemical Experiments. *J. Chem. Educ.* **2000**, *77* (7), 900–902.
- (20) American Society for Testing and Materials (ASTM) Terrestrial Reference Spectra for Photovoltaic Performance Evaluation <http://rredc.nrel.gov/solar/spectra/am1.5/> (accessed Aug 15, 2015) (accessed Jan 1, 2015).
- (21) Galbavy, E. S.; Ram, K.; Anastasio, C. 2-Nitrobenzaldehyde as a Chemical Actinometer for Solution and Ice Photochemistry. *J. Photochem. Photobiol. A Chem.* **2010**, *209* (2–3), 186–192.
- (22) Zepp, R. G. Quantum Yields for Reaction of Pollutants in Dilute Aqueous Solution. *Environ. Sci. Technol.* **1978**, *12* (3), 327–329.
- (23) Nielsen, A. T.; Jonsson, S. Trace Determination of Volatile Sulfur Compounds by Solid-Phase Microextraction and GC-MS. *Analyst* **2002**, *127* (8), 1045–1049.

- (24) Sander, R, Henry's Law data, NIST Chemistry WebBook, NIST Standard Reference Database Number 69, National Institute of Standards and Technology, (retrieved October 15, 2017). Henry's Law data.
- (25) CWA Methods Team. *Definition and Procedure for the Determination of the Method Detection Limit, Revision 2*; U.S. Environmental Protection Agency, Washington, DC, 2016.
- (26) Rijstenbil, J. .; Wijnholds, J. . HPLC Analysis of Nonprotein Thiols in Planktonic Diatoms : Pool Size, Redox State and Response to Copper and Cadmium Exposure. *Mar. Biol.* **1996**, *127* (1), 45–54.
- (27) Ianni, J. . in Kintecus, Windows Version 5.2, (<http://www.kintecus.com>).
- (28) Elliott, S.; Lu, E.; Rowland, F. S. Rates and Mechanisms for the Hydrolysis of Carbonyl Sulfide in Natural Waters. *Environ. Sci. Technol.* **1989**, *23* (4), 458–461.
- (29) Elliott, S. Effect of Hydrogen Peroxide on the Alkaline Hydrolysis of Carbon Disulfide. *Environ. Sci. Technol.* **1990**, *24* (2), 264–267.
- (30) Mopper, K.; Kieber, D.; Stubbins, A. Chapter 8 - Marine Photochemistry of Organic Matter: Processes and Impacts. In *Biogeochemistry of Marine Dissolved Organic Matter (Second Edition)*; Academic Press: Burlington, 2015; pp 389–450.
- (31) Pos, W. H.; Riemer, D. D.; Zika, R. G. Carbonyl Sulfide (OCS) and Carbon Monoxide (CO) in Natural Waters: Evidence of a Coupled Production Pathway. *Mar. Chem.* **1998**, *62* (1–2), 89–101.
- (32) Berry, J.; Wolf, A.; Campbell, J. E.; Baker, I.; Blake, N.; Blake, D.; Denning, a. S.; Kawa, S. R.; Montzka, S. a.; Seibt, U.; et al. A Coupled Model of the Global Cycles of Carbonyl Sulfide and CO₂: A Possible New Window on the Carbon Cycle. *J. Geophys. Res. Biogeosciences* **2013**, *118* (2), 842–852.
- (33) Lennartz, S. T.; Marandino, C. A.; von Hobe, M.; Cortes, P.; Quack, B.; Simo, R.; Booge, D.; Pozzer, A.; Steinhoff, T.; Arevalo-Martinez, D. L.; et al. Direct Oceanic Emissions Unlikely to Account for the Missing Source of Atmospheric Carbonyl Sulfide. *Atmos. Chem. Phys.* **2017**, *17* (1), 385–402.
- (34) Brimblecombe, P.; Shooter, D. Photo-Oxidation of Dimethylsulphide in Aqueous Solution. *Mar. Chem.* **1986**, *19* (4), 343–353.

- (35) Bouillon, R.-C.; Miller, W. L. Photodegradation of Dimethyl Sulfide (DMS) in Natural Waters: Laboratory Assessment of the Nitrate-Photolysis-Induced DMS Oxidation. *Environ. Sci. Technol.* **2005**, *39* (24), 9471–9477.
- (36) Guo, H.; Tang, L.; Li, K.; Ning, P.; Sun, X.; Liu, G.; Bao, S.; Zhu, T.; Jin, X.; Duan, Z.; et al. The Hydrolysis Mechanism and Kinetic Analysis for COS Hydrolysis: A DFT Study. *Russ. J. Phys. Chem. B* **2016**, *10* (3), 427–434.
- (37) Andersen, W. C.; Bruno, T. J. Kinetics of Carbonyl Sulfide Hydrolysis. 1. Catalyzed and Uncatalyzed Reactions in Mixtures of Water + Propane. *Ind. Eng. Chem. Res.* **2003**, *42* (5), 963–970.
- (38) Zhao, S.; Yi, H.; Tang, X.; Jiang, S.; Gao, F.; Zhang, B.; Zuo, Y.; Wang, Z. The Hydrolysis of Carbonyl Sulfide at Low Temperature: A Review. *Sci. World J.* **2013**, 2013.

CHAPTER 3. **ROLE OF ORGANIC SULFUR PRECURSORS AND WATER QUALITY CONSTITUENTS ON PHOTOCHEMICAL FORMATION OF COS AND CS₂**

A version of this chapter has been previously published in Environmental Science and Technology Journal.

Modiri Gharehveran, M.; Shah, A. D. Indirect Photochemical Formation of Carbonyl Sulfide and Carbon Disulfide in Natural Waters: Role of Organic Sulfur Precursors, Water Quality Constituents, and Temperature. *Environ. Sci. Technol.* **2018**, 52 (16), 9108–9117.

DOI: 10.1021/acs.est.8b01618

3.1 Abstract

This chapter evaluated how different organic sulfur precursors and water quality constituents, which can form important reactive intermediates (RIs) affected COS and CS₂ formation. Nine natural waters ranging in salinity were spiked with cysteine, cystine, dimethylsulfide (DMS) or methionine and exposed to simulated sunlight over 4 h under varied water quality conditions. COS and CS₂ formation were strongly affected by the DOC concentration, organic sulfur precursor type, and O₂ concentration while salinity differences and CO addition did not play a significant role.

3.2 Introduction

This chapter evaluated the role of different organic sulfur precursors and water quality constituents on forming COS and CS₂ in the presence of sunlight. Nine natural waters ranging from freshwater to seawater were evaluated. Selected waters were spiked with 14μM cysteine (thiol), cystine (a disulfide formed via thiol oxidation by O₂, ¹O₂, •OH¹), DMS (thioether), or methionine (thioether) and were also varied in dissolved O₂, Cl⁻, and CO concentrations at a fixed sunlight exposure dose. Overall, this study helped identify the key factors and reaction mechanisms

involved in generating COS and CS₂ in natural waters with sunlight, which may ultimately control the concentrations emitted into the atmosphere.

3.3 Material and Methods

3.3.1 Description of standards, reagents, and stock preparation

The standards, reagents and stocks used were identical to those in chapter 2. In addition, cystine and methionine were purchased at $\geq 97\%$ purity from Sigma Aldrich. Suwannee River Fulvic Acid (SRFA) was purchased from the International Humic Substances Society (IHSS). The SRFA stock solution was prepared by adding 4.5 mg SRFA to 10 ml of purified water. The final stock concentration was 237 mg-C/L based on the elemental percentage of C reported by IHSS. CO was purchased as calibration gas standards at 10 ppm (mol/mol) in N₂ from Gasco. CO stock solutions were prepared by first creating a CO stock in the gas phase (8%_{vol} CO). Synthetic water (2 mL) was then injected into this gas phase, which was left overnight at 4°C to create a liquid stock.

3.3.2 Natural water samples

The natural waters used for this study were identical to those in chapter 2.

3.3.3 Experimental procedure

Characterization of photochemical reactors, the sunlight intensity measurement and pathlength determination

A solar simulator (OAI Tri-Sol; AM 1.5G filter), identical to the one used in chapter 2, was used to simulate collimated sunlight. The reactors contained various types of synthetic solutions with no headspace and were placed below the sunlight beam under constant mixing and temperature conditions (20±1°C). The reactors used in these experiments was identical to those described in chapter 2. The sunlight intensity from the solar simulator (OAI Tri-Sol) and the average path length were measured similar to the conditions described in chapter 2.

Single exposure dose experiments

Experiments were performed at one exposure dose of 4 h at 20°C following a procedure similar to the kinetic experiments in chapter 2, except for the following changes which evaluated the effect of: (i) organic sulfur precursor type where cysteine, cystine, DMS, or methionine (all at 14 μM) were spiked into the LA-B1 water, (ii) water type where all nine waters were spiked with cysteine or DMS, (iii) dissolved O_2 , by irradiating a LA-B1 water that was either purged with N_2 for 10 min or left as is where the $[\text{O}_2]_0 \approx 8.9 \text{ mg/L}$ at 20°C since these waters were left in equilibrium with the atmosphere during storage, and (iv) Cl^- , by varying its concentration for two cysteine-spiked waters (FL-F and LA-F) from 5- 35 ppt (g/L) (FL-F) and 8-35 ppt (LA-F), where NaClO_4 was used as an ionic strength (IS) control, and (v) CO, which was varied from 6.9-20.9 μM in cysteine-spiked LA-B1 water or synthetic water ($[\text{DOC}]_0 = 2.9 \text{ mg/L-C SRFA}$ ((equaling the $[\text{DOC}]_0$ of the LA-B1 water (Table 2-1)) and pH 8 (phosphate buffer)).

3.3.4 Analytical methods

COS, CS_2 , DMS, cysteine, methionine, and CO were analyzed as described in Chapter 2.

3.4 Results and Discussion

3.4.1 Comparison between water types

COS and CS_2 formation from the nine waters tested varied slightly in the dark but varied more widely in the presence of light, especially when cysteine and DMS were added (Fig. 3-1). For example, in the dark, all of the waters did not form COS above the DL when not spiked or spiked with DMS (Fig. 3-1c), while the waters spiked with cysteine formed between 0.3 to 1 nM (0.7 nM differential) (Fig. 3-1a). Upon irradiation, COS formation widened further between 0.2 to 3.4 nM (3.2 nM differential) (Fig. 3-1a). Upon irradiation, COS formation widened further between 0.2 to 3.4 nM (3.2 nM differential) when not spiked while generating 2.5 to 8.5 nM (6.0 nM differential) with

cysteine (Fig. 3-1a) and 1.5 to 5.2 nM (3.7 nM differential) with DMS (Fig. 3-1c). This general pattern was similarly repeated for CS₂ (Fig. 3-1). Overall, these findings indicated that the wider range of COS and CS₂ formed with light were due to the varied photosensitizers present in these different waters, which were driven by photochemical processes rather than dark ones. This conclusion was made by assuming that the COS and CS₂ levels formed from the dark-based reactions occurred to the same degree during irradiation. This assumption seems especially valid when cysteine and DMS were present, since the system was not limited by organic sulfur precursor content.

To then better evaluate the identity of these reactants, COS and CS₂ formation were plotted against different water quality parameters to investigate how they correlated with each other. The water quality parameters included the initial DOC concentration (Fig. 3-1), UV₃₆₀ (Fig. 3-2 and 3-3), salinity (measured as Cl⁻) (Fig. 3-1) and the total carbonate concentration (Fig. 3-2 and 3-3). In the end, the DOC concentration and UV₃₆₀ (the UV₃₆₀ value serves as a surrogate for the CDOM content while UV₂₅₄ can estimate the degree of aromaticity in CDOM²) were the only water quality parameters that correlated with COS and CS₂. These effects were especially striking for COS formation with cysteine and DMS and CS₂ formation with DMS which increased fairly consistently with increasing DOC (Fig. 3-1). COS formation also incurred similar trends with increasing UV₃₆₀, although the MA-S water was as an outlier (Fig. 3-2 and 3-3). These findings suggested that COS, and to a lesser extent CS₂, increased in formation due to the: (i) inherent DOS concentration (factor 1), (ii) CDOM-based moieties that are responsible for forming key RIs (e.g. ³DOM*³ and •OH^{4,5}) (factor 2), as suggested previously for forming COS and CS₂,⁶ and/or (iii) for COS, functional groups (e.g. carbonyl (-C=O)) that may react with the reduced sulfur compounds to form COS (factor 3), as suggested previously,⁶⁻⁸ since O₂ is not likely involved (see

later results). The importance and weight of each of these factors remains unknown. However, factors 2 and/or 3 (for COS only) do appear to play a significant role given that the gap in COS and CS₂ formation between these waters increased when moving from the irradiated non-spiked waters to the cysteine- and DMS-spiked waters (Fig. 3-1). Thus, by adding cysteine and DMS, the role of organic sulfur precursors became less limiting, suggesting that the presence of other reactants, e.g. formed through factors 2 or 3, controlled formation instead.

Moreover, no correlations were observed against salinity (as observed previously for COS⁸) (Fig. 3-4) and the carbonate concentration (Fig. 3-2 and 3-3). The results of these correlations do not necessarily mean that the halide or carbonate species did not affect COS or CS₂ by either quenching key RIs (e.g. •OH),^{1,10,11} forming RIs (e.g. RHS species or CO₃^{•-}),¹¹ or incurring other effects (e.g. ionic strength¹² or heavy atom effects¹³). Rather, it indicated that these variables did not appear to outcompete other factors and control formation.

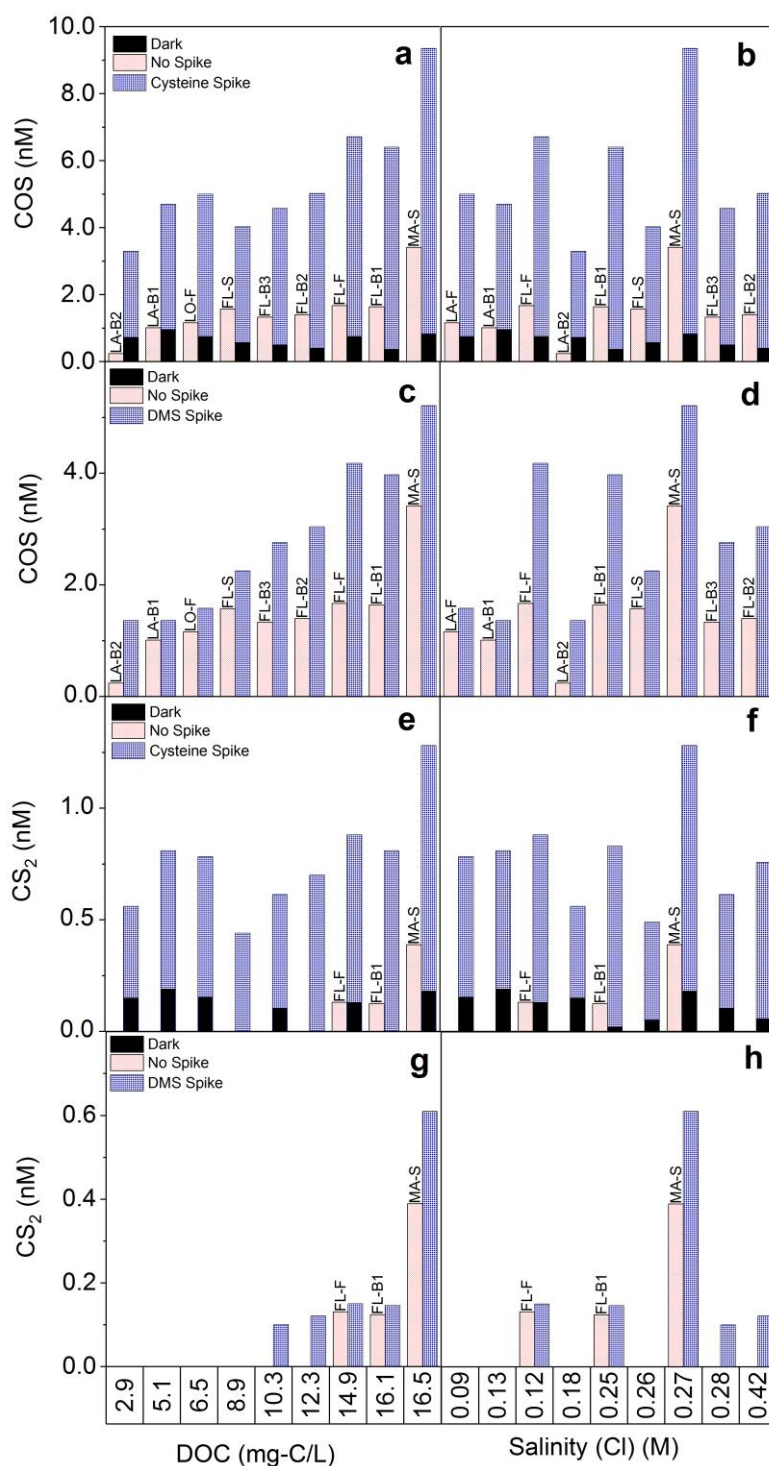


Figure 3-1. The effect of different water types on COS and CS₂ photoproduction for (a,c,e,g) based on DOC values and (b,d,f,h) based on [Cl] values when waters spiked or not spiked with cysteine or DMS ([cysteine or DMS]₀ = 14 μM, temperature: 20±1°C, pH: FL-F: 7.8, FL-B1: 8.0, FL-B2: 8.0, FL-B3: 7.9, FL-S: 8.0, LA-F: 8.0, LA-B1: 8.1, LA-B2: 8.17, MA-S: 7.8).

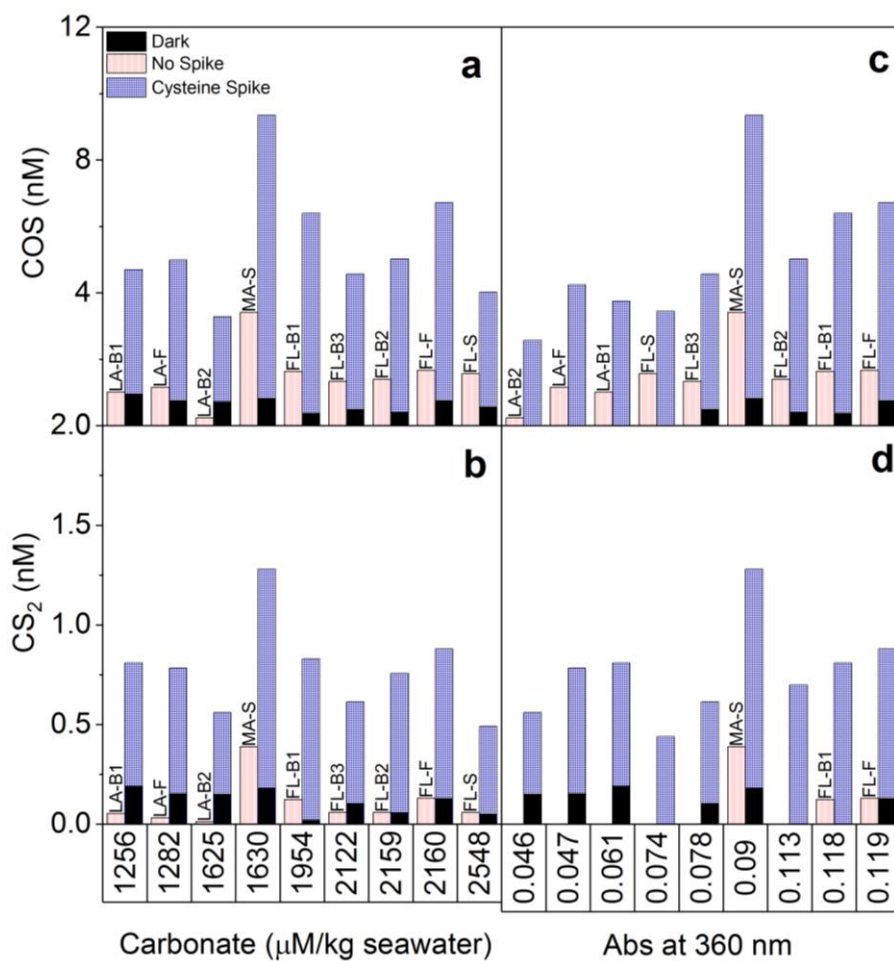


Figure 3-2. The effect of different water types on COS and CS₂ photoproduction for (a,b) based on carbonate values and (c,d) based on absorbance at 360 nm values when waters spiked or not spiked with cysteine ([cysteine]₀ = 14 µM, temperature: 20±1 °C, pH: FL-F: 7.8, FL-B1: 8.0, FL-B2: 8.0, FL-B3: 7.9, FL-S: 8.0, LA-F: 8.0, LA-B1: 8.1, LA-B2: 8.17, MA-S: 7.8).

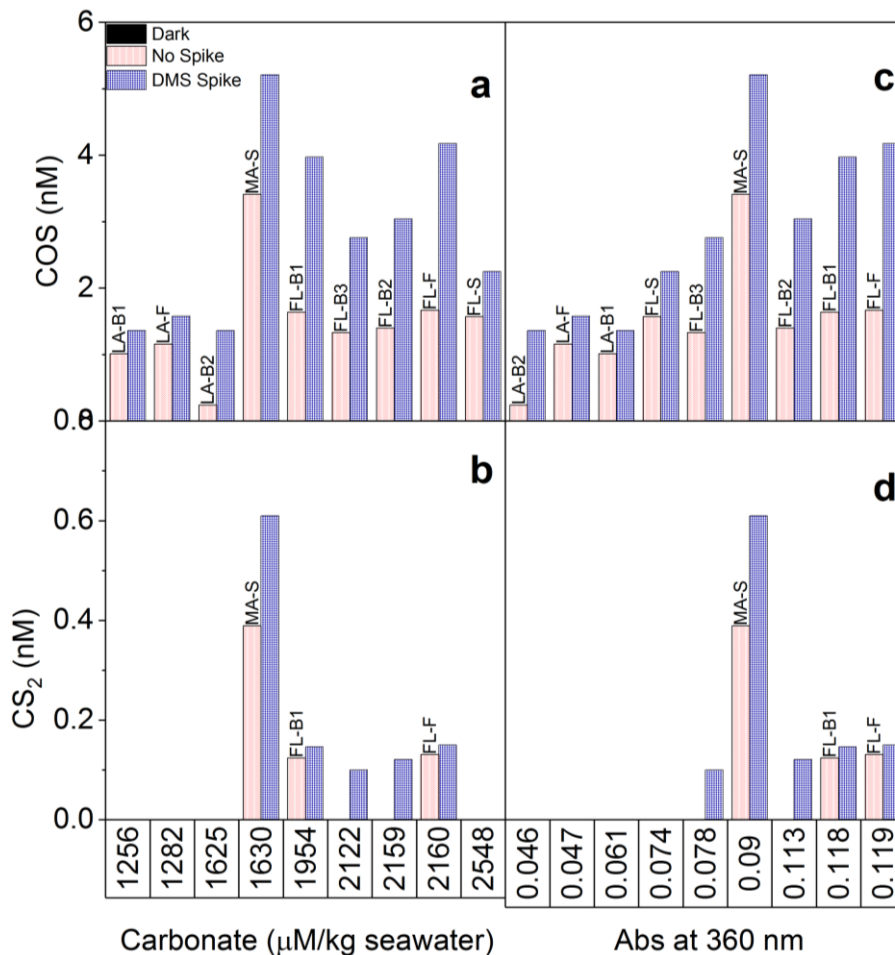


Figure 3-3. The effect of different water types on COS and CS₂ photoproduction for (a,b) based on carbonate values and (c,d) based on absorbance at 360 nm values when waters spiked or not spiked with DMS ([DMS]₀ = 14 μM, temperature: 20±1 °C, pH: FL-F: 7.8, FL-B1: 8.0, FL-B2: 8.0, FL-B3: 7.9, FL-S: 8.0, LA-F: 8.0, LA-B1: 8.1, La-B2: 8.17, MA-S: 7.8).

3.4.2 Effect of salinity

Further attempts to elucidate the role of salinity were carried out under a more controlled water matrix regime where cysteine-spiked low salinity LA-F and FL-F waters were amended with NaCl or NaClO₄ (Fig. 3-4). In general, an increase in either NaCl or NaClO₄ led to either no change or no consistent change in COS and CS₂ formation trends in these waters (Fig. 3-4), suggesting again that NaCl does not control COS and CS₂ formation. It should also be noted that testing the effect of bromide, which could also produce RHS species (e.g. Br[•] and Br₂^{•-}),^{1,10,11} was not possible due

to analytical limitations, since bromide cannot be accurately measured by the IC in high chloride-containing natural waters.¹⁴

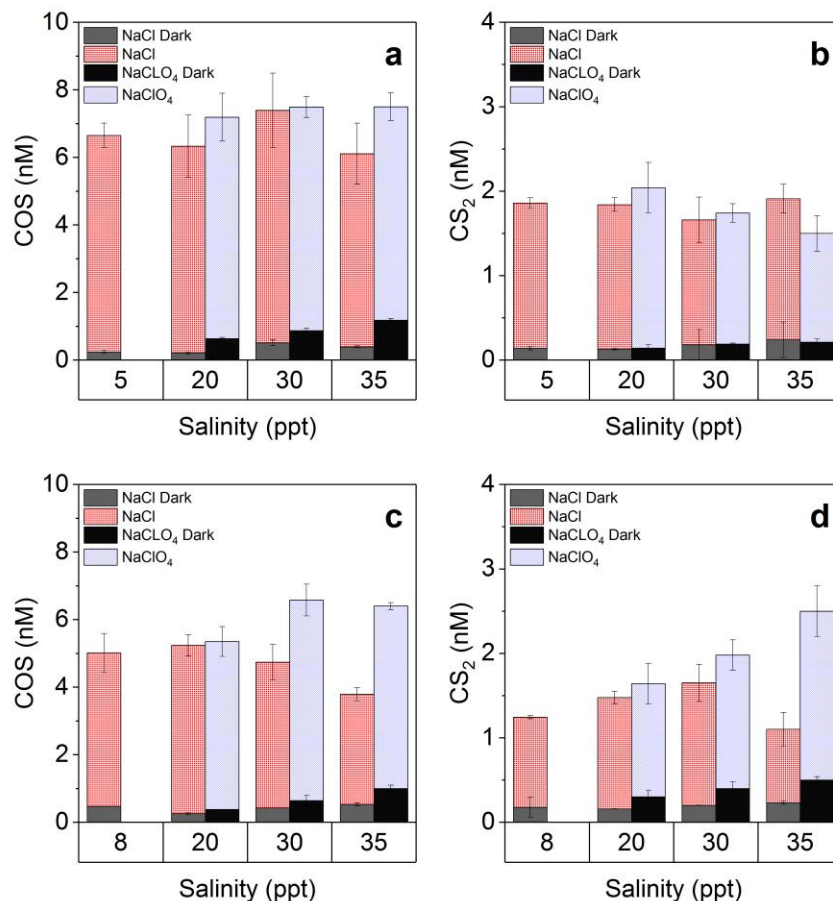


Figure 3-4. The effect of chloride on COS and CS₂ photoproduction for (a,b) the FL-F water and (c,d) the LA-F water spiked with cysteine ([cysteine]₀ = 14 μM, temperature: 20±1 °C, pH: LA-B1: 8.1, FL-F: 7.8). The error bars represent the standard errors for three replicates.

3.4.3 Role of organic sulfur precursor

Along with cysteine and DMS, methionine and cystine were spiked into the LA-B1 water (Fig. 3-5). For COS, the results indicated that the type of precursor added affected formation under both dark and light conditions. In the dark, only cysteine and cystine formed COS at > DL concentrations (Fig. 3-5a) (a previous study also observed no COS formation with methionine⁷).

With light, COS decreased in formation according the following order where cysteine (3.9 nM) > cystine (1.8 nM) > DMS (1.5 nM) > methionine (0.92 nM) (Fig. 3-5a). This trend was not solely due to the dark controls since the dark values were then subtracted from the light-generated COS, where the net formation again following the order of where cysteine (2.4 nM) > cystine (1.6 nM) > DMS (1.5 nM) > methionine (0.92 nM) (Fig. 3-5a). Two studies also found that cysteine > methionine by 2.8-3:1 (cysteine: methionine) when forming COS^{6,11}. Alternatively, CS₂ formation, while similarly matching COS in terms of its dark formation (only cysteine led to > DL concentrations (Fig. 3-5b)), behaved differently with different precursors with light (Fig. 3-5b). In this case, CS₂ decreased in formation where cysteine (0.62 nM) > cystine (0.4 nM) > methionine (0.23 nM) > DMS (< DL) (Fig. 3-5b) but this order slightly changed for net formation where cystine (0.38 nM) > cysteine (0.32 nM) > DMS (0.17 nM) > methionine (< DL) (Fig. 3-5b). Other studies observed that CS₂: (i) qualitatively formed from cysteine¹⁵, (ii) did not form¹⁵ or formed at 1-4 nM with methionine⁶, or (iii) decreased according to cysteine > methionine⁶. In parallel, no methionine decay was observed over time, unlike cysteine and DMS (Fig. 3-5).

Overall, these trends indicated that organic sulfur precursor type impacted COS and CS₂ formation, but their sequences for net formation were not identical (thiols > disulfides > thioethers for COS and disulfides > thiols > thioethers for CS₂). In both cases, the thiol (cysteine) consistently generated greater levels of COS and CS₂ than the thioethers (DMS and methionine), but the disulfide (cystine) formed higher levels of CS₂ than the other precursors. Different functional groups adjacent to the sulfur atom thus appear to alter COS and CS₂ formation. These functional groups are not directly linked to S oxidation number since the sulfur oxidation states for COS and CS₂ are -2 which is the same for cysteine, methionine, and DMS and in fact lower than cystine

(sulfur oxidation state of -1).¹⁵ Instead, these patterns are controlled by a more complex set of reaction mechanisms (see later sections).

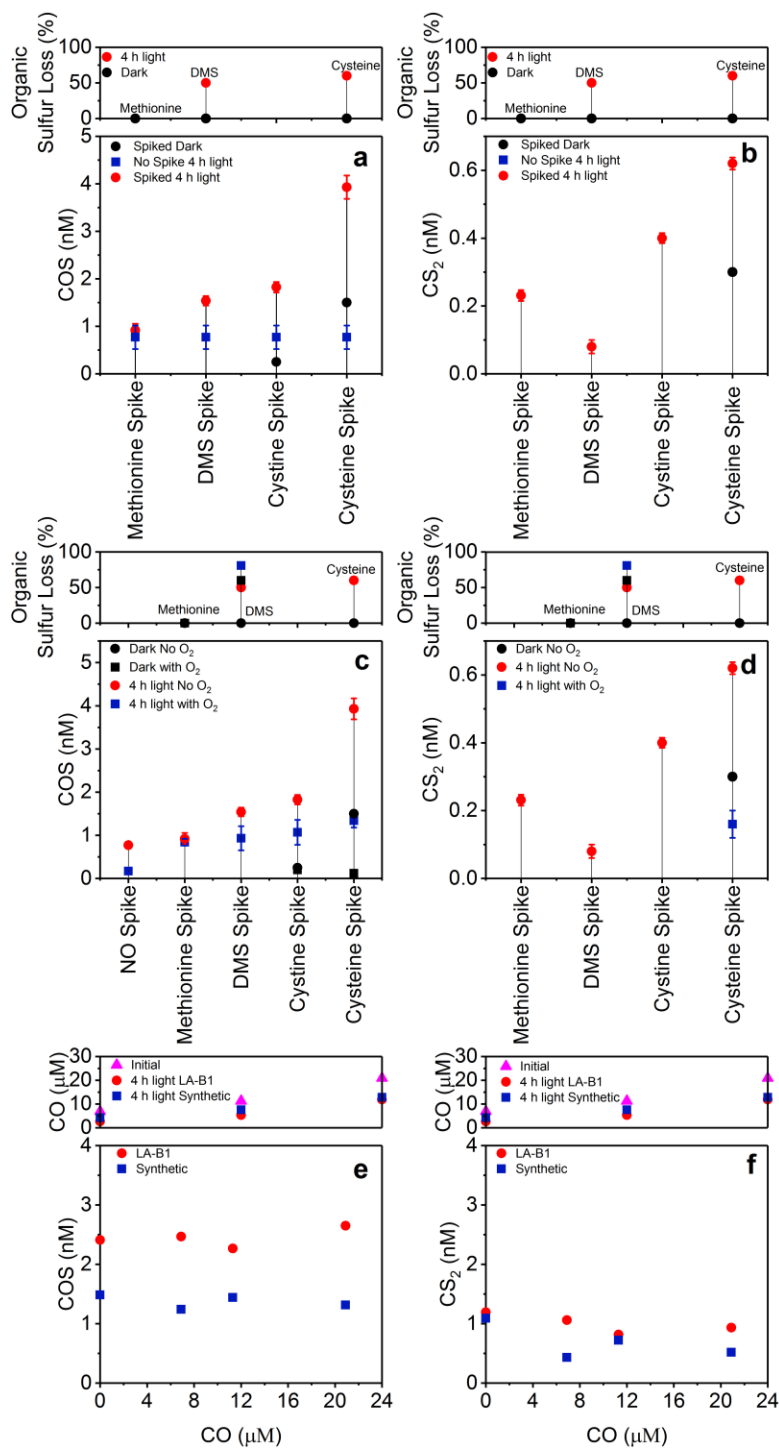


Figure 3-5. COS and CS₂ formation when exposed to (a,b) different organic sulfur precursors ($[\text{cysteine}]_0 = [\text{cystine}]_0 = [\text{DMS}]_0 = [\text{methionine}]_0 = 14 \mu\text{M}$) with the LA-B1 water, (c,d) when amended with O₂ for the LA-B1 water, and (e,f) when amended with CO for the LA-B1 and synthetic water (temperature: $20 \pm 1 \text{ }^\circ\text{C}$, pH of LA-B1 = 8.1, pH of synthetic water = 8.15), $[\text{CO}]_0 = 6.9 \mu\text{M}$, $[\text{CO}]_0 = 11.3 \mu\text{M}$, $[\text{CO}]_0 = 20.9 \mu\text{M}$. The error bars represent the standard errors for three replicates.

3.4.4 Role of O₂

The presence of O₂ ([O₂]₀ ≈ 8.9 mg/L at 20°C) inhibited COS and CS₂ formation under both dark and light conditions in the no spike and cysteine-, DMS-, methionine-, and cysteine- spiked LA-B1 water (Fig. 3-5). This effect was especially dramatic with light where the presence of O₂ decreased COS by 0.2× with no precursor added but decreased by 0.3, 0.6, 0.6, and 0.9× with cysteine, cystine, DMS, or methionine, respectively (Fig. 3-5c). For methionine, the decrease observed with O₂ was considerably lower than that observed without the precursor (Fig. 3-5c). This result indicated that O₂ quenched methionine or the intermediates generated from it to some extent, although this likely occurred to a small degree since no observable % methionine loss occurred with O₂ (Fig. 3-5c). Previously, studies found that O₂ either decreased^{6,11} or increased COS formation,⁹ but they used a 254 nm light source^{6,9}. O₂ also decreased CS₂ levels to < DL, < DL, and by 0.25× for cysteine, cystine, or methionine, respectively (Fig. 3-5d), as observed previously (CS₂ decreased by 0.13× with O₂ in a no-spike natural water)⁶. Overall, O₂ is believed to deter COS and CS₂ formation by directly reacting with the organic sulfur precursor to form various oxidized by-products instead⁶ and by potentially quenching potential key RIs such as ³DOM*,⁵ and carbon-centered radicals¹⁷ as well as sulfur-centered radicals⁶. This former effect also matched the organic sulfur precursor loss where cysteine and DMS decayed to a greater extent by > 60% and 80%, respectively, with O₂ (Fig. 3-5c) than without O₂. Thus, O₂ does not appear to be directly involved in forming the COS and CS₂, but more likely appears to be indirectly involved by quenching the various reactants involved in their formation. For COS, this is opposite to a previously proposed mechanism, although no direct experimental evidence was provided in this case to support it.⁶

3.4.5 Role of CO

COS and CS₂ concentrations remained relatively unchanged and exhibited no trend when amending CO to the cysteine-spiked LA-B1 or cysteine-spiked synthetic water (Fig. 3-5). These results were expected for CS₂ since no oxygen is needed but less expected for COS, which was proposed to form when thiols react with CO.⁸ Interestingly, a former study did find that the CO concentration simultaneously decreased with increasing COS formation in a cysteine-spiked natural water⁷. However, this study further proposed that this correlation was not due to having CO serve as a reactant for COS, but instead having it serve as a competing product from a common precursor⁷. One precursor tested was acetylacetonate which reacted with bisulfide to form both CO and COS.⁷ Our results further support the claim that CO is not involved in COS formation.

3.4.6 Proposed mechanisms

Based on these results, several photochemical and dark pathways for COS and CS₂ formation have been proposed that depend on the structure of the organic sulfur precursor (Scheme 3-1). The photochemical reactions are: (i) not expected to involve O₂ or CO, (ii) likely involve DOM-based moieties, which are predicted to form key RIs (e.g. ³DOM*) and for COS, contribute oxygen, and (iii) less likely involve halides or carbonate species.

Cysteine: Cysteine is hypothesized to form considerable levels COS and CS₂, as compared to the other precursors, through several steps which involve either the thiol (-SH) or thiolate (R-S⁻) moieties, given that its pK_a of 8.4¹ falls within the pH range of the waters tested (Table 2-1). In fact, the thiolate moiety is expected to be more reactive than the thiol since R-S⁻ is a better nucleophile than SH.¹⁸ Both the thiol and thiolate are then expected to undergo one electron transfer with RIs potentially including ³DOM*, •OH, or ROO•, as observed previously in biological matrices,¹⁸ to form R-S• (Scheme 3-1). Notably, the thiol may also undergo hydrogen

abstraction by the RI, as observed previously with $^3\text{DOM}^*$ and $\bullet\text{OH}$ (Scheme 3-1),^{8,19} and especially in low O_2 environments²⁰ (Scheme 3-1). Hydrogen abstraction has been shown to either form R-S^\bullet or a carbon centered radical ($-\alpha\text{C}^\bullet$) by attacking the S-H or $^\alpha\text{C-H}$ moiety, respectively.^{19,21,22} $^\alpha\text{C}^\bullet$ is predicted to form more readily than R-S^\bullet since the C-H bond exhibits a lower bond dissociation energy than the S-H bond.¹⁹ Although, they can convert back and forth by rearranging via hydrogen transfer (Scheme 3-1).²³ After these radicals are formed, COS is proposed to form through some sequence of: (i) hydrogen abstraction, (ii) disproportionation, which is known to occur in peptides containing cysteine,²¹ and/or (iii) β -cleavage²¹ (Scheme 3-1). Within this sequence, oxygen also becomes bonded to carbon through some unknown steps but which likely include attack by various DOM-derived oxygen based radicals (e.g. $\bullet\text{OH}$, RO^\bullet , ROO^\bullet , and $\text{R-C}^\bullet(\text{O})^7$) (Scheme 3-1).

CS_2 is also likely generated from the $-\alpha\text{C}^\bullet$ or R-S^\bullet radicals but where different steps are required to form a S-C-S linkage and then generate CS_2 . One possibility is that the $-\alpha\text{C}^\bullet$ and/or R-S^\bullet radicals undergo some sequence of reactions involving: (i) reaction with each other to form a S-C bond, as previously proposed,⁶ (ii) hydrogen abstraction, (iii) disproportionation and/or (iv) β -cleavage (Scheme 3-1). A second possibility is that the thioaldehyde ($-\text{C}(\text{S})\text{HR}_1$) moiety, generated via the COS pathway, undergoes nucleophilic attack by another cysteine thiolate moiety (R-S^-), as also observed in multiple cysteine-containing peptide chains²⁴, to form the S-C-S bond. Following this, it becomes less evident how the S-C-S linkage then forms CS_2 . Clearly, several bonds need to be cleaved, but this is not hypothesized to occur by radical pathways induced by RIs since this is not supported by the CS_2 diurnal cycling results. Instead, some long-lasting intermediate is involved (e.g. , R-S^-) (Scheme 3-1), but further research is required to confirm its identity. In addition, it should be noted that CS_2 has been observed to react with $\bullet\text{OH}$ in the aqueous phase to form COS.²⁵

However, the linear formation of CS₂ during diurnal cycling and the fact that CS₂ formation after 12 h light exposure and 12 h of diurnal cycling closely matched each other (Fig. 2-14b) indicated that this was not likely the dominate route for forming COS.

Moreover, in the dark, cysteine is hypothesized to form COS and CS₂ via two possible routes where: (i) R-S• is generated through metal-catalyzed auto-oxidation.²⁶ Trace concentrations of metals are expected in these waters, even though < DL concentrations of Cu, Pb, Hg were measured (Table 2-1) or (ii) through other pathways, since cysteine can react with DOM in the dark.²⁷⁻²⁹

Cystine: Cystine is believed to form COS and CS₂ through two major proposed pathways. The first pathway suggests that its C-S bond can undergo homolytic bond cleavage when reacting with various sensitizers (e.g. n, π* and π, π* type- ³DOM* sensitizers) to form the RSS• intermediate, as similarly observed for other disulfides³⁰. In the second pathway, cystine could react with ³DOM* through a one electron transfer to form the disulfide radical anion, RSSR^{-•}, which is known to readily dissociate and form R-S^{-•}, and R-S•.^{18,22,31} Once R-S^{-•} and R-S• are formed, pathways similar to cysteine would be adopted. Both proposed pathways support the fact that cystine formed greater levels of CS₂ than other precursors, since the two reactive S moieties formed from one cystine molecule would be in close proximity to each other.

DMS and Methionine: The mechanisms driving DMS and methionine to form COS and CS₂ are less clear, although their attached methyl groups and the absence of R-S^{-•} implies that forming R-S• is more difficult. This is especially true if R-S• is formed through homolytic bond cleavage, where DMS and methionine would generate less stable radicals as compared to cysteine³². Alternatively, hydrogen abstraction could occur at the C-H bond adjacent to the sulfur group,²⁰ leading to a carbon centered radical. In addition, methionine has previously been reported to react

with $^3\text{DOM}^*$ to form a sulfur centered radical cation, $\text{R-S}^{\bullet+}$.³³ More detailed investigations are needed to assess how the carbon centered radical \cdot and/or $\text{R-S}^{\bullet+}$ would then form COS or CS₂.

3.5 Conclusions

Since COS and CS₂ formation were found to be enhanced in the presence of sunlight, the aim of this study was to evaluate how different water quality parameters, type of organic sulfur precursors and O₂ affected their indirect photochemical formation with natural waters in the presence of light. These effects were assessed with nine different natural waters ranging from freshwater to seawater. The results indicated the type of natural waters affected COS and CS₂ formation slightly in the dark while this effect was stronger in the presence of light specially when cysteine and DMS were added to solutions. However, among all water quality constituents, the DOC concentration and UV₃₆₀ were the only water quality parameters that correlated with COS and CS₂. In a further attempt, the effect of salinity was also tested by spiking some of the natural waters with NaCl, where the results indicated that the formation of COS and CS₂ were not influenced by salinity. Alternatively, their formation was highly dependent on the type of organic sulfur precursors. Specifically, the net COS formation followed the order of cysteine (2.4 nM) > cystine (1.6 nM) > DMS (1.5 nM) > methionine (0.92 nM), and the net formation of CS₂ followed the order of cystine (0.38 nM) > cysteine (0.32 nM) > DMS (0.17 nM) > methionine (< DL). This implied that, while the type of organic sulfur precursor impacted COS and CS₂ formation, their sequences for net formation were not identical (thiols > disulfides > thioethers for COS and disulfides > thiols > thioethers for CS₂). Additionally, the COS and CS₂ formation were both hampered with O₂ under both dark and light conditions with all organic sulfur precursors tested. For example, the COS formation decreased by 0.3, 0.6, 0.6, and 0.9× with cysteine, cystine, DMS, or methionine, respectively. O₂ also decreased CS₂ levels to < DL, < DL, and by 0.25× for cysteine, cystine, or methionine, respectively. Furthermore, COS and CS₂ formation did not change upon addition of CO to the system, which implied that CO is not involved in COS formation pathways. Lastly, given these results, several photochemical and dark pathways for COS and CS₂ formation

were also proposed for each organic sulfur precursors. These proposed pathways appeared to depend on the structure of the organic sulfur precursors and did not include CO, O₂, halides or carbonate radicals.

3.6 References

- (1) Chu, C.; Erickson, P. R.; Lundeen, R. A.; Stamatelatos, D.; Alaimo, P. J.; Latch, D. E.; McNeill, K. Photochemical and Nonphotochemical Transformations of Cysteine with Dissolved Organic Matter. *Environ. Sci. Technol.* **2016**, *50* (12), 6363–6373.
- (2) Pugach, S. P.; Pipko, I. I.; Shakhova, N. E.; Shirshin, E. A.; Perminova, I. V.; Gustafsson, Ö.; Bondur, V. G.; Ruban, A. S.; Semiletov, I. P. Dissolved Organic Matter and Its Optical Characteristics in the Laptev and East Siberian Seas: Spatial Distribution and Interannual Variability (2003–2011). *Ocean Sci.* **2018**, *14* (1), 87–103.
- (3) Canonica, S. Oxidation of Aquatic Organic Contaminants Induced by Excited Triplet States. *CHIMIA International Journal for Chemistry*. pp 641–644.
- (4) Vione, D.; Minella, M.; Maurino, V.; Minero, C. Indirect Photochemistry in Sunlit Surface Waters: Photoinduced Production of Reactive Transient Species. *Chem. – A Eur. J.* **2014**, *20* (34), 10590–10606.
- (5) McNeill, K.; Canonica, S. Triplet State Dissolved Organic Matter in Aquatic Photochemistry: Reaction Mechanisms, Substrate Scope, and Photophysical Properties. *Environ. Sci. Process. Impacts* **2016**, *18* (11), 1381–1399.
- (6) Du, Q.; Mu, Y.; Zhang, C.; Liu, J.; Zhang, Y.; Liu, C. Photochemical Production of Carbonyl Sulfide, Carbon Disulfide and Dimethyl Sulfide in a Lake Water. *J. Environ. Sci.* **2016**, *51* (September), 1–11.
- (7) Pos, W. H.; Riemer, D. D.; Zika, R. G. Carbonyl Sulfide (OCS) and Carbon Monoxide (CO) in Natural Waters: Evidence of a Coupled Production Pathway. *Mar. Chem.* **1998**, *62* (1–2), 89–101.
- (8) Flöck, O. R.; Andreae, M. O.; Dräger, M. Environmentally Relevant Precursors of Carbonyl Sulfide in Aquatic Systems. *Mar. Chem.* **1997**, *59* (1–2), 71–85.
- (9) Ferek, R.; Andreae, M. Photochemical Production of Carbonyl Sulphide in Marine Surface Waters. *Nature* **1984**, *370*, 148–150.

- (10) Huang, J.; Mabury, S. A. Steady-State Concentrations of Carbonate Radicals in Field Waters. *Environ. Toxicol. Chem.* **2009**, *19* (9), 2181–2188.
- (11) Zepp, R. G.; Andreae, M. O. Factors Affecting the Photochemical Production of Carbonyl Sulfide in Seawater. *Geophys. Res. Lett.* **1994**, *21* (25), 2813–2816.
- (12) Parker, K. M.; Pignatello, J. J.; Mitch, W. A. Influence of Ionic Strength on Triplet-State Natural Organic Matter Loss by Energy Transfer and Electron Transfer Pathways. *Environ. Sci. Technol.* **2013**, *47* (19), 10987–10994.
- (13) Turro, N. J. *Principles of Molecular Photochemistry: An Introduction*; Ramamurthy, V., Scaiano, J. C. (Juan C. ., Eds.; Sausalito, Calif.: University Science Books: Sausalito, Calif., 2009.
- (14) Chen, Z. L.; Megharaj, M.; Naidu, R. Determination of Bromate and Bromide in Seawater by Ion Chromatography, with an Ammonium Salt Solution as Mobile Phase, and Inductively Coupled Plasma Mass Spectrometry. *Chromatographia* **2007**, *65* (1), 115–118.
- (15) Xie, H.; Moore, R. M.; Miller, W. L. Photochemical Production of Carbon Disulphide in Seawater. *J. Geophys. Res. Ocean.* **1998**, *103* (C3), 5635–5644.
- (16) Kennepohl, D.; Farmer, S.; Reusch, W.; Soderberg, T.; Schaller, C. P. Thiols and Sulfides https://chem.libretexts.org/Core/Organic_Chemistry/Thiols_and_Sulfides/Thiols_and_Sulfides#Oxidation_States_of_Sulfur_Compounds (accessed Mar 18, 2018).
- (17) Wright, J.; Hooman, S.; L., C. L. Stability of Carbon-centered Radicals: Effect of Functional Groups on the Energetics of Addition of Molecular Oxygen. *J. Comput. Chem.* **2008**, *30* (7), 1016–1026.
- (18) Trujillo, M.; Alvarez, B.; Radi, R. One- and Two-Electron Oxidation of Thiols: Mechanisms, Kinetics and Biological Fates. *Free Radic. Res.* **2016**, *50* (2), 150–171.
- (19) Rauk, A.; Yu, D.; Armstrong, D. A. Oxidative Damage to and by Cysteine in Proteins: An Ab Initio Study of the Radical Structures, C–H, S–H, and C–C Bond Dissociation Energies, and Transition Structures for H Abstraction by Thiyl Radicals. *J. Am. Chem. Soc.* **1998**, *120* (34), 8848–8855.
- (20) Davies, M. J. Protein Oxidation and Peroxidation. *Biochem. J.* **2016**, *473* (Pt 7), 805–825.

- (21) Mozziconacci, O.; Sharov, V.; Williams, T. D.; Kerwin, B. A.; Schöneich, C. Peptide Cysteine Thiyl Radicals Abstract Hydrogen Atoms from Surrounding Amino Acids: The Photolysis of a Cystine Containing Model Peptide. *J. Phys. Chem. B* **2008**, *112* (30), 9250–9257.
- (22) Pattison, D. I.; Rahmanto, A. S.; Davies, M. J. Photo-Oxidation of Proteins. *Photochem. Photobiol. Sci.* **2012**, *11* (1), 38–53.
- (23) Schöneich, C. Thiyl Radicals and Induction of Protein Degradation. *Free Radic. Res.* **2016**, *50* (2), 143–149.
- (24) Mozziconacci, O.; Kerwin, B. A.; Schöneich, C. Photolysis of an Intrachain Peptide Disulfide Bond: Primary and Secondary Processes, Formation of H₂S, and Hydrogen Transfer Reactions. *J. Phys. Chem. B* **2010**, *114* (10), 3668–3688.
- (25) Fang, H.; Ouyang, B.; Qin, Y.; Dong, W.; Hou, H. Study on the Reaction of Carbon Disulfide with Hydroxyl Radical in Aqueous Solution. *Chinese Sci. Bull.* **2005**, *50* (24), 2832–2835.
- (26) Von Hobe, M.; Cutter, G. A.; Kettle, A. J.; Andreae, M. O. Dark Production: A Significant Source of Oceanic COS. *J. Geophys. Res. Ocean.* **2001**, *106* (C12), 31217–31226.
- (27) Klüpfel, L.; Piepenbrock, A.; Kappler, A.; Sander, M. Humic Substances as Fully Regenerable Electron Acceptors in Recurrently Anoxic Environments. *Nat. Geosci.* **2014**, *7*, 195–200.
- (28) Aeschbacher, M.; Vergari, D.; Schwarzenbach, R. P.; Sander, M. Electrochemical Analysis of Proton and Electron Transfer Equilibria of the Reducible Moieties in Humic Acids. *Environ. Sci. Technol.* **2011**, *45* (19), 8385–8394.
- (29) Aeschbacher, M.; Sander, M.; Schwarzenbach, R. P. Novel Electrochemical Approach to Assess the Redox Properties of Humic Substances. *Environ. Sci. Technol.* **2010**, *44* (1), 87–93.
- (30) Byers, G. W.; Gruen, H.; Giles, H. G.; Schott, H. N.; Kampmeier, J. A. Photochemistry of Disulfides. I. Carbon-Sulfur Cleavage in the Photosensitized Decomposition of Simple Disulfides. *J. Am. Chem. Soc.* **1972**, *94* (3), 1016–1018.
- (31) Creed, D. The Photophysics and Photochemistry of the Near-UV Absorbing Amino Acids-III. Cysteine and Its Simple Derivatives. *Photochem. Photobiol.* **1984**, *39* (4), 577–583.
- (32) Jones, M. *Organic Chemistry*; W. W. Norton & Company: New York, USA, 1997.

- (33) Filipiak, P.; Bobrowski, K.; Hug, G. L.; Pogocki, D.; Schöneich, C.; Marciniak, B. New Insights into the Reaction Paths of 4-Carboxybenzophenone Triplet with Oligopeptides Containing N- and C-Terminal Methionine Residues. *J. Phys. Chem. B* **2017**, *121* (20), 5247–5258.

CHAPTER 4. INFLUENCE OF DOM ON COS AND CS₂ FORMATION FROM CYSTEINE DURING SUNLIGHT PHOTOLYSIS

4.1 Abstract

The role of DOM type and concentration on COS and CS₂ formation with cysteine was assessed. Cysteine (14 μM) and one type of DOM isolate (5 mg-C/L) were spiked into buffered synthetic water at pH 8.3. Five different types of DOM isolates were chosen ranging from freshwater to ocean water. These isolates included two freshwater isolates, Suwanee River fulvic acid (SRFA) and Aldrich humic acid, a river DOM isolate (Altamaha River, GA), and two ocean water isolates (Gulf Stream in the Atlantic Ocean). These solutions were exposed to simulated sunlight for up to 4 h. Surprisingly, CS₂ was not formed under any conditions with any type of DOM which was ascribed to the complexity of natural waters which formed a host of RIs when compared to the synthetic solutions with DOM isolates. However, the presence of DOM enhanced COS formation while increasing DOM concentration had a reverse effect on COS formation. The role of Reactive Intermediates (RIs) such as ³DOM* and •OH was also investigated by adding selective quenching agents. Results indicated that, with isopropanol, an efficient •OH scavenger, COS formation was not affected. Whereas, with ³DOM* quenching agents, COS formation decreased but this was highly dependent on the type of quenching agent added. For example, adding phenol did not influence COS formation, the presence of trimethylphenol, sorbic acid and O₂ dramatically decreased its concentration during 4 h irradiation. Treating DOM isolates with sodium borohydride to reduce ketone/aldehydes to corresponding alcohols, increased COS formation.

4.2 Introduction

DOM is an important substrate to explore in detail since it generates a host of RIs (e.g., triplet states of dissolved organic matter ($^3\text{DOM}^*$) and hydroxyl radicals ($\bullet\text{OH}$)) when exposed to sunlight in natural waters.¹ However, the formation of such RIs is highly dependent on the type of DOM involved and its chemical composition. Notably, the differences in chemical composition result in various optical properties (i.e., absorbance and fluorescence) of DOM, which can be measured by different analytical tools.²⁻⁴ Thus, these optical measurements can be directly correlated to the formation of different RIs. For example, autochthonous DOM, which originates through microbial activity, has been found to have lower absorbance at the longer wavelength which may lead to greater values of E_2/E_3 (the ratio of the absorbance values at 250 nm and 365 nm) compared to allochthonous DOM which is derived from terrestrial sources.⁵ In other words, the absorbance at longer wavelength is associated with charge transfer interaction between singlet electronic ground state phenolic electron donors and excited triplet state aromatic ketone/quinone acceptors.⁶ The lower absorbance at the longer wavelength or higher E_2/E_3 value implies the lower fractional content of phenols in comparison to aromatic ketone sensitizers which may lead to lower extent of charge transfer interactions, thus higher RIs formation.⁷⁻¹⁰ It has been shown that charge transfer interactions hamper the formation of RIs (e.g., $^3\text{DOM}^*$) by de-activating $^1\text{DOM}^*$ and reducing its chance to form $^3\text{DOM}^*$ through intersystem crossing.^{3,11} While aromatic ketone/quinone groups have been reported to be involved in the photochemical production of RIs,^{3,6} phenolic moieties are most likely quenching the RIs^{12,13}. In a previous study,¹⁴ it was found that the formation of the RIs (e.g., $^3\text{DOM}^*$) were directly correlated to E_2/E_3 values while the quenching rates of RIs (e.g., $^3\text{DOM}^*$) were inversely correlated with E_2/E_3 values.¹⁵ This implies that while allochthonous DOM likely has more quenching capacity than autochthonous DOM, the latter one has more RIs forming capacity.

The indirect photochemical formation of COS and CS₂ has been observed in different natural waters,^{1,15-20} likely containing different DOM types and concentrations, with different organic sulfur precursors such as cysteine.^{21,22} For example, in our previous study,¹⁵ COS and CS₂ formation were evaluated in nine different natural waters which ranged in DOM concentration from 2.9-16.5 mg-C/L. While it was found that COS and CS₂ formation was correlated to DOC concentration, it was hard to investigate how DOM type/concentration specifically matters since natural waters are more complex mixtures. Overall, the presence of DOM is expected to enhance the COS and CS₂ formation by forming different RIs which can react with organic sulfur precursors^{1,16-20}. However, no known studies have tried to investigate the effect of DOM type/concentration or specifically the role of RIs on COS and CS₂ formation.

In order to further elucidate the RIs involved, studies have also used probe compounds and quenching agents.^{1,13,16,23,24} The quenching agents can selectively react with target RIs to remove them from the system which helps to assess the importance of missing RIs. Therefore, different quenching agents are used in this study in order to evaluate the importance of selective RIs in COS and CS₂ formation. For example, isopropanol is used to primarily quench •OH²⁴⁻²⁷ while phenol, trimethylphenol, sorbic acid, and O₂ are used to primarily quench ³DOM*.^{1,16,28} These compounds can quench ³DOM* with different reaction rates and through different mechanisms, including energy transfer (e.g. with sorbic acid and O₂) or oxidation (e.g. with phenol and trimethylphenol). The reaction rates of these quenching agents with reactive intermediates such as •OH and ³DOM* are listed in Table 4-1.

Table 4-1. The scavenging reaction rates of quenching agents with $\bullet\text{OH}$ and ${}^3\text{DOM}^*$

Quenching agent	$\bullet\text{OH}$	${}^3\text{DOM}^*$ ($\text{M}^{-1}\text{s}^{-1}$)
Isopropanol	$(4.3 \pm 1.3 \times 10^9 \text{ M}^{-1} \text{ s}^{-1})^{29}$	-
Phenol	$(0.841 \pm 0.042 \times 10^{-10} \text{ M}^{-1} \text{ s}^{-1})^{30}$	4×10^8 (pH 8) ²⁸
Trimethylphenol	$(9.75 \pm 0.98 \times 10^{-8} \text{ L molecule}^{-1} \text{ s}^{-1})^{31}$ or $(1.61 \pm 0.16 \times 10^{-31} \text{ M}^{-1} \text{ s}^{-1})^{31}$	43×10^8 (pH 10) ¹⁶
Sorbic acid	-	$(4.4 \pm 4.29 \times 10^9)^1$
O ₂	-	$(2 \times 10^9)^1$

Given this information, there is a lack of clarity related to how DOM and its resulting RIs affect COS and CS₂ formation. This study was intended to address this scientific gap by answering three major questions: (i) how do different types and concentrations of DOM affect COS and CS₂ formation, (ii) if DOM does play an important role, what are the contributions of different RIs in forming COS and CS₂, and (iii) how does the role of DOM compare to the role of the organic sulfur compound precursor, such as cysteine, in forming COS and CS₂, when assessed as a function of concentration or speciation? To address these questions, five different DOM isolates ranging from freshwater to seawater were evaluated. Synthetic solutions containing cysteine and one DOM isolate over varied concentrations were exposed to simulated sunlight for 4 h. Certain solutions were amended with isopropanol, phenol, trimethylphenol, sorbic acid, or O₂ to selectively quench ${}^3\text{DOM}^*$ or $\bullet\text{OH}$. In addition, NaBH₄ was used to selectively reduce ketones to their corresponding alcohols to assess if the RIs derived from ketones were involved in COS and CS₂ formation. The results indicated that CS₂ did not form above the DL under any condition with any type of the DOM isolate tested. However, the presence of DOM at any concentrations enhanced COS formation with cysteine under sunlight, where DOM was found to be the limiting reactant rather than cysteine. However, higher concentrations of DOM inhibited COS formation. While $\bullet\text{OH}$ was not suggested to be involved in COS formation, ${}^3\text{DOM}^*$ seemed to be the major contributing RI.

Finally, this study suggested that DOM can enhance COS formation in the presence of cysteine by forming RIs, especially ³DOM*; however, for the formation of CS₂, the presence of other water quality constituents seemed necessary, as happened in natural waters.

4.3 Materials and Methods

4.3.1 Description of standards, reagents, and stock preparation

In addition to the standards and reagents used in Chapter 2 and 3, other reagents used in these experiments included: sodium borohydride (NaBH₄), sephadex G-10, phenol, trimethylphenol and sorbic acid (HDA), which were purchased at ≥ 97% purity from Sigma Aldrich. NaBH₄ was stored under inert gas (N₂) condition immediately after it was purchased. Isopropanol was purchased from Alfa Aesar. Tris buffer was purchased from Roche Diagnostics. Humic acid was purchased from Aldrich. Overall, these and other chemicals were purchased at reagent grade or higher.

The stock solutions of cysteine and Suwanee River fulvic acid (SRFA) were prepared in the same way as described in Chapter 2 and 3, respectively. In addition, the humic acid stock solution was prepared by adding 10 mg of humic acid to 100 ml of purified water. The final humic acid stock solution concentration of 42.3 mg-C/L was measured by a TOC-V Shimadzu Total Organic Carbon Analyzer. The phenol and trimethylphenol stock solutions were prepared by adding known amounts of phenol and trimethylphenol to 20% ACN/80% water, respectively. The sorbic acid stock solution was prepared by adding known amount of sorbic acid to ACN.

4.3.2 Collection, characterization and modification of different DOM isolates

Five different DOM isolates were assessed from sources ranging from freshwater to ocean water. Two of these isolates, humic acid and SRFA, were purchased commercially (as noted above). The three remaining isolates were collected in 2013 by Dr. Perdue (Ball State University,

Indiana) either from the Altamaha River or the Gulf Stream within and off the eastern coast of the US, respectively. The specific sampling sites of these waters are shown in Fig. 4-1. These isolates were chosen to test because they were already collected and were available. So, there was no rationale for selection of the sampling sites.

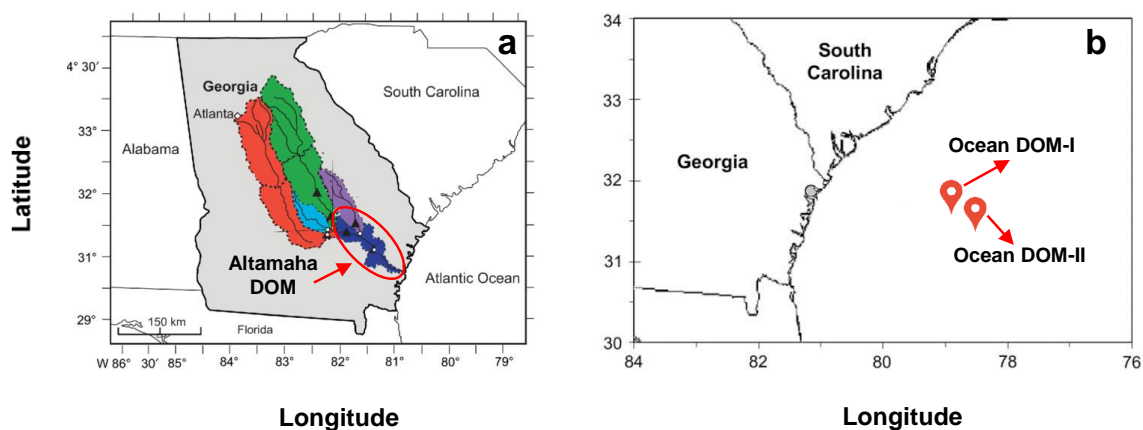


Figure 4-1. The location of sampling sites for: (a) Altamaha and (b) gulf stream isolates (ocean DOM-I and ocean DOM-II)³¹. The right map is similar to the one used by a previous study and thus adopted from a picture provided in it.³¹

Once collected, these sampled waters were treated by reverse osmosis–electrodialysis to remove salts and also to reduce the water volume.³² These samples were then stored at -20°C until they were transported to Purdue in one day, where they were again stored in the dark at -20°C before use. The total organic carbon content of these isolates was measured using a TOC-V Shimadzu Total Organic Carbon Analyzer.

In general, these isolates represented freshwater to open ocean DOM types, where: (i) SRFA and humic acid, the latter of which is typically derived from vegetable soil, peat, and/or soft coal, represented freshwater DOM, (ii) the sample from the Altamaha river represented freshwater to brackish water DOM (henceforth labeled as “Altamaha DOM”), and (iii) samples from the Gulf Stream represented open ocean DOM (henceforth labeled as “Ocean DOM-I” and “Ocean DOM-II”). Several optical characteristics of these isolates were also measured including: (i) absorbance

spectra from 200-800 nm (Shimadzu UV-VIS spectrophotometer) and (ii) fluorescence spectra at an excitation wavelength range of 229-700 nm ($\lambda_{\text{excitation}}$) and an emission wavelength range of 242-824 nm ($\lambda_{\text{emission}}$) (measured using an Aqualog fluorometer (Horiba Scientific) by Ethan Hain and Lee Blaney at the University of Maryland, Baltimore County (UMBC)).

In addition, these DOM isolates were further modified using sodium borohydride (NaBH_4), which was used to reduce ketone and aldehyde functional groups to their corresponding alcohols. This procedure was undertaken in order to investigate if ketone- and aldehyde containing sensitizers were important precursors in forming COS and CS_2 . This reduction was performed by following a modified procedure provided in previously reported methods.^{6,33,34} Briefly, known concentrations of different DOM isolates were transferred to 20 ml vials and were purged with N_2 for 30 min. The vials were immediately capped after purging and transferred into the glove box where NaBH_4 was added to the DOM-containing solutions at a 30:1 NaBH_4 :DOC mass ratio. The vials were then capped and allowed to react in the dark for up to 24 h. The pH values of the samples were also measured prior to and following the 24 h reduction where the pH increased from 6.7-8.7 to ~ 10 , respectively. To readjust the pH back to the stocks' original pH values (6.7-8.7) and ensure complete removal of excess NaBH_4 , the samples were then passed through a small G-10 packed size-exclusion column (1×10 cm, equilibrated with Milli-Q water). In some cases, a small amount of phosphoric acid was used to further adjust the pH after samples went through the column. At different reaction times (2,4, and 24 h) of NaBH_4 treatment, the UV absorbance (200-800 nm) of these solutions was also measured and was compared to its original pre-treatment value. The UV absorbance was used to validate if the ketone and aldehyde moieties of these DOM isolates were reduced since previous literature has shown that NaBH_4 reduction of DOM creates a preferential loss of visible absorption and enhanced, blue-shifted fluorescence emission.³⁵ When the UV

absorbance was assessed after 2, 4, and 24 h, a decrease in absorbance was observed at 2 h and it stayed at same levels for 24 h, where it was assumed that the reaction was complete. The final UV absorbance values of treated DOM isolates (24 h) were then compared to original absorbance values before treating the DOM isolates (Fig. 4-2). While this loss was more significant in certain cases like humic acid and SRFA (Fig. 4-2a and b), with other DOM isolates, the effect was minor (Fig. 4-2c, d and e). A similar effect was seen by previous literature when treating humic acid with NaBH_4 .²² These modified DOM stock solutions were then immediately used for the irradiation.

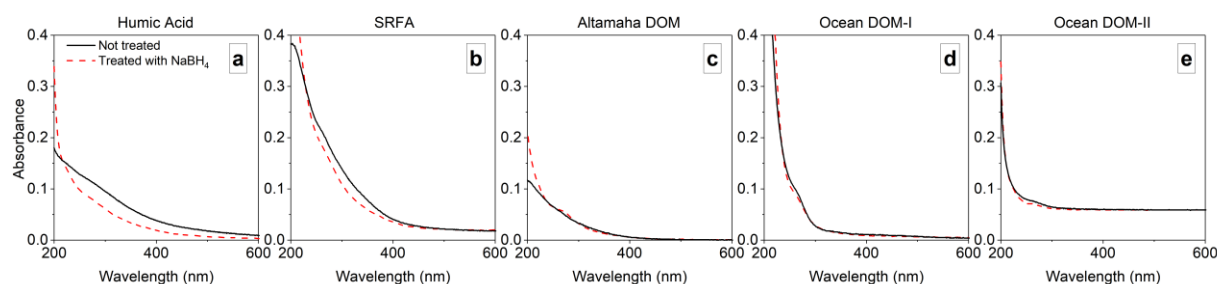


Figure 4-2. Effect of sodium borohydride treatment on DOM absorbance spectra

4.3.3 Photochemical reactor setup

The solar simulator (OAI Tri-Sol; AM 1.5G filter), photochemical reactors and the experimental conditions were identical to those described in previous chapters.

4.3.4 Experimental procedure

Kinetic experiments were performed using synthetic solutions that contained $14 \mu\text{M}$ cysteine, and one DOM isolate (humic acid, SRFA, Altamaha DOM, ocean DOM-I, or ocean DOM-II). These synthetic solutions were also buffered at pH 8.3 (a relevant pH at natural waters) with 10 mM tris buffer and were initially purged with N_2 for 30 min to remove dissolved O_2 . These solutions (11 mL) were then placed into the reactors and either left in the dark or exposed to simulated sunlight over 4 h. These experiments were then repeated, where each DOM isolate was

instead pre-treated with NaBH₄. Additional experiments were also performed in which solutions varied in: (i) DOM concentration (0.5-20 mg-C/L), (ii) cysteine concentration (1- 100 μM), and (iii) pH (pH 7 to 10 using tris buffer). Certain solutions were also: (i) amended with isopropanol (10 mM), (ii) phenol (1 mM), (iii) trimethylphenol (0.125 mM), (iv) sorbic acid (0.5 mM), or (v) O₂ (in this case, the waters were not purged with N₂ but were left as is where the [O₂]₀ ≈ 8.9 mg/L at 20°C since the DOM isolates were left in equilibrium with the atmosphere during storage). Isopropanol was used to primarily scavenge •OH whereas phenol, trimethylphenol, sorbic acid, and O₂ were used to primarily scavenge ³DOM* (Table 4-1).

4.3.5 Analytical methods

COS and CS₂ were analyzed by headspace GC-MS (Agilent 6420), as described in Chapter 2.

4.4 Results and Discussion

4.4.1 Characterization of DOM

Two important optical properties of the DOM isolates were measured including the absorbance (Fig. A1 in Appendix) and Fluorescence Emission Excitation Matrices (EEMs) spectra (Fig. A2 in Appendix). From these figures, various spectral metrics were extracted. Several of these parameters were not important in COS and CS₂ formation and thus are included in text A1 in appendix. These parameters included the absolute absorbance or fluorescence intensity at a specific wavelength, ratios of different wavelengths, carbon-normalization of optical properties, and the slopes across specific regions of the optical spectrum were also calculated based on previously described methods^{36,37} and are summarized in text A1. However, among these parameters, the fluorescence index (FI) and the ratio of the absorbance values at 250 nm (E₂) and 365 nm (E₃) (=E₂/E₃) (table 4-2) were found to be most relevant for understanding the

photochemical processes behind COS and CS₂ formation. The fluorescence index (FI) is defined as the ratio of the fluorescence intensity at 450 nm to that at 500 nm when excited at 370 nm.^{37,38} Fluorescence index represents the level of the aromaticity of the source of the organic material, which is defined as the % of sp²-hybridized carbon atom which can be determined by ¹³C-NMR [nuclear magnetic resonance].³⁷ This suggests that FI can serve as a surrogate for the general structural features of the carbon skeleton which have been found to be related to the organic materials of different sources. Given this, FI is typically used to distinguish the source of DOM, with lower values suggesting terrestrial sources and higher values suggesting microbial sources.^{37,38} For the DOM isolates evaluated in this study, humic acid had the lowest FI value, indicating that it was the most terrestrial DOM while Ocean DOM-I had the highest FI value, indicating that it was the least terrestrial and most microbial-based DOM (Table 4-2). Overall, the FI values decreased for the DOM isolates such that ocean DOM-I > ocean DOM-II > Altamaha DOM > SRFA > humic acid (Table 4-2). The other index, E₂/E₃, has often been used as an indicator for the average molecular size of DOM, whose value is inversely proportional to size.³⁹ The molecular weight dependence of this index is believed to stem from an increase in probability of electronic interactions between different chromophores in larger DOM molecules. Humic acid exhibited the lowest E₂/E₃ value, indicating that it may have the highest average molecular weight whereas ocean DOM-II had the lowest average molecular weight. Overall, the average molecular weight decreased for the DOM isolates such that humic acid > Altamaha DOM > SRFA > ocean DOM-I > ocean DOM-II (Table 4-2).

Table 4-2. The fluorescence index (FI) and E₂/E₃ values for DOM isolates, calculated based on previously described methods.^{35,36}

Sample	Fluorescence index	E ₂ :E ₃
Humic acid	1.00	2.62
SRFA	1.38	5.24
Altamaha DOM	1.48	5.12
Ocean DOM-I	1.80	5.41
Ocean DOM-II	1.65	9.80

4.4.2 COS and CS₂ formation from different DOM isolates

When cysteine and each type of DOM isolate were added to the reaction solutions, CS₂ was surprisingly not formed under any tested conditions. This result contradicted our previous findings in chapters 2 and 3,¹⁵ where CS₂ was photochemically generated to up to 1.5 nM when nine different natural waters spiked with cysteine were exposed to simulated sunlight over 4 h.¹⁵ This difference is likely attributed to the fact that the natural waters tested in this previous case were directly collected from the field with no considerable pre-treatment (waters were only filtered through a 0.7 μm filter). Thus, these waters contained a more complicated matrix of reactive water constituents (e.g., halides, carbonates, and possibly others). These water constituents can generate RIs (see eqs. 1- 7 in chapter 1), that potentially affected CS₂ formation. Also, RIs formed by DOM were consumed in the pathways forming COS. In this current experimental regime where DOM isolates were used instead, such additional RIs were not present. Such results indicated that any RIs generated from DOM did not lead to CS₂ formation, which was not the case for COS, as discussed in the following sections.

Unlike CS₂, COS formation increased when DOM was present. With all five DOM isolates, COS did not form above the DL in the dark with no cysteine but increased to similar low concentrations for all DOM isolates with cysteine, ranging between 0.25-0.3 nM after 4 h (Fig. 4-3).

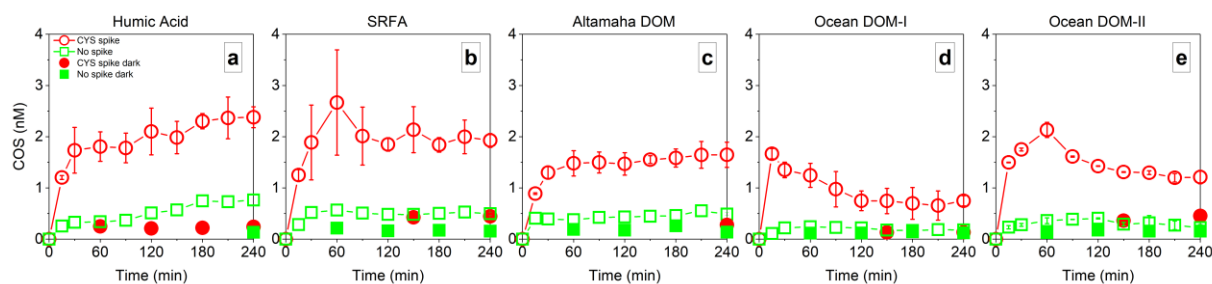


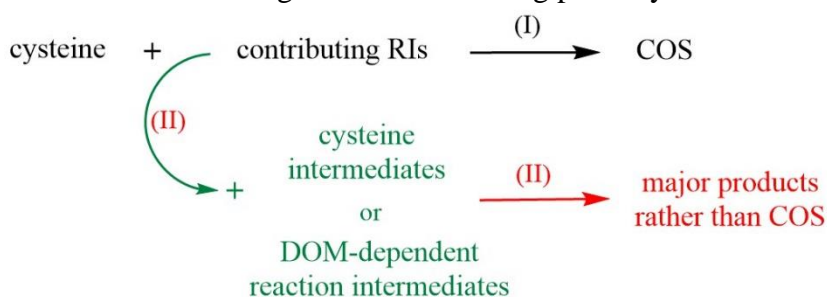
Figure 4-3. Effect of DOM type on COS formation ($[CYS]= 14 \mu M$, $[DOM]= 5 \text{ mg-C/L}$, $pH= 8.3$, temperature= $21 \pm 1 \text{ } ^\circ\text{C}$).

The ability for cysteine to form COS in the dark has been observed in previous studies.^{14,20} COS formation then increased with sunlight to a slightly higher level over 4 h with no cysteine while increasing even further with cysteine to up to 18 \times higher concentrations (1.2 to 2.4 nM) compared to dark (Fig. 4-3). Initially, these results suggested that the precursors derived from the inherent dissolved organic sulfur (DOS) present in these DOM isolates were able to form some degree of COS. However, COS increased further once cysteine was added. These increased COS levels with sunlight also matched prior results where COS increased by 1.8-7 \times ,^{15,18,21,22} in the presence of sunlight compared to dark. Surprisingly though, these different DOM isolates formed similar amount of COS (1.2-2.4 nM) which suggested that the RI involved in COS formation possibly formed at similar quantum yields (Φ) from these DOM isolates. The RIs that are likely involved include low-energy triplet states ($ET < 250 \text{ kJ mol}^{-1}$) of chromophoric dissolved organic matter (CDOM), which appear to form at similar quantum yields for a wide range of DOM types¹³. Further support of these RIs serving as the primary candidates for COS formation will also be

provided by results discussed in later sections. Also, it should be noted that COS formed at very low yields (<0.01%) from cysteine which implies that there are some other non-COS major products formed from cysteine as discussed in chapter 2.

Unlike COS formation levels, the kinetics of COS formation were slightly different for different DOM isolates (Fig. 4-3). Specifically, COS formation from humic acid and Altamaha DOM followed the same trend, where the COS concentration continuously increased over the 4 h irradiation time (Fig. 4-3a and c). However, COS formation with SRFA and the ocean DOM isolates (ocean DOM I and II) decreased after specific time points (Fig. 4-3b, d and e). COS formation decreased after one hour for SRFA and Ocean DOM-II and after 15 min for ocean DOM-I (Fig. 4-3b, d and e). These results implied that the formation of COS was limited by the concentration of RIs which were possibly further consumed by cysteine intermediates or other DOM-dependent reaction intermediates that formed other major products rather than COS (scheme 4-1, path (II)).

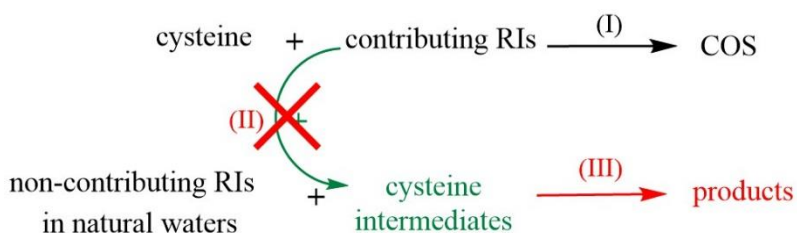
Scheme 4-1. Proposed mechanisms for consumption of contributing RIs in COS formation by other intermediates through non-COS forming pathways



Once the RIs were consumed, COS hydrolysis then appeared to outcompete COS formation at various time points, which resulted in a decrease in its formation. This counter effect seemed more dominant for SRFA and the ocean DOM isolates (ocean DOM I and II) than for the other isolates (Fig. 4-3b, d and e), although it is currently unclear why this is the case.

Moreover, it should be noted that kinetics for all of the isolates were considerably different from those observed with natural waters, where COS formation continuously kept increasing during irradiation.^{15,21,22,40} For example, in one of these studies, they tested a synthetic seawater (NE Atlantic seawater) which was firstly spiked with 4.4 μM of cysteine and then 0.5 mg-C/L of humic acid, and the COS formation increased by 4 \times in presence of humic acid while following an increasing trend for the whole irradiation period.²¹ In the same study, COS formation was also tested with other organic sulfur precursors in the presence of Aldrich humic acid and SRFA, where COS formation continuously increased over irradiation time but to different degrees. However, it should be noted that they compared COS formation while using different precursors and natural water types, NE Atlantic seawater was assessed with sodium glutathione (4.4 μM) and SRFA (0.25 mg-C/L) while North Sea seawater was tested with 3-mercaptopropionic acid (4.4 μM) and humic acid (0.25 mg-C/L).²¹ In other studies, adding 2.85 and 3.5 mg-C/L SRFA with 10 μM cysteine to natural waters increased COS formation, following an similar increasing trend, by 7 and 10 \times , respectively, compared to no SRFA (pH 8).²² Overall, most of these studies observed a similar increase in COS formation upon addition of DOM, although they tested natural waters, but the COS formation kinetics were different than those observed here. This difference in kinetics can be attributed to the concomitant presence of other RIs in natural waters, which possibly were quenching the reaction intermediates (e.g., cysteine intermediates) that were consuming the contributing RIs of COS formation (scheme 4-2, path (III)).

Scheme 4-2. Proposed mechanisms for scavenging of cysteine intermediates by non-contributing RIs of COS formation in natural waters



These additional RIs were not present in synthetic solutions with DOM isolates. Consequently, COS formation in DOM isolates were limited by RIs while in natural waters it followed an increasing trend and the reaction was not likely limited by contributing RIs.

Interestingly, these results, which did not have a strong dependence on DOM type, also differed from other studies that evaluated organic precursor degradation where DOM type had a strong effect.^{5,25,26} However, these previous studies investigated the organic precursors and not the products specially the minor products like COS. For example, Sulfadimethoxine was found to undergo higher photodegradation rates with Pony Lake Fulvic Acid (PLFA) than SRFA.^{5,25} This can be explained through different optical properties of these DOM isolates which lead to different capacities in forming and quenching RIs (see next section for more details). Similar results were obtained with sulfadiazine, as its photo-transformation trends for PLFA were found to be thoroughly different than SRFA, and the rate constants of PLFA were higher than those of SRFA.²⁶ It is possible that similar effects happened with cysteine although it was not possible to observe it since cysteine was not measured. This was not seen through COS formation since it was a minor path. This effect was seen with COS formation but only when the effect of DOM concentration was tested (see later discussions).

4.4.3 Effect of DOM concentration

The results with varying DOC concentration from 0.5 to 20 mg-C/L indicated that increasing DOM concentration decreased COS formation for most of tested DOM isolates (Fig. 4-4). The strongest effect was observed for the humic acid and Altamaha DOM isolates whereas the Ocean DOM-I also exhibited the same effect but to a slightly lower degree (Fig. 4-4a, c and d).

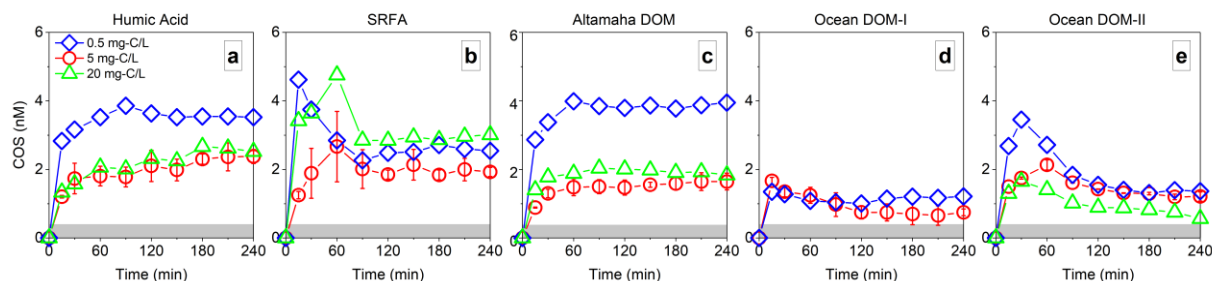


Figure 4-4. Effect of DOM concentration on COS formation ($[CYS] = 14 \mu M$, $pH = 8.3$, temperature = $21 \pm 1 \text{ } ^\circ C$). The grey box shows the general level of dark formation, which was similar for all scenarios. The stock concentration of ocean DOM-I was 12.7 mg-C/L and it was not possible to test 20 mg-C/L .

Overall, this effect is likely attributed to the dual role that DOM has on simultaneously producing and scavenging RIs.^{4,12,13,41} In general, DOM can inhibit the degradation process of organic compounds through three main mechanisms. The first mechanism includes light screening, which is not of concern in COS formation since the precursor, cysteine, does not absorb sunlight,¹⁶ and thus does not compete with DOM in receiving photons. The second mechanism includes scavenging RIs (eqs. 1- 3), as found previously where DOM acted as a scavenger of reactive species⁴²⁻⁴⁴ such as $^3DOM^*$,^{4,12} $\bullet OH$ and $CO_3^{\bullet -}$.^{45,46}



Therefore, higher DOM concentration can inhibit the photoproduction of COS by scavenging the RIs involved in COS formation, and possibly decreasing cysteine degradation, similar to how it inhibits the degradation of probe compounds (e.g., trimethylphenol) and organic contaminants.^{41,47} For example, trimethylphenol oxidation was inhibited by 50-60% when the concentration of effluent organic matter (EfOM) isolates in the solution increased from 3 to 25 mg-C/L.⁹ This finding can be applied to the formation of COS from cysteine degradation since both

trimethylphenol and cysteine can react with $^3\text{DOM}^*$.^{1,16} Lastly, the third mechanism is related to the potential for DOM to reduce organic compound reaction intermediates. In this case, the organic compound can react with an oxidizing radical or/and excited triplet state to form a radical cation which can be later reduced by DOM to reform the parent compound while generating an oxidized DOM radical, DOM^{*+} (eqs. 4- 5).⁴¹



It is speculated that such a reversal may similarly happen with the thiolate (R-S^-) moiety, which is the deprotonated form of cysteine. For this proposed reaction, the thiolate (R-S^-) moiety would initially react with $^3\text{DOM}^*$ to form the thiyl radical through electron transfer, which is known to occur from previous literature⁴⁸. The thiyl radical could then accept an electron from another DOM moiety to reform the thiolate (R-S^-) moiety. However, further experiments need to be conducted to confirm that this reaction sequence occurs. In the end though, both the second and third mechanisms could possibly hamper cysteine degradation towards forming COS.

It also should be noted that other DOM isolates either exhibited no effect of DOM concentration (e.g. for Ocean DOM-I) or a fluctuating effect of DOM concentration (e.g. for SRFA) on COS formation (Fig. 4-4 b and d). Thus, these overall differences observed between the five isolates can likely be attributed to the RI quenching capacity of each particular organic matter. This quenching capacity is linked to the source of the DOM resulting from its chemical composition.⁴ For example, humic acid and Altamaha DOM were found to have more terrestrial origin (lower FI values, see table 4-2) and more phenolic content than other DOM isolates, specifically ocean DOM-I, which has been shown to lead to greater RI quenching capacity.¹³ On

the other hand, Ocean DOM-I had the most microbial content (higher BI value) which implied a lower RI quenching capacity.¹³ In addition, terrestrial DOMs have higher molecular weights (lower E₂:E₃ values) which are found to have a greater RI quenching capacity.¹⁴ Furthermore, terrestrial DOMs have also more phenolic content than microbial-based DOMs¹³, and such phenolic moieties are also well known to quench RIs such as ³CDOM*^{1,12,13}. One interesting outlier for all of these results included SRFA, which is considered as a terrestrial-based DOM isolate. In this case, by increasing the concentration of SRFA from 0.5 to 5 mg-C/L, COS formation decreased, which implied that a greater percentage of contributing RIs were quenched than were formed when increasing the DOM concentration (Fig. 4.4b). However, when the DOM concentration increased from 5 to 20 mg-C/L, COS formation subsequently increased, which implied that this balance shifted such that a greater level of RIs were generated to form COS rather than being quenched (Fig. 4.4b). A similar effect has been also observed in a previous study,⁴ where increasing the concentration of SRFA from 0 to ~5 mg-C/L decreased the steady state concentration of ³DOM* while increasing the concentration further up to 40 mg-C/L increased the steady state concentration of ³DOM*.⁴ Currently, it is unclear why SRFA exhibited this switch in forming and quenching RIs, while other DOM isolates did not exhibit a similar effect. A more complex set of chemical reactions seems to be taking place with SRFA, and future experiments are needed to determine why this is the case.

Moreover, this effect of DOM concentration falls in direct contrast to the results observed in chapters 2 and 3, which have been reported in a previous paper.¹⁵ In these chapters, results for nine different natural waters indicated that COS formation was positively correlated to the waters' DOM concentrations.¹⁵ This difference can be attributed to the fact that two different types of water matrices were assessed. This study assessed DOM isolates in clean water matrices while the

former work involved natural waters¹⁵. This difference especially impacted the kinetics of COS formation for both scenarios, such that with natural waters, the additional RIs involved, as discussed previously, led to a constant formation of COS over time.¹⁵ It is likely that the concentrations of these additional RIs increased with increasing DOM concentrations, and these RIs were not present in synthetic solutions with DOM isolates.

4.4.4 Effect of cysteine concentration

Given that the RI concentration is likely the key factor in controlling COS formation, additional experiments were conducted to confirm that, alternatively, the cysteine concentration was not a limiting reagent in forming COS under these experimental conditions. It was expected that cysteine would not limit the reaction, especially since it was added at μM concentrations, but to further prove this, solutions were varied in their initial cysteine concentration (1-100 μM) when one type of DOM isolate, ocean DOM-II, was added. Results indicated that increasing the concentration of cysteine slightly increased COS formation in the dark while a greater increase occurred in the presence of light (Fig. 4-5). Also, the kinetics were slightly affected by increasing the cysteine concentration. This effect was especially true with 100 μM cysteine where COS formation continued to increase for 80 min and then subsequently decrease due to COS hydrolysis (Fig. 4-5). Therefore, the results further supported the fact that COS formation was limited by RIs and not cysteine since increasing cysteine's concentration by 100 \times only increased COS formation by 3 \times (Fig. 4-5). In addition, these results also matched results from previous literature⁴⁰ where the COS formation increased by 2.5 \times when cysteine concentration increased from 0 to 2.5 μM .⁴⁰ However, the effect of cysteine concentration was investigated only through single dose experiments, and thus it was not possible to compare the formation kinetics.⁴⁰ Overall, it should be noted that the presence of cysteine enhanced COS formation even at low formation yields.

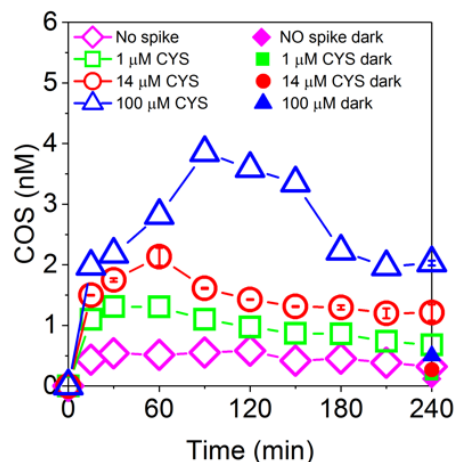


Figure 4-5. Effect of CYS concentration on COS formation during the sunlight photolysis with ocean DOM-II ([ocean DOM-II]= 5 mg-C/L, pH= 8.3, temperature= 21±1 °C)

4.4.5 Effect of pH

In addition to the cysteine concentration, the effect of cysteine speciation ($pK_a = 8.4$),¹⁶ was also investigated by adjusting the pH of the reaction solutions between pH 7 to 10. Results indicated that COS formation was strongly influenced by pH where the highest COS formation occurred at the lowest pH of 7.0 (Fig. 4-6). However, it was not possible to experimentally assess whether either cysteine species, the thiol (-SH) or its dissociated form, the thiolate ($-S^-$), led to greater reactivity, since COS can also undergo base-catalyzed hydrolysis, which is a pH-dependent process. Here, base-catalyzed hydrolysis can increase with increasing pH, as estimated through its pseudo-order rate constants of COS with OH^- ($k_{OH^-} (M^{-1}s^{-1}) \times [OH^-] (M)$). As shown in chapter 2, these rate constants increased from 12.9×10^{-7} , 25.8×10^{-6} , and $12.9 \times 10^{-4} (s^{-1})$ when pH increased from 7, 8.3, and 10, respectively. While the previous literature has found that the thiolate moiety possibly will be more reactive than the thiol since $R-S^-$ is a better nucleophile than SH ,⁴⁸ it was difficult to ascertain this effect in COS formation due to the hydrolysis effect.

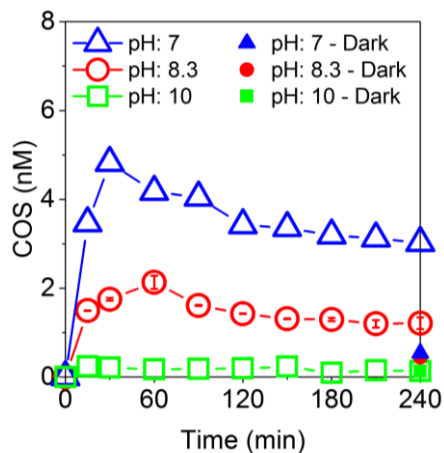


Figure 4-6. Effect of pH on COS formation during the sunlight photolysis of cysteine with ocean DOM-II ([ocean DOM-II]= 5 mg-C/L, [CYS]= 14 μ M, temperature= 21 \pm 1 $^{\circ}$ C).

4.4.6 Role of quenching agents

Influence of \bullet OH

Given the important role that the RIs generated from DOM have on forming COS, additional experiments were conducted to isolate which specific RIs were involved in the reaction pathway. First, the influence of \bullet OH was evaluated by spiking solutions containing each DOM isolate with 10 mM isopropanol to immediately quench \bullet OH once it was formed in solution (Table 4-1). As expected, isopropanol addition did not affect COS dark formation. Interestingly, isopropanol addition also did not affect COS formation with light for most of the DOM isolates (excluding the Altamaha DOM) (Fig. 4-7), which implied that \bullet OH was not involved in forming COS.

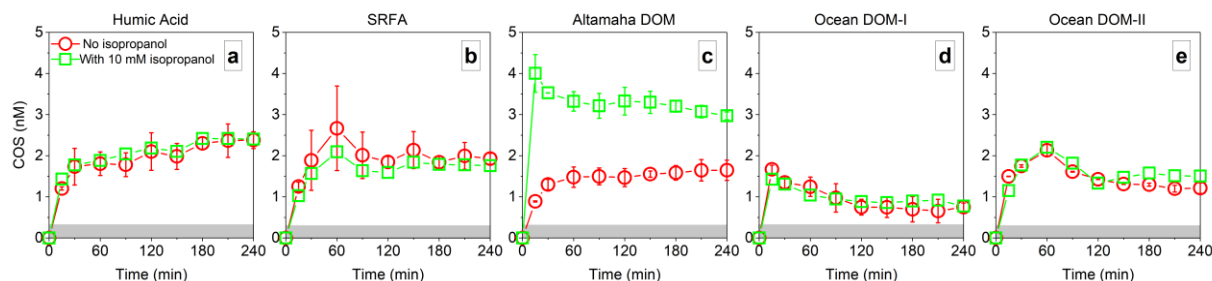


Figure 4-7. Influence of isopropanol on COS formation ($[CYS]= 14 \mu M$, $[DOM]= 5 \text{ mg-C/L}$, $pH= 8.3$, temperature= $21 \pm 1 \text{ } ^\circ\text{C}$). The grey box shows the general level of dark formation, which was similar for all scenarios.

The influence of isopropanol was however different with Altamaha DOM, where adding isopropanol dramatically increased COS formation (Fig. 4-7c). One possibility driving this effect could be attributed to the presence of other RIs, specifically generated by the Altamaha DOM (eq. 6), which react with cysteine or more likely the cysteine-based intermediates to initiate other non-COS forming pathways (eq. 7) but that are quenched by isopropanol (eq. 8). This quenching would then leave cysteine or its intermediates to instead form COS (eq. 9). The ability for isopropanol to quench other unknown long-lived RIs generated by DOM, aside from $\bullet\text{OH}$, has been previously suggested when photolyzing SRFA.⁴⁹ Further research is needed to ascertain what RIs these might be, that seem specific to Altamaha DOM.



Influence of $^3\text{DOM}^$*

Since $\bullet\text{OH}$ was not found to be a key RI involved in forming COS, the influence of $^3\text{DOM}^*$ was evaluated next by adding various quenching agents that quenched $^3\text{DOM}^*$ to varying degrees

and rates (Table 4-1). These quenching agents included phenol²⁸, trimethylphenol²⁸, sorbic acid¹ and O₂¹. Initially, each of these quenching agents was added to solutions containing humic acid (Fig. 4-8a). As expected, these quenching agents did not affect COS formation in the dark (Fig. 4-8a). However, with light, COS concentrations decreased but did so to varying degrees depending on the type of quenching agent added (Fig. 4-8a). Phenol then did not have any influence on COS formation whereas trimethylphenol, sorbic acid and O₂ dramatically decreased COS formation by ~60, 60 and 80%, respectively, after 4 h irradiation (Fig. 4-8a). Thus, COS formation decreased in these solutions according to the following pattern of quenching agents where no quenching agent \approx phenol > sorbic acid \approx trimethylphenol > O₂ (Fig. 4-8a).

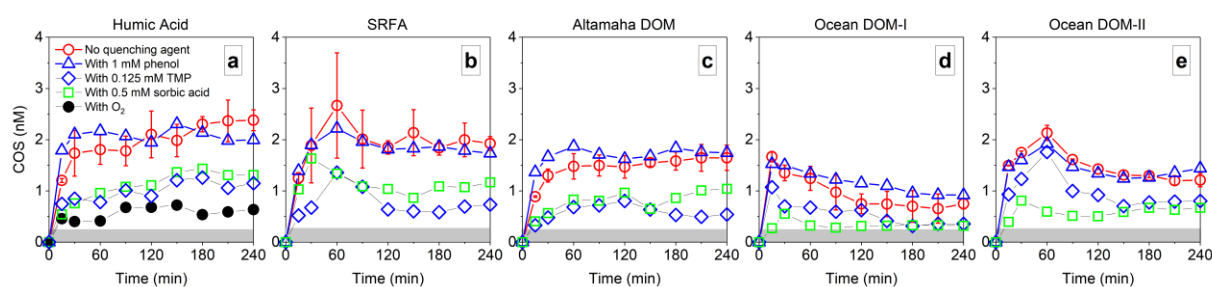


Figure 4-8. Influence of phenol, trimethylphenol (TMP), sorbic acid, and dissolved oxygen on COS formation ([CYS]= 14 μ M, [DOM]= 5 mg-C/L, pH= 8.3, temperature= 21 \pm 1 $^{\circ}$ C). The grey box shows the general level of dark formation, which was similar for both quenched and non-quenched samples.

Interestingly, these results suggested that ³DOM* is an important group of RIs involved in forming COS. The RIs that are likely involved include low-energy triplet states (³DOM*_{Low-energy}, ET < 250 kJ mol⁻¹) of CDOM rather than the high-energy triplet states (³DOM*_{High-energy}, ET > 250 kJ mol⁻¹) of CDOM. This statement is supported by several pieces of evidence, including the fact that, as noted in section 4.4.2, COS formation was found to be independent of DOM type. This independent behavior suggests that the responsible RIs form at similar quantum yields for different DOM isolates. One group of RIs that have shown such behavior include low-energy triplet states

($\Phi_{\text{low-triplet}}$), where similar quantum yields were found for a wide range of different DOM isolates.¹³ These isolates included four terrestrial isolates (e.g., SRFA), one autochthonous (e.g., Pony Lake fulvic acid (PLFA)) and eleven effluent DOMs from 2 municipal sewage plants and wastewater-contaminated rivers and lakes located in Shanghai.¹³ Thus, these RIs seem to be the most likely candidates for forming COS.¹³ Alternatively, the quantum yields ($\Phi_{\text{high-triplet}}$) of high-energy triplet states of CDOM vary significantly for different DOM isolates.¹³ In addition, the low-energy triplet states have been also found to have similar electron transfer capacities for different DOM isolates which implies that these triplet states possibly show similar reactivities toward different organic compounds.¹³ It is also critical to know that low-energy triplet states have been shown to be formed from quinone moieties of DOM, which subsequently serve as the source for the low-energy triplet pool of CDOM.¹³ This differs for the high-energy triplet states, which have been shown to be derived from ketone moieties of DOM and as a result, serve as the source for the high-energy triplet pool of CDOM.¹³ The fact that triplet states with different energies form from different DOM functional groups will also be relevant in later discussions (see section 4.4.7).

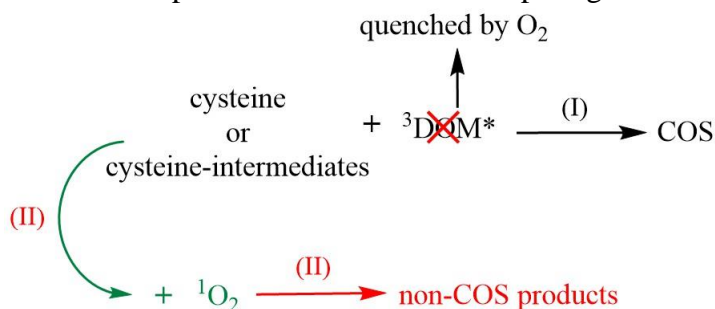
Moreover, the differences observed between quenching agents also seem to be well correlated to the ability for each quenching agent to compete with cysteine in reacting with $^3\text{DOM}^*$. However, no known studies have tried to investigate the reactions of these quenching agents specifically with low-energy triplet states of CDOM. Instead, these studies have evaluated the reaction rates with the high-energy triplet states or simply natural DOM isolates without distinguishing between high- and the low-energy triplet states.^{1,16,28,34,50} Nevertheless, it is hypothesized that the general pattern of high-energy triplet state reactivity with organic compounds and especially quenching agents can also be applied to those of the low-energy triplet states, even if high-energy triplet states are in general more reactive.^{13,50} However, there are controversial findings regarding the reaction of

phenolic compounds with the low-energy triplet states. For example, in one study,¹³ it was found that phenolic compounds like trimethylphenol can react with the low-energy triplet states although they were more reactive toward high-energy triplet states.¹³ In another study, though it was suggested that trimethylphenol can react with the vast majority of triplets excited states produced in EfOM, but the lower energy triplets may not be capable of oxidizing trimethylphenol.⁷ Overall, for high-energy-triplet-states, the pattern indicates that the $k_{quenching\ agent}^{3Sen*} \times [quenching\ agent]$ values of these quenching agents toward $^3DOM^*$ follows the pattern of sorbic acid = $2.2 \times 10^6 (s^{-1})^{22}$ > $O_2 = 5.6 \times 10^5 (s^{-1})^{49}$ > trimethylphenol = $5.4 \times 10^5 (s^{-1})^{15}$ > phenol = $4 \times 10^5 (s^{-1})^{27}$ > $k_{cysteine}^{3Sen*} \times [cysteine] = 0.56-1.54 \times 10^4 (s^{-1})^{16}$. Given these, all of the quenching agents are expected to react with $^3DOM^*$ at higher rates than cysteine. Thus, the hypothesis seemed relevant in this system as adding most of these quenching agents (excluding phenol) to DOM solutions decreased COS formation which supports the reaction of quenching agents with the low-energy triplet states at a similar pattern. Therefore, the reaction rates of quenching agents and cysteine with high-energy triplet states suggested that they can be used as proxy for the reaction of these compounds with the low-energy triplet states. In general, the decrease in COS formation followed the reactivity pattern although there were two outliers (see next paragraphs).

The COS formation was deterred by O_2 at higher degree (Fig. 4-8a) compared to other quenching methods (e.g., trimethylphenol and sorbic acid) falling out of the reactivity pattern. This can be explained through two main reasons. First, O_2 can quench more $^3DOM^*$ due to its lower singlet energy value ($E_S = 94 \text{ kJ Mol}^{-1}$)^{1,50}. Second, O_2 can increase cysteine degradation rate by forming 1O_2 through reaction with $^3DOM^*$ ¹ (see eqs. 1-4 in chapter 1), thus decreasing the chance of cysteine or most likely cysteine-based intermediates to form COS in the system (scheme 4-3).

$^1\text{O}_2$ has been shown to react with cysteine (pH 7.9) at a rate of $2 \pm 0.1 \times 10^{-5} \text{ (s}^{-1}\text{)}$ with $[\text{}^1\text{O}_2]_{\text{ss}} = 3.8 \times 10^{-14} \text{ (M)}$.¹⁶

Scheme 4-3. Proposed mechanisms for hampering the COS formation by O_2



However, the phenol was also an outlier that its presence did not decrease COS formation (Fig. 4.8a), which can be attributed to the capability of $^3\text{DOM}^*$ in oxidizing different phenols, which are shown to be highly modulated by phenol electron-richness.¹ Therefore, the results were different with trimethylphenol as an alkyl-substituted phenol which can be more readily oxidized by $^3\text{DOM}^*$ than phenol. More specifically, the reaction rate of trimethylphenol by SRFA has been reported to be 20× higher than that for phenol.²⁸ Overall, it is possible that phenol did not compete with cysteine to react with $^3\text{DOM}^*$, thus adding phenol did not influence COS formation.

Similar results were achieved with other DOM isolates when adding the same set of quenching agents, although the role of O_2 was not tested (Fig. 4-8). For this data, phenol did not influence COS formation. However, trimethylphenol decreased it by 60, 70, 40, and 20%, and sorbic acid by 50, 50, 40, and 25% with SRFA, Altamaha DOM, ocean DOM-I and DOM-II isolates, respectively (Fig. 4-8b, c, d and e). This again seems to imply that the types of $^3\text{DOM}^*$ species generating COS for all of these water types seem to be quite similar, which further supports the role of low-energy-triplet-states in these systems.

Lastly, it should be noted that CS_2 formation was actually observed when the Altamaha DOM was treated with trimethylphenol or sorbic acid under both dark and light conditions (Fig. 4-9).

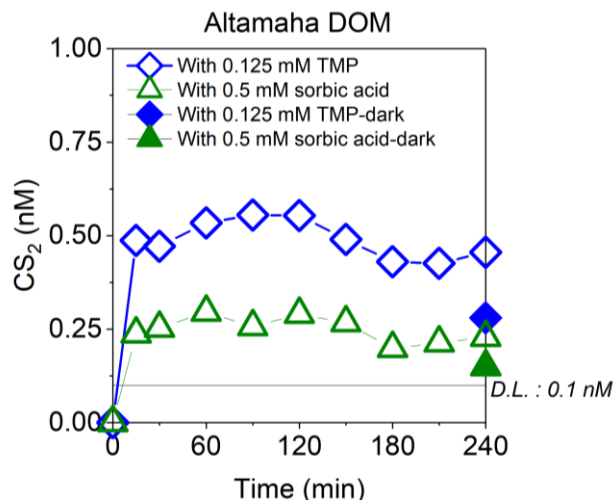
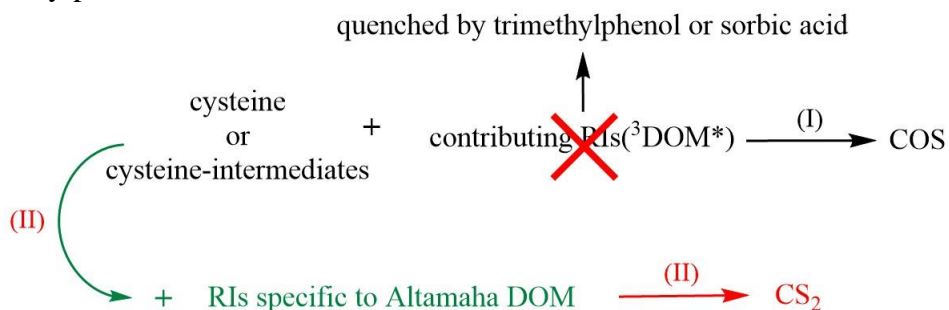


Figure 4-9. CS₂ formation upon the addition of trimethylphenol (TMP) or sorbic acid to solutions with Altamaha DOM ([CYS]= 14 μM, [DOM]= 5 mg-C/L, pH= 8.3, temperature= 21±1 °C). The DL for CS₂ is represented by a horizontal line.

In the dark, its concentration increased with trimethylphenol and sorbic acid, respectively, to 0.28 and 0.15 nM while in the presence of light, it further increased up to 2×, ranging between 0.4-0.55 and 0.2-0.3 nM (Fig. 4-9). Interestingly, these results suggested that ³DOM* is not involved in forming CS₂. It is likely that there are some specific RIs in this DOM isolate that can react with cysteine to form CS₂, as proposed in scheme 4-4, and their formation was increased in the presence of trimethylphenol or sorbic acid .

Scheme 4-4. Proposed mechanisms for CS₂ formation upon scavenging the ³DOM* by trimethylphenol or sorbic acid with Altamaha DOM



These RIs possibly are not quenched by these quenching agents. Interestingly, given the results with Altamaha DOM, where unlike to other DOM isolates, adding isopropanol increased COS formation (see section 4.4.6, *Influence of [•]OH*) or adding trimethylphenol or sorbic acid resulted in CS₂ formation, this DOM isolate possibly has some capacities in generating specific RIs which is not the case for other DOM isolates. However, further research is required to explore these specific RIs and the pathways which formed both COS and CS₂ under aforementioned experimental conditions.

4.4.7 Role of sodium borohydride treatment

Additional experiments were conducted with NaBH₄-treated DOM isolates. NaBH₄ was used to reduce the carbonyl functional groups (-C=O) in ketones to their corresponding alcohols. This reduction was conducted to remove ketones which were initially expected to be relevant precursors of ³DOM* to form COS in the system. However, the results indicated removing ketones from the solutions did not decrease COS formation suggesting that the ³DOM* derived from ketones were not involved in COS formation. These results further supported our previous data which suggested that high-energy-triplet-states, mainly derived from ketones, possibly are not involved in COS formation. For all DOM isolates, treating the DOM isolates with NaBH₄ increased COS formation by a factor of 1.1 to 2× (Fig. 4-10).

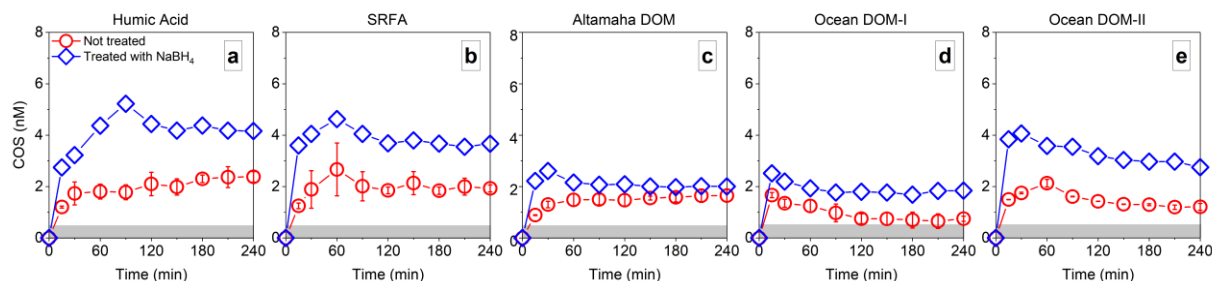
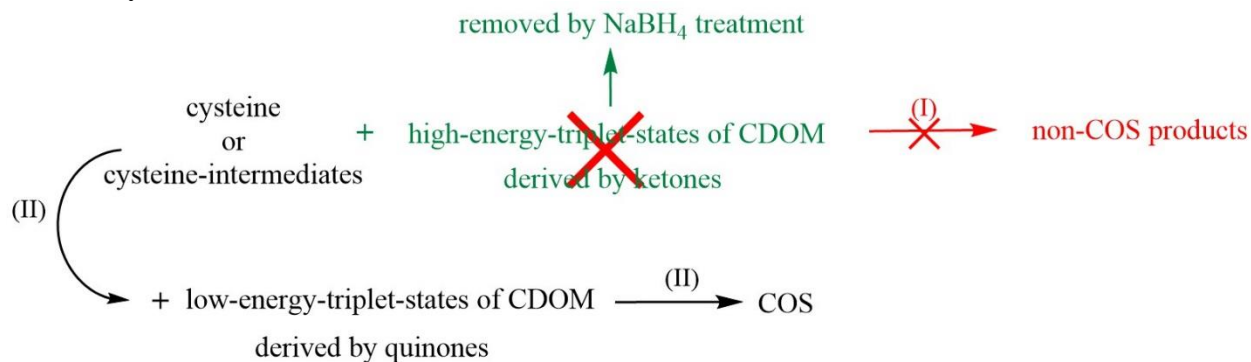


Figure 4-10. Role of sodium borohydride treatment on COS formation ($[CYS]= 14 \mu\text{M}$, $[DOM]= 5 \text{ mg-C/L}$, $\text{pH}= 8.3$, $\text{temperature}= 21\pm 1 \text{ }^\circ\text{C}$). The grey box shows the general level of dark formation, which was similar for all scenarios.

The resulting increase can be explained through by two possible reasons. First, since the carbonyl functional groups in ketones were removed from the system, their corresponding non-COS formation pathways (scheme 4-5, path (I)) were likely stopped as well, thus a more COS formation capacity was achieved in the system (scheme 4-5, path (II)).

Scheme 4-5. Proposed mechanisms for COS formation upon scavenging the $^3\text{DOM}^*$ derived from ketones by NaBH_4 treatment



Second, although the carbonyls were removed from the system, quinones were still present which are expected to form the low-energy-triplet-states of CDOM that have been already suggested as contributing RIs in COS formation (scheme 4-5, path (II)). Additionally, the inverse effect of carbonyls on COS formation has been also proposed by a previous study.⁴⁰ It was found that the COS formation dramatically decreased upon addition of different amounts of formaldehyde (the simplest carbonyl group) ranging from 0.1 to 6 mM to Aahai lake water (an artificial lake, Beijing

city).⁴⁰ Overall, these results further supported the findings of the effect of DOM type on COS formation (section 4.4.2) where the contribution of low-energy-triplet-states derived from quinones was suggested. However, further research is recommended to better investigate the contribution of quinones in COS formation by using other reduction treatments such as using dithionite to selectively reduced quinones to hydroquinones².

4.5 Conclusions

The aim of this study was to evaluate how different types/concentrations of DOM and the RIs formed by DOM (e.g., $^3\text{DOM}^*$ and $\bullet\text{OH}$) affected the photochemical formation of COS and CS_2 with organic sulfur compounds such as cysteine. This effect was evaluated with five different natural DOM isolates ranging from freshwater to seawater. The results indicated CS_2 did not form above the DL with any of the DOM isolates under any condition. Whereas, COS formation increased with DOM and cysteine under both dark and light conditions while the effect was more strong in the light. This increase was similar for all of the DOM isolates where COS formation increased with light over 4 h with cysteine to up to 1.2 to 2.4 nM. Unlike to similar formation levers, the kinetics of COS formation was slightly different with different DOM isolates, but the general trend implied that the formation was limited by RIs. This was further supported when the effect of the concentration or speciation of cysteine was tested where the formation kinetics were still the same but shifted at some time points. In addition, increasing DOM concentration decreased COS formation which implied the dual role of DOM on concomitantly forming and quenching the RIs. It was also found that when isopropanol, the quenching agent of $\bullet\text{OH}$, was added to solutions, the COS formation was not affected which suggested that $\bullet\text{OH}$ was not involved in the formation pathways. However, when phenol, trimethylphenol, sorbic acid or O_2 , the $^3\text{DOM}^*$ quenching agents, were added to the solutions, the COS formation was affected but depending on the type of

the quenching agent. With phenol, COS formation was not affected while with trimethylphenol, sorbic acid or O₂ the formation was dramatically decreased up to 80% with O₂. This result suggested that ³DOM* could be a major contributing RI in forming COS with cysteine. Furthermore, treating the DOM isolates with NaBH₄ to reduce the ketones/aldehydes to their corresponding alcohols, increased COS formation which implied that the RIs derived from ketones were not involved in COS formation pathways. Overall, these findings indicate that COS formation can be dramatically enhanced with DOM since the RIs formed by DOM in the sunlight, specially the ³DOM*, can react with cysteine to form COS.

4.6 References

- (1) McNeill, K.; Canonica, S. Triplet State Dissolved Organic Matter in Aquatic Photochemistry: Reaction Mechanisms, Substrate Scope, and Photophysical Properties. *Environ. Sci. Process. Impacts* **2016**, *18* (11), 1381–1399.
- (2) Del Vecchio, R.; Schendorf, T. M.; Blough, N. V. Contribution of Quinones and Ketones/Aldehydes to the Optical Properties of Humic Substances (HS) and Chromophoric Dissolved Organic Matter (CDOM). *Environ. Sci. Technol.* **2017**, *51* (23), 13624–13632.
- (3) Dalrymple, R. M.; Carfagno, A. K.; Sharpless, C. M. Correlations between Dissolved Organic Matter Optical Properties and Quantum Yields of Singlet Oxygen and Hydrogen Peroxide. *Environ. Sci. Technol.* **2010**, *44* (15), 5824–5829.
- (4) Mangalgi, K. P.; Blaney, L. Elucidating the Stimulatory and Inhibitory Effects of Dissolved Organic Matter from Poultry Litter on Photodegradation of Antibiotics. *Environ. Sci. Technol.* **2017**, *51* (21), 12310–12320.
- (5) Guerard, J. J.; Chin, Y.-P.; Mash, H.; Hadad, C. M. Photochemical Fate of Sulfadimethoxine in Aquaculture Waters. *Environ. Sci. Technol.* **2009**, *43* (22), 8587–8592.
- (6) Ma, J.; Del Vecchio, R.; Golanoski, K. S.; Boyle, E. S.; Blough, N. V. Optical Properties of Humic Substances and CDOM: Effects of Borohydride Reduction. *Environ. Sci. Technol.* **2010**, *44* (14), 5395–5402.

- (7) O'Connor, M.; Helal, S. R.; Latch, D. E.; Arnold, W. A. Quantifying Photo-Production of Triplet Excited States and Singlet Oxygen from Effluent Organic Matter. *Water Res.* **2019**, *156*, 23–33.
- (8) McKay, G.; Couch, K. D.; Mezyk, S. P.; Rosario-Ortiz, F. L. Investigation of the Coupled Effects of Molecular Weight and Charge-Transfer Interactions on the Optical and Photochemical Properties of Dissolved Organic Matter. *Environ. Sci. Technol.* **2016**, *50* (15), 8093–8102.
- (9) Bodhipaksha, L. C.; Sharpless, C. M.; Chin, Y.-P.; Sander, M.; Langston, W. K.; MacKay, A. A. Triplet Photochemistry of Effluent and Natural Organic Matter in Whole Water and Isolates from Effluent-Receiving Rivers. *Environ. Sci. Technol.* **2015**, *49* (6), 3453–3463.
- (10) Cawley, K. M.; Korak, J. A.; Rosario-Ortiz, F. L. Quantum Yields for the Formation of Reactive Intermediates from Dissolved Organic Matter Samples from the Suwannee River. *Environ. Eng. Sci.* **2014**, *32* (1), 31–37.
- (11) Sharpless, C. M.; Blough, N. V. The Importance of Charge-Transfer Interactions in Determining Chromophoric Dissolved Organic Matter (CDOM) Optical and Photochemical Properties. *Environ. Sci. Process. Impacts* **2014**, *16* (4), 654–671.
- (12) Wenk, J.; Eustis, S. N.; McNeill, K.; Canonica, S. Quenching of Excited Triplet States by Dissolved Natural Organic Matter. *Environ. Sci. Technol.* **2013**, *47* (22), 12802–12810.
- (13) Zhou, H.; Yan, S.; Lian, L.; Song, W. Triplet-State Photochemistry of Dissolved Organic Matter: Triplet-State Energy Distribution and Surface Electric Charge Conditions. *Environ. Sci. Technol.* **2019**.
- (14) Maizel, A. C.; Remucal, C. K. Molecular Composition and Photochemical Reactivity of Size-Fractionated Dissolved Organic Matter. *Environ. Sci. Technol.* **2017**, *51* (4), 2113–2123.
- (15) Modiri Gharehveran, M.; Shah, A. D. Indirect Photochemical Formation of Carbonyl Sulfide and Carbon Disulfide in Natural Waters: Role of Organic Sulfur Precursors, Water Quality Constituents, and Temperature. *Environ. Sci. Technol.* **2018**, *52* (16), 9108–9117.
- (16) Chu, C.; Erickson, P. R.; Lundeen, R. A.; Stamatelatos, D.; Alaimo, P. J.; Latch, D. E.; McNeill, K. Photochemical and Nonphotochemical Transformations of Cysteine with Dissolved Organic Matter. *Environ. Sci. Technol.* **2016**, *50* (12), 6363–6373.

- (17) Adams, G. E.; Aldrich, J. E.; Bisby, R. H.; Cundall, R. B.; Redpath, J. L.; Willson, R. L. Selective Free Radical Reactions with Proteins and Enzymes: Reactions of Inorganic Radical Anions with Amino Acids. *Radiat. Res.* **1972**, *49* (2), 278–289.
- (18) Zepp, R. G.; Andreae, M. O. Factors Affecting the Photochemical Production of Carbonyl Sulfide in Seawater. *Geophys. Res. Lett.* **1994**, *21* (25), 2813–2816.
- (19) Vione, D.; Minella, M.; Maurino, V.; Minero, C. Indirect Photochemistry in Sunlit Surface Waters: Photoinduced Production of Reactive Transient Species. *Chem. – A Eur. J.* **2014**, *20* (34), 10590–10606.
- (20) Huang, J.; Mabury, S. A. Steady-State Concentrations of Carbonate Radicals in Field Waters. *Environ. Toxicol. Chem.* **2009**, *19* (9), 2181–2188.
- (21) Flöck, O. R.; Andreae, M. O.; Dräger, M. Environmentally Relevant Precursors of Carbonyl Sulfide in Aquatic Systems. *Mar. Chem.* **1997**, *59* (1–2), 71–85.
- (22) Pos, W. H.; Riemer, D. D.; Zika, R. G. Carbonyl Sulfide (OCS) and Carbon Monoxide (CO) in Natural Waters: Evidence of a Coupled Production Pathway. *Mar. Chem.* **1998**, *62* (1–2), 89–101.
- (23) Grebel, J. E.; Pignatello, J. J.; Mitch, W. A. Sorbic Acid as a Quantitative Probe for the Formation, Scavenging and Steady-State Concentrations of the Triplet-Excited State of Organic Compounds. *Water Res.* **2011**, *45* (19), 6535–6544.
- (24) Rosario-Ortiz, F. L.; Canonica, S. Probe Compounds to Assess the Photochemical Activity of Dissolved Organic Matter. *Environ. Sci. Technol.* **2016**, *50* (23), 12532.
- (25) Guerard, J. J.; Miller, P. L.; Trouts, T. D.; Chin, Y.-P. The Role of Fulvic Acid Composition in the Photosensitized Degradation of Aquatic Contaminants. *Aquat. Sci.* **2009**, *71* (2), 160–169.
- (26) Bahnmüller, S.; Von Gunten, U.; Canonica, S. Sunlight-Induced Transformation of Sulfadiazine and Sulfamethoxazole in Surface Waters and Wastewater Effluents. *Water Res.* **2014**, *57*, 183–192.
- (27) Zeng, T.; Arnold, W. A. Pesticide Photolysis in Prairie Potholes: Probing Photosensitized Processes. *Environ. Sci. Technol.* **2013**, *47* (13), 6735.
- (28) Canonica, S.; Jans, U.; Stemmler, K.; Hoigne, J. Transformation Kinetics of Phenols in Water: Photosensitization by Dissolved Natural Organic Material and Aromatic Ketones. *Environ. Sci. Technol.* **1995**, *29* (7), 1822–1831.

- (29) Lloyd, A. C.; Darnall, K. R.; Winer, A. M.; Pitts, J. N. Relative Rate Constants for the Reactions of OH Radicals with Isopropyl Alcohol, Diethyl and DI-n-Propyl Ether at 305 ± 2 K. *Chem. Phys. Lett.* **1976**, *42* (2), 205–209.
- (30) Bonin, J.; Janik, I.; Janik, D.; Bartels, D. M. Reaction of the Hydroxyl Radical with Phenol in Water Up to Supercritical Conditions. *J. Phys. Chem. A* **2007**, *111* (10), 1869–1878.
- (31) Aschmann, S. M.; Arey, J.; Atkinson, R. Rate Constants for the Reactions of OH Radicals with 1,2,4,5-Tetramethylbenzene, Pentamethylbenzene, 2,4,5-Trimethylbenzaldehyde, 2,4,5-Trimethylphenol, and 3-Methyl-3-Hexene-2,5-Dione and Products of OH + 1,2,4,5-Tetramethylbenzene. *J. Phys. Chem. A* **2013**, *117* (12), 2556–2568.
- (32) Koprivnjak, J.-F.; Pfromm, P. H.; Ingall, E.; Vetter, T. A.; Schmitt-Kopplin, P.; Hertkorn, N.; Frommberger, M.; Knicker, H.; Perdue, E. M. Chemical and Spectroscopic Characterization of Marine Dissolved Organic Matter Isolated Using Coupled Reverse Osmosis–electrodialysis. *Geochim. Cosmochim. Acta* **2009**, *73* (14), 4215–4231.
- (33) Tinnacher, R. M.; Honeyman, B. D. A New Method to Radiolabel Natural Organic Matter by Chemical Reduction with Tritiated Sodium Borohydride. *Environ. Sci. Technol.* **2007**, *41* (19), 6776–6782.
- (34) Golanoski, K. S.; Fang, S.; Del Vecchio, R.; Blough, N. V. Investigating the Mechanism of Phenol Photooxidation by Humic Substances. *Environ. Sci. Technol.* **2012**, *46* (7), 3912–3920.
- (35) Schendorf, T. M.; Del Vecchio, R.; Koech, K.; Blough, N. V. A Standard Protocol for NaBH₄ Reduction of CDOM and HS. *Limnol. Oceanogr. Methods* **2016**, *14* (6), 414–423.
- (36) Hansen, A. M.; Kraus, T. E. C.; Pellerin, B. A.; Fleck, J. A.; Downing, B. D.; Bergamaschi, B. A. Optical Properties of Dissolved Organic Matter (DOM): Effects of Biological and Photolytic Degradation. *Limnol. Oceanogr.* **2016**, *61* (3), 1015–1032.
- (37) McKnight, D. M.; Boyer, E. W.; Westerhoff, P. K.; Doran, P. T.; Kulbe, T.; Andersen, D. T. Spectrofluorometric Characterization of Dissolved Organic Matter for Indication of Precursor Organic Material and Aromaticity. *Limnol. Oceanogr.* **2001**, *46* (1), 38–48.
- (38) Cory, R. M.; McKnight, D. M.; Chin, Y.-P.; Miller, P.; Jaros, C. L. Chemical Characteristics of Fulvic Acids from Arctic Surface Waters: Microbial Contributions and Photochemical Transformations. *J. Geophys. Res. Biogeosciences* **2007**, *112* (G4).

- (39) Peuravuori, J.; Pihlaja, K. Molecular Size Distribution and Spectroscopic Properties of Aquatic Humic Substances. *Anal. Chim. Acta* **1997**, *337* (2), 133–149.
- (40) Du, Q.; Mu, Y.; Zhang, C.; Liu, J.; Zhang, Y.; Liu, C. Photochemical Production of Carbonyl Sulfide, Carbon Disulfide and Dimethyl Sulfide in a Lake Water. *J. Environ. Sci.* **2016**, *51* (September), 1–11.
- (41) Canonica, S.; Laubscher, H.-U. Inhibitory Effect of Dissolved Organic Matter on Triplet-Induced Oxidation of Aquatic Contaminants. *Photochem. Photobiol. Sci.* **2008**, *7* (5), 547–551.
- (42) Brezonik, P. L.; Fulkerson-Brekken, J. Nitrate-Induced Photolysis in Natural Waters: Controls on Concentrations of Hydroxyl Radical Photo-Intermediates by Natural Scavenging Agents. *Environ. Sci. Technol.* **1998**, *32* (19), 3004–3010.
- (43) Zepp, R. G.; Hoigne, J.; Bader, H. Nitrate-Induced Photooxidation of Trace Organic Chemicals in Water. *Environ. Sci. Technol.* **1987**, *21* (5), 443–450.
- (44) Buxton, G.; Greenstock, C.; Helman, W.; Ross, A. Critical Review of Rate Constants for Reactions of Hydrated Electrons, Hydrogen Atoms and Hydroxyl Radicals ($\cdot\text{OH}/\cdot\text{O}^{\text{sup}} - ^{\wedge}$ in Aqueous Solution. *J. Phys. Chem. Ref. Data* **2015**, *44* (1), 1.
- (45) Larson, R. A.; Zepp, R. G. Reactivity of the Carbonate Radical with Aniline Derivatives. *Environ. Toxicol. Chem.* **1988**, *7* (4), 265–274.
- (46) Canonica, S.; Kohn, T.; Mac, M.; Real, F. J.; Wirz, J.; von Gunten, U. Photosensitizer Method to Determine Rate Constants for the Reaction of Carbonate Radical with Organic Compounds. *Environ. Sci. Technol.* **2005**, *39* (23), 9182–9188.
- (47) Wenk, J.; Aeschbacher, M.; Sander, M.; Gunten, U. von; Canonica, S. Photosensitizing and Inhibitory Effects of Ozonated Dissolved Organic Matter on Triplet-Induced Contaminant Transformation. *Environ. Sci. Technol.* **2015**, *49* (14), 8541–8549.
- (48) Trujillo, M.; Alvarez, B.; Radi, R. One- and Two-Electron Oxidation of Thiols: Mechanisms, Kinetics and Biological Fates. *Free Radic. Res.* **2016**, *50* (2), 150–171.
- (49) Jacobs, L. E.; Fimmen, R. L.; Chin, Y.-P.; Mash, H. E.; Weavers, L. K. Fulvic Acid Mediated Photolysis of Ibuprofen in Water. *Water Res.* **2011**, *45* (15), 4449–4458.
- (50) Zepp, R. G.; Schlotzhauer, P. F.; Sink, R. M. Photosensitized Transformations Involving Electronic Energy Transfer in Natural Waters: Role of Humic Substances. *Environ. Sci. Technol.* **1985**, *19* (1), 74–81.

- (51) Barbosa, M. O.; Ribeiro, A. R.; Ratola, N.; Hain, E.; Homem, V.; Pereira, M. F. R.; Blaney, L.; Silva, A. M. T. Spatial and Seasonal Occurrence of Micropollutants in Four Portuguese Rivers and a Case Study for Fluorescence Excitation-Emission Matrices. *Sci. Total Environ.* **2018**, *644*, 1128–1140.

CHAPTER 5. INFLUENCE OF DOM ON COS AND CS₂ FORMATION FROM DIMETHYL SULFIDE (DMS) DURING SUNLIGHT PHOTOLYSIS

5.1 Abstract

The role of DOM type and concentration on COS and CS₂ formation with DMS was evaluated. DMS (14 μM) and one type of DOM isolate (5 mg-C/L) were spiked into buffered synthetic water at pH 8.3. Five different types of DOM isolates were chosen ranging from freshwater to ocean water. These isolates included two freshwater isolates, Suwanee River fulvic acid (SRFA) and Aldrich humic acid, a river DOM isolate (Altamaha River, GA), and two ocean water isolates (Gulf Stream in the Atlantic Ocean). These solutions were exposed to simulated sunlight for up to 4 h. Results indicated that CS₂ did not form under any of the conditions with any type of DOM. However, the presence of DOM with DMS enhanced COS formation while increasing DOM concentration further increased COS formation. The role of RIs such as ³DOM* and •OH was also investigated by adding selective quenching agents. Results indicated that, with isopropanol, an efficient •OH scavenger, COS formation was dramatically decreased. Similarly, with ³DOM* quenching agents, COS formation decreased but to a higher degree. Adding phenol, trimethylphenol, sorbic acid and O₂ substantially decreased COS concentration during 4 h irradiation. Moreover, treating DOM isolates with sodium borohydride to reduce ketone/aldehydes to corresponding alcohols, increased COS formation. These results indicated that both •OH and ³DOM* were involved in COS formation with DMS while •OH was not found to be a contributing RI with cysteine. Overall, these findings implied that the COS formation mechanisms with DMS were likely different than cysteine and involved different RIs such as •OH.

5.2 Introduction

DMS is an important organic sulfur compound to evaluate in terms of forming COS and CS₂ since it represents one of the major marine sources of organic sulfur in the oceans.¹⁻³ Previously, it has been observed that DMS can form COS and CS₂ by photoreacting in natural waters.^{4,5} In one study, the COS formation with DMS was reported upon irradiation of the synthetic natural waters (coastal Atlantic water (near Jekyll Island, GA) and Gulf of Mexico (near Turkey Point, FL)) with xenon lamp, which were amended with 3.4 mg-C/L SRFA prior to irradiation.⁵ Also, in our previous study,⁴ DMS was found to form COS and CS₂ with some of the natural waters when irradiated by simulated sunlight for 4 h.⁴ While natural waters have different water quality constituents which can form variety of RIs (³DOM*,⁶ •OH and ¹O₂^{6,7}, Br• and Cl•,^{5,8,9} and the carbonate radical (CO₃•⁻)⁶) in the presence of sunlight, it has been shown that DOM plays an important role in terms of forming RIs such as ³DOM* and •OH.⁷ The type and concentration of DOM vary substantially in different natural waters.^{10,11} For example, in our previous study, nine different natural waters varied widely in DOM concentration ranging from 2.1-16.5 mg-C/L DOC.⁴ In addition, it was found that COS and CS₂ formation was correlated to DOC concentration in the presence of DMS.⁴ However, it was hard to investigate the role of DOM type/concentration or the role of specific RIs on COS and CS₂ formation since natural waters are more complex matrices. Therefore, a cleaner matrix is required in order to better investigate the role of DOM or the specific RIs in COS and CS₂ formation with DMS.

However, no known studies have experimentally assessed how DOM type/concentration or the role of the specific RIs generated from it affects COS and CS₂ formation with DMS during sunlight photolysis. Therefore, this study attempted to clarify this issue by answering three major questions: (i) how do different concentrations and types of DOM affect COS and CS₂ formation with DMS,

(ii) if DOM does play an important role, what are the contributions of different RIs in forming COS and CS₂, and (iii) how does the role of DOM concentration compare to the role of DMS concentration, in forming COS and CS₂? To address these questions, five different DOM isolates ranging from freshwater to seawater were evaluated. Synthetic solutions containing DMS and one DOM isolate over varied concentrations were exposed to simulated sunlight for 4 h. Certain solutions were amended with isopropanol, phenol, trimethylphenol, sorbic acid, or O₂ to selectively quench RIs. In addition, NaBH₄ was used to selectively reduce ketones to their corresponding alcohols to assess if the RIs formed by ketones were involved in COS and CS₂ formation with DMS. The results indicated that CS₂ did not form above the DL under any condition with any type of the DOM isolate tested. However, COS formation with DMS increased in the presence of DOM, where DOM was found to be the limiting reactant rather than DMS. In addition, increasing the concentration of DOM further increased COS formation. When the role of RIs were assessed, both •OH and ³DOM* seemed to be involved in COS formation with DMS. Finally, this study suggested that DOM can enhance COS formation in the presence of DMS by forming RIs specially •OH and ³DOM*. Interestingly, the RIs involved in forming COS from DMS differed from those involved in forming COS from cysteine (see chapter 4). However, CS₂ formation from DMS, as observed with cysteine, also seemed to require RIs generated from other water quality constituents present in natural waters, rather than from those generated from DOM alone.

5.3 Materials and Methods

5.3.1 Description of standards, reagents, and stock preparation

Most of the standards, reagents and the stock solutions used were identical to those described in chapters 2-4. In addition, stock solutions of DMS were prepared by placing 10 μL of pure liquid

DMS (=0.0084 g DMS with $\rho = 840 \text{ kg/m}^3$) into 10 mL acetonitrile to reach a final concentration of 13.5 mM.

5.3.2 Collection, characterization and modification of different DOM isolates

The different DOM isolates tested were identical to those used in chapter 4. The location, characterization and sodium borohydride (NaBH_4) modification of these isolates are also described in chapter 4.

5.3.3 Photochemical reactor setup

The solar simulator (OAI Tri-Sol; AM 1.5G filter), photochemical reactors and the experimental conditions used for the reactor were identical to those described in previous chapters.

5.3.4 Experimental procedure

Kinetic experiments were performed using synthetic solutions that contained 14 μM DMS and 5 mg-C/L of one DOM isolate (humic acid, SRFA, Altamaha DOM, ocean DOM-I, and ocean DOM-II). These synthetic solutions were also buffered at pH of 8.3 (a relevant pH in natural waters) with 10 mM tris buffer and were initially purged with N_2 for 30 min to remove dissolved O_2 . These solutions (11 mL) were then placed into the reactors and either left in the dark or exposed to simulated sunlight over 4 h. These experiments were then repeated, where each DOM isolate was instead pre-treated with NaBH_4 . Additional experiments were also performed in which the synthetic solutions varied in: (i) DOM concentrations ranging between 0.5-20 mg-C/L, and (ii) pH from 7 to 10 using tris buffer. Some of the solutions were also amended with: (i) isopropanol (10 mM), (ii) phenol (1 mM), (iii) trimethylphenol (0.125 mM), (iv) sorbic acid (0.5 mM), or (v) O_2 (for O_2 experiments, the solutions were not purged with N_2 to contain $[\text{O}_2]_0 \approx 8.9 \text{ mg/L}$ at 20°C since DOM isolates were left in equilibrium with the atmosphere during storage). Isopropanol was

used to primarily scavenge $\bullet\text{OH}$ whereas phenol, trimethylphenol, sorbic acid, and O_2 were used to primarily scavenge $^3\text{DOM}^*$ (for reaction rates see Table 4-1).

5.3.5 Analytical methods

COS , CS_2 , and DMS were analyzed by headspace GC-MS (Agilent 6420), as described in Chapter 2.

5.4 Results and Discussion

5.4.1 Characterization of DOM

The characterizations and optical properties of DOM isolates are identical to those in chapter 4.

5.4.2 COS and CS_2 formation from different DOM isolates

When DMS along with each type of DOM isolate were added to the reaction solutions, CS_2 did not form above the DL under any conditions with any type of DOM isolate. These results matched our previous study, where CS_2 did not form above the DL with DMS in most of the natural waters tested.⁴ Unlike CS_2 , the presence of DOM increased COS formation with DMS slightly in the dark and more dramatically in the presence of light (Fig. 5-1). With all five DOM isolates, COS did not form above the DL in the dark with no DMS but increased to similar low concentrations for all DOM isolates in the presence of DMS , ranging between 0.1-0.15 nM after 4 h irradiation (Fig. 5-1). This slight increase in formation of COS with DMS in the dark was different from our previous results where COS did not form above the DL in the dark when nine different natural waters were spiked with DMS .⁴ Moreover, with light after 4 h irradiation, COS formation was increased between 0.17 to 0.76 nM without DMS while increasing even further with DMS to up to 10 \times higher concentrations (0.8 to 1.5 nM) when compared to the DMS -spiked dark control (Fig. 5-1).

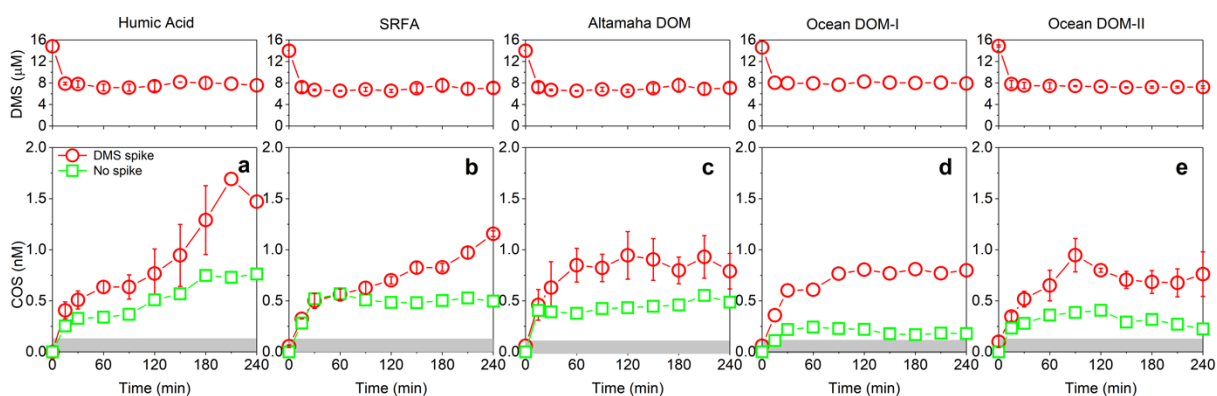


Figure 5-1. Effect of DOM type on COS formation during sunlight photolysis when not spiked or spiked with DMS ($[DMS]_0 = 14 \mu\text{M}$, $[DOM]_0 = 5 \text{ mg-C/L}$, $\text{pH} = 8.3$, $\text{temperature} = 21 \pm 1 \text{ }^\circ\text{C}$). The grey box shows the dark formation which was similar for all scenarios.

These results suggested that the precursors derived from the inherent dissolved organic sulfur (DOS) present in these DOM isolates were able to form some degree of COS. However, COS increased further once DMS was added. This result matched the findings of previous studies where DMS increased COS formation in the presence of sunlight.^{4,5} In one of these studies, a qualitative increase was reported for COS formation.⁹ However, in our previous study DMS increased COS formation up to 1.5 nM in the presence of sunlight while DMS did not form COS above the DL in the dark when different natural waters were tested.⁴

Surprisingly though, these different DOM isolates formed relatively similar amount of COS (0.8 to 1.5 nM) which suggested that one of the major RIs involved in COS formation with DMS possibly formed at similar quantum yields (Φ) from these DOM isolates. The RIs that are likely involved include low-energy triplet states ($\text{ET} < 250 \text{ kJ mol}^{-1}$) of chromophoric dissolved organic matter (CDOM), which appear to form at similar quantum yields for a wide range of DOM types¹². Further support of these RIs serving as the primary candidates for COS formation with DMS will also be provided by results discussed in later sections. Unlike COS formation levels, the kinetics

of COS formation were slightly different with DOM isolates (Fig. 5-1). These kinetics with DMS were similar to those with cysteine, which implied that with most of the DOM isolates, the formation reaction was limited by RIs rather than DMS (for details see chapter 4).

Furthermore, the degradation rates and kinetics of DMS loss were also very similar when testing all DOM isolates both under dark and light conditions. DMS degradation was ~10% in the dark while in the light DMS concentration sharply decreased by 45% just after 15 min and slowly decreased to 50% over 4 h of irradiation (Fig. 5-1). These results suggested that the DOM isolates generated RIs that degraded DMS through similar photochemical pathways. Interestingly, these results, which did not have a strong dependence on DOM type, also differed from other studies that evaluated organic precursor degradation where DOM type had a strong effect.¹³⁻¹⁵ However, none of these studies investigated the degradation of DMS. Although the photosensitized loss of DMS has been reported in presence of DOM,¹⁶⁻¹⁸ the role of DOM type on DMS photochemical breakdown is poorly understood. It is proposed previously¹⁷ that the photochemical loss of DMS occurs through a binding (or catalytic) mechanism, presumably involving components of DOM and perhaps reactive species that are generated by DOM. These species included photochemically generated singlet oxygen ($^1\text{O}_2$), $\bullet\text{OH}$ and hydrogen peroxide, but for all these RIs, reaction rates were too slow to be a significant removal mechanism for DMS.¹⁷ For example, a photochemical loss of 15% has been reported for DMS through forming its only identified photochemical product, DMSO.¹⁷ It should also be noted that, the predominant products of DMS photodegradation have not been identified.¹⁷ Therefore, it is hard to investigate the photochemical degradation of DMS through assessing its minor product COS with a very low yield formation (<0.01% yield). Further research will be helpful to explore the effect of DOM type or RIs formed by DOM on photochemical loss of DMS.

Moreover, it is noteworthy that COS formed in less degree with DMS than cysteine, which is consistent with previous findings.^{4,5} With DMS, the COS formation was $< 0.3\times$ lower than with cysteine (for details see chapter 4) when averaging for all DOM isolates. Similarly, in previous studies,^{4,5} COS formation was also lower with DMS than cysteine by $0.3\times$ in two different natural waters ($[\text{cysteine or DMS}]_0 = 10 \mu\text{M}$)⁵, and $< 0.5\times$ with one natural water from Louisiana ($[\text{cysteine or DMS}]_0 = 14 \mu\text{M}$)⁴ (for details see chapter 3). These results further supported our previous work where cysteine was proposed to be a stronger precursor for COS formation than DMS.⁴ The results also indicated that with both DMS and cysteine (chapter 4), COS formation was independent of DOM type. This can suggest the presence of a common RI involved in both pathways, such as low-energy triplet states of DOM. This RI has been proposed to be involved in COS formation with cysteine (for details see chapter 4), and its presence will be assessed in more details with DMS in later sections.

5.4.3 Effect of DOM concentration

The results with varying DOC concentration from 0.5 to 20 mg-C/L indicated that increasing DOM concentration did not affect COS dark formation, but increased COS formation in the presence of light (Fig. 5-2). For example, COS formation increased by up to $11\times$ with SRFA when DOM concentration increased from 0.5 to 20 mg-C/L after 4 h irradiation (Fig. 5-2).

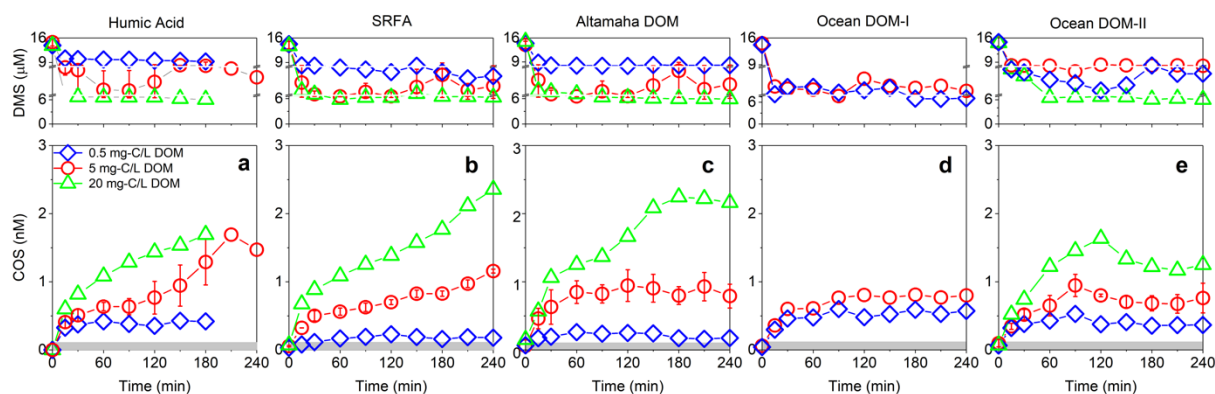


Figure 5-2. Effect of DOM concentration on COS formation ($[DMS]= 14 \mu M$, $[DOM]= 5 \text{ mg-C/L}$, $pH= 8.3$, temperature= $21 \pm 1 \text{ }^\circ C$). The grey box shows the general level of dark formation, which was similar for all scenarios. The stock concentration of ocean DOM-I was 12.7 mg-C/L and it was not possible to test 20 mg-C/L .

The degradation of DMS was also increased by increasing DOM concentration, which matched the previous results where the photochemical degradation of DMS was found to be correlated to the concentration of DOM.^{16,17}

However, when compared to cysteine, different effects of DOM concentration on COS formation was observed. This implied that possibly there are different RIs involved in COS formation with DMS versus cysteine which the formation rates of these RIs were correlated with DOM concentration. This RI is likely the $\bullet OH$ (see later sections) which was not involved in COS formation with cysteine (for details see chapter 4). Previously, a linear relationship between the rate of $\bullet OH$ production and SRFA concentration was reported under anaerobic conditions.¹⁹ When the DOM concentration was increased from 3 to 18 mg/L , the $\bullet OH$ production rate was also increased under irradiation at both 310 and 320 nm ($pH= 8.5$).¹⁹ In another study, higher apparent steady-state $\bullet OH$ concentrations were observed when 5 different DOM isolates were increased in concentration from 0 to 16 mg-C/L .²⁰ So, possibly higher DOM concentrations favored higher RIs production such as $\bullet OH$ which were involved in producing COS with DMS (see later sections)

and consequently increased COS formation. Moreover, it should also be noted that, similar to cysteine, DOM could also quench the RIs²¹⁻²³ such as $^3\text{DOM}^*$ ^{24,25}, $\bullet\text{OH}$ and $\text{CO}_3^{\bullet-}$ ^{26,27} (for details see eqs. 1- 3 in chapter 4). However, these results implied that in this case a greater percentage of contributing RIs were formed than were quenched when increasing the DOM concentration, and this can explain the increase of COS formation by increasing the concentration of DOM (Figure 5-2).

5.4.4 Effect of pH

To further elucidate the effect of DMS on COS formation, the effect of pH was also investigated (only with humic acid) since it has been shown previously that pH can affect the photo-degradation of DMS in nitrate-photolysis-induced natural waters.²⁸ Results indicated that DMS photodegradation slightly decreased by increasing the pH of the solutions (Fig. 5-3). Specifically, DMS decreased by 4 and 15% when pH increased from 7 to 8.3 and 10, respectively (Fig. 5-3). Alternatively, the COS formation was also decreased by increasing the pH but more significantly, as it decreased by 60 and 92% when pH increased from 7 to 8.3 and 10, respectively (Fig. 5-3). However, it is unclear as whether this substantial loss in COS formation was due to the slight decrease in DMS photo-degradation or not, since base-catalyzed hydrolysis of COS can also occur, which is highly pH-dependent (for details see chapter 4). However, future research is required to elucidate if there is any pH dependency on this reactivity although it needs to be assessed by controlling the effect of hydrolysis.

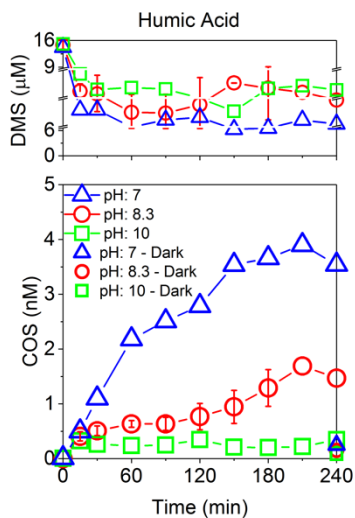


Figure 5-3. Effect of pH on COS formation ([DOM]= 5 mg-C/L, [DMS]= 14 μ M, temperature= 21 \pm 1 $^{\circ}$ C)

5.4.5 Role of quenching agents

Influence of \bullet OH

In order to further elucidate the role of \bullet OH in forming COS, 10 mM isopropanol was added to the reaction solutions. As expected, isopropanol addition did not affect COS dark formation (Fig. 5-4). However, in the presence of light, isopropanol addition led to decrease in COS formation for all of the tested DOM isolates (Fig. 5-4). Specifically, COS concentration after 4 h irradiation decreased by 65, 60, 35, 40, and 35% with humic acid, SRFA, Altamaha DOM, ocean DOM-I and ocean DOM-II, respectively (Fig. 5-4).

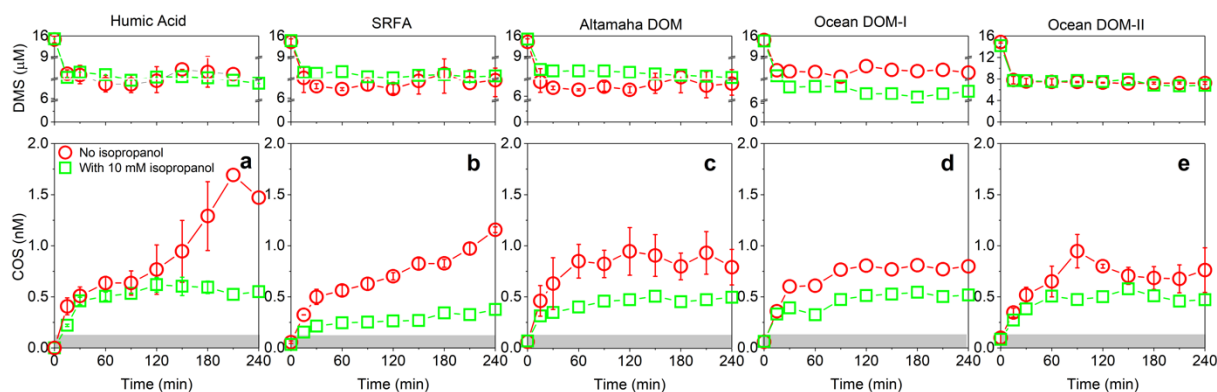


Figure 5-4. Influence of isopropanol on COS formation ($[DMS]= 14 \mu M$, $[DOM]= 5 \text{ mg-C/L}$, $pH= 8.3$, $temperature= 21\pm 1 \text{ }^\circ\text{C}$). The grey box shows the general level of dark formation, which was similar for all scenarios.

Interestingly, these results implied that $\bullet\text{OH}$ was involved in COS formation with DMS. These findings also help to explain the fact that COS formation increased with increasing DOM concentration (Fig. 5-2) since $\bullet\text{OH}$ formation has similarly been shown to increase with increasing DOM concentration.^{19,20} While $\bullet\text{OH}$ formation from DOM has been reported,^{7,20,29} one source of $\bullet\text{OH}$ is known to come from quinones which it is believed to be an important functional group leading to COS formation (see later discussions). However, it is not well understood from a mechanistic perspective and there are controversy concerning regarding details of quinones role on $\bullet\text{OH}$ formation. Specially, their photoreactivity with H_2O , and whether quinones can form $\bullet\text{OH}$ by photo-oxidation of H_2O or not. Some quinones are postulated as water-photooxidizing agents when irradiated in the visible or UV light ranges.³⁰ For example, the role of benzoquinone, which is the simplest member of the quinone family, has been investigated on $\bullet\text{OH}$ formation.³⁰⁻³² It was reported that the excited triplet state of benzoquinone and certain substituted benzoquinones were capable of abstracting a hydrogen atom from water to generate $\bullet\text{OH}$.³⁰⁻³² In a further attempt, it was also found that the absorption band of benzoquinone was felt in the same wavelength range

in which anaerobic $\bullet\text{OH}$ generation was observed (300-350 nm),¹⁹ which further supported the role of benzoquinone on $\bullet\text{OH}$ formation. In addition, it has been reported that the type of quinone could affect generation of $\bullet\text{OH}$ in the visible light.³⁰ While some quinone compounds like 1,4-benzoquinone (BQ) and 2-methyl-1,4-benzoquinone (MBQ) were able to photoxidize water upon irradiation with wavelengths within the solar radiation range (>310 nm), with the consequent production of $\bullet\text{OH}$, 9,10-anthraquinone-1,5-disulfonate (AQDS) was not found to form $\bullet\text{OH}$.³⁰ Alternatively, other works reported quinones could photochemically produce low energy hydroxylating species and not free $\bullet\text{OH}$ ⁴⁷⁻⁵⁰, but they were hypothesized to contribute at least in part to the photochemical $\bullet\text{OH}$ production of DOM¹⁹. In another study, it was proposed that quinones can be one of the prime suspects in the CDOM-sensitized formation of $\bullet\text{OH}$ or lower energy hydroxyl radical-like species.⁷ Recently, this process was investigated from a more detailed mechanistic perspective.³⁷ The photo-oxidation of water via sensitisation of benzoquinone with ultraviolet (UV) light in the hydrogen-bonded complex of benzoquinone with a single water molecule was proposed.³⁷ Where, the mechanisms of electron/proton transfer reactions between photoexcited benzoquinone and water were characterized.³⁷ Specifically, it was proposed that the proton transfer in this reaction possibly led to the formation of the triplet $\text{BQH}\bullet\text{-}\bullet\text{OH}$ biradical, which could dissociate to free $\text{BQH}\bullet$ and $\bullet\text{OH}$ radicals through more proton-transfer reactions. Given all of these controversy findings, it is obvious that the roles of quinones on $\bullet\text{OH}$ formation (in visible light) needs further investigations.

It is also known that DMS can react with $\bullet\text{OH}$, as previously reported.³⁸ Although it is not clear where $\bullet\text{OH}$ exactly reacts in the full mechanism of COS formation, it is likely involved in the first step of the reaction (for more details see chapter 3)⁴. Moreover, it should be noted that, adding isopropanol did not inhibit COS formation completely, which suggested two possibilities: (i)

isopropanol partially quenched the reaction. One previous study indicated that it can quench ~80% of the $\bullet\text{OH}$ species generated from different DOM isolates,¹³ and thus it was still present to some degree and contributed in COS formation, or (ii) $\bullet\text{OH}$ was only partially responsible for COS formation and there were other RIs which contributed in COS formation such as $^3\text{DOM}^*$. The role of $^3\text{DOM}^*$ was assessed next by adding selective quenching agents of this RI.

Moreover, it was found that the reaction of DMS with $\bullet\text{OH}$ cannot be a significant photochemical removal mechanism for DMS.¹⁷ Given this, it is likely that in this system, DMS mainly was removed (~50 % loss) through the reaction with some other RIs rather than $\bullet\text{OH}$, which adding isopropanol did not affect their concentrations.

Influence of $^3\text{DOM}^$*

The role of $^3\text{DOM}^*$ was also evaluated by adding various quenching agents that quenched $^3\text{DOM}^*$ to varying degrees and rates (for details see Table 4-1). These quenching agents included phenol³⁹, trimethylphenol³⁹, sorbic acid⁷ and O_2 ⁷. Initially, each of these quenching agents was added to solutions containing humic acid (Fig. 5-5a). As expected, adding any of these compounds to solutions did not affect COS formation in the dark (Fig. 5-5a). However, with light, the presence of phenol, trimethylphenol, sorbic acid and O_2 dramatically decreased COS formation during 4 h irradiation (Fig. 5-5a). Specifically, with phenol, trimethylphenol, sorbic acid, and O_2 , COS formation was deterred by ~70, 80, 68 and 86%, respectively, after 4 h irradiation (Fig. 5-5a). Thus, COS formation decreased in these solutions according to the following pattern of quenching agents where no quenching agent > sorbic acid > phenol > trimethylphenol > O_2 (Fig. 5-5a).

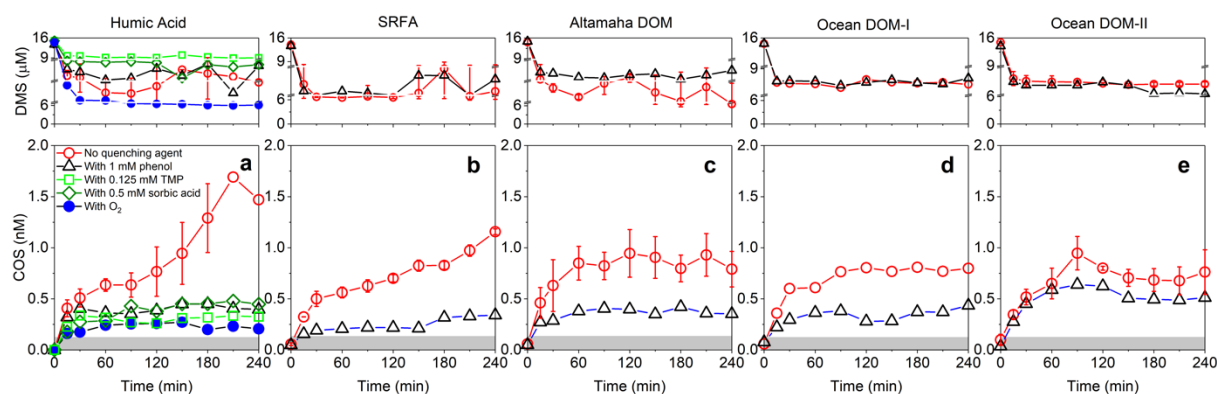


Figure 5-5. Influence of phenol, trimethylphenol (TMP), sorbic acid, and dissolved oxygen (O_2) on COS formation ($[DMS]= 14 \mu M$, $[DOM]= 5 \text{ mg-C/L}$, $pH= 8.3$, $temperature= 21\pm 1 \text{ }^\circ C$). The grey box shows the general level of dark formation, which was similar for all scenarios.

Interestingly, these results suggested that ${}^3DOM^*$ is another important RI in forming COS with DMS. Moreover, similar to cysteine (for details see chapter 4), it can be proposed that this RI likely is the low-energy triplet states (${}^3DOM^*_{\text{Low-energy}}$, $ET < 250 \text{ kJ mol}^{-1}$) of CDOM rather than the high-energy triplet states (${}^3DOM^*_{\text{High-energy}}$, $ET > 250 \text{ kJ mol}^{-1}$). This statement is supported by several pieces of evidence, including the fact that, as noted in section 5.4.2, COS formation was found to be independent of DOM type. This independent behavior suggests that the responsible RIs form at similar quantum yields for different DOM isolates. As it has been found previously,¹² one group of RIs that have shown such behavior include low-energy triplet states ($\Phi_{\text{low-triplet}}$), where similar quantum yields were found for a wide range of different DOM isolates¹² (for more details about the low-energy-triplet-states of CDOM see chapter 4 section 4.4.2).

Moreover, the differences observed between quenching agents also seem to be well correlated to the ability for each quenching agent to compete with DMS in reacting with ${}^3DOM^*$. However, since no known studies have investigated the DMS reaction rates specifically with the low-energy-triplet-states of CDOM, similar logic to chapter 4 was used (for details see section 4.4.6 in chapter

4). Briefly, the general pattern of high-energy triplet state reactivity with DMS and quenching agents were applied to those of the low-energy triplet states. Given this, it was found that the overall effect was similar to cysteine when comparing the $k_{quenching\ agent}^{3Sen*} \times [quenching\ agent]$ values of these quenching agents and DMS toward $^3DOM^*$. However, it is likely that DMS competed with these quenching agents at lower degree than cysteine which made the overall effect of the quenching agents stronger in this case.

Moreover, similar results were achieved with other DOM isolates when adding phenol, although the role of other quenching agents were not tested. With phenol, the COS formation decreased by 75, 60, 35, and 25% with SRFA, Altamaha DOM, ocean DOM-I and ocean DOM-II, respectively (Fig. 5-5). Interestingly, it seemed that there is an effect of DOM type on the quenching power of phenol, where phenol seemed to lose power on quenching $^3DOM^*$ when moving to less terrestrial source DOM isolates such as ocean DOM-I and ocean DOM-II (see FI values in chapter 4) (Fig. 5-5). The DOM isolates with less terrestrial sources have been found to have higher percentages of high-energy-triplet-states compared to low-energy-triplet-states.¹² Since high-energy-triplet-states have higher reactivity toward phenolic compounds,¹² it is likely that phenol mostly quenched high-energy-triplet-states which decreased the chance of phenol to quench low-energy-triplet-states, which are likely the contributing RIs (see later discussions). Similar effects were observed with DMS degradation but to a lower degree (Fig 5-5). In this case, adding phenol decreased DMS degradation but this effect was less strong when moving to less terrestrial source DOM isolates (Fig. 5-5). Since less terrestrial source DOM isolates form the high-energy-triplet-states at a higher degree, these results implied that DMS did not compete with phenol in reacting with high-energy-triplet-states.

DMS degradation was also affected by adding other quenching agents. Specifically, the DMS degradation decreased in these solutions according to the following pattern of quenching agents where no quenching agent > sorbic acid ~ trimethylphenol > phenol > O₂ (Fig. 5-5a). These results supported the reaction of DMS with ³DOM* since removing these RIs from the solutions hampered the degradation of DMS. As expected, DMS degradation increased with O₂ at the highest degree because DMS can react with O₂ at a reaction rate of $5 \times 10^7 \text{ M}^{-1}\text{s}^{-1}$ ⁴⁰. The results of O₂ effect on COS formation matched our previous study (chapter 3),⁴ where O₂ had similar effects on COS formation with 14 μ DMS in brackish water from Louisiana, under similar pH (~8) and temperature (20 ± 1 °C) conditions. However, DMS degraded to a higher degree in our previous study in natural waters (80% with O₂),⁴ which could be attributed to the presence of carbonate radicals which are known to react with organic sulfides (DMS)⁴¹ to form DMSO which possibly enhanced DMS removal.

Overall, the results indicated that in addition to •OH, ³DOM* was likely another contributing RI in COS formation with DMS. However, in order to better elucidate the COS formation from these RIs, the net formation of COS from •OH and ³DOM* was compared to the total formation with humic acid. Specifically, the portion of each RI in forming COS was calculated by subtracting the formation with each corresponding quenching agent, isopropanol for •OH and phenol, trimethylphenol and sorbic acid for ³DOM*, from the total formation. Interestingly, the overall formation with •OH and ³DOM* was found to match the total formation (Fig. 5-6).

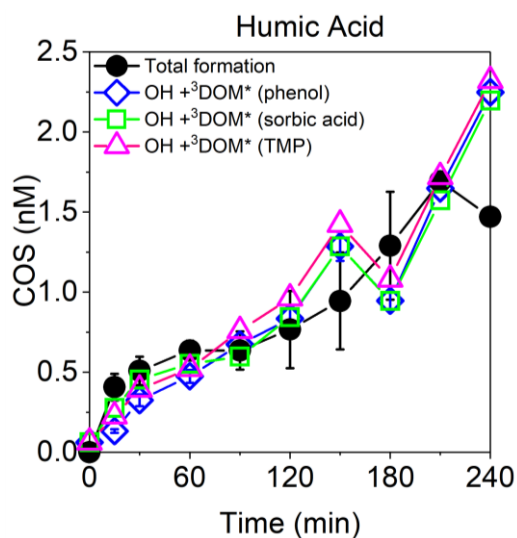


Figure 5-6. Comparison of net formation from $\bullet\text{OH}$ and ${}^3\text{DOM}^*$ to the total formation with humic acid. The loss in COS formation due to the removing of each specific RI was considered as net formation with that specific RI.

This implied that $\bullet\text{OH}$ and ${}^3\text{DOM}^*$ are likely the only major contributing RIs in forming COS with this DOM isolate, when O_2 was not present. However, it was not possible to do the same analysis with other DOM isolates since only phenol was used as the quenching agent of ${}^3\text{DOM}^*$ which was found not to be an efficient quenching agent for less terrestrial source DOM isolates.

5.4.6 Role of sodium borohydride treatment

When additional experiments were conducted with NaBH_4 -treated DOM isolates, no consistent results were found with DMS. NaBH_4 treatment subsequently led to either no change, an increase or a decrease in COS formation (Fig. 5-7). The increase in COS formation, which happened with SRFA and Altamaha DOM (Fig. 5-7), can be explained through similar reasons described for cysteine in chapter 4 (for details see chapter 4). However, it is not clear why COS formation decreased with humic acid or did not change with ocean DOM-I and ocean DOM-II. In general, this inconsistency can be attributed to the various characteristics of DOM, especially the

presence of different types of quinones in DOM isolates^{42,43} since the ketones were removed from the system. It is likely that there is some complex chemistry behind the forming and quenching of different RIs, which possibly are also involved in some other non-COS forming pathways.

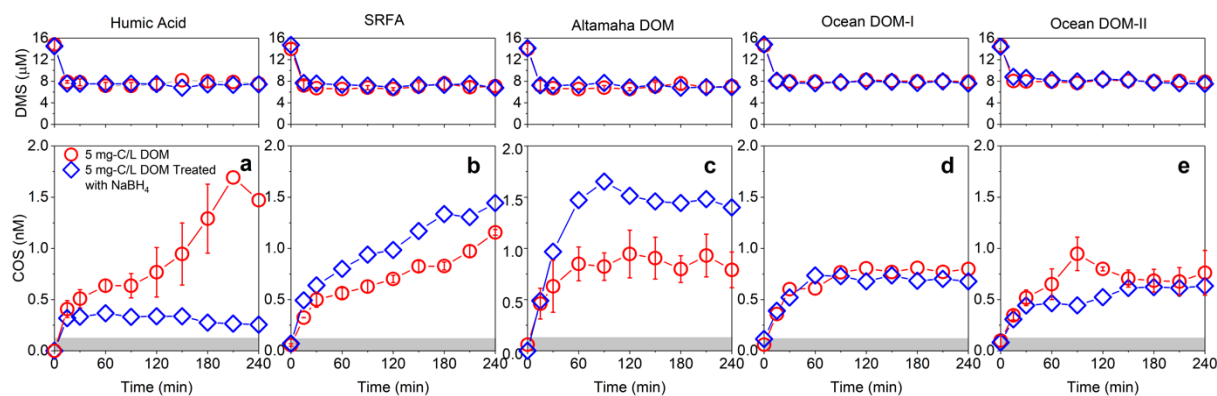


Figure 5-7. Effect of sodium borohydride treatment on COS formation ($[DMS]= 14 \mu M$, $[DOM]= 5 \text{ mg-C/L}$, $pH= 8.3$, $temperature= 21 \pm 1 \text{ } ^\circ C$). The grey box shows the general level of dark formation, which was similar for all scenarios.

Interestingly, the degradation of DMS was not affected by removing ketone/aldehydes from solutions while adding the quenching agents of $^3DOM^*$ decreased its degradation. This implied that DMS could react with $^3DOM^*$ but possibly with the low-energy-triplet-states of CDOM since removing the high-energy-triplet-states from the solutions did not affect its degradation. Overall, these results further supported the claim that the low-energy-triplet states, mainly formed by quinones, were involved in forming COS with DMS, rather than high-energy-triplet-states, which are mainly formed by ketones. However, as noted in chapter 4, further research will be helpful to better investigate the contribution of quinones in COS formation with different organic sulfur precursors.

5.5 Conclusions

The aim of this chapter was to evaluate how different types/concentrations of DOM and the RIs formed by DOM (e.g., $^3\text{DOM}^*$ and $\bullet\text{OH}$) affected the photochemical formation of COS and CS_2 with DMS. This effect was evaluated with five different natural DOM isolates ranging from freshwater to seawater. The results indicated that CS_2 did not form above the DL with any of the DOM isolates under any condition. Alternatively, COS formation increased with DOM, under both dark and light conditions while the effect was more strong in the light. This increase was similar for all of the DOM isolates. Slight differences were instead observed when assessing the kinetics of COS formation for different DOM isolates, where the kinetics for some isolates seemed to plateau and, in some cases, decrease after increasing over greater sunlight exposure. Such results implied that the formation was limited by RIs when only DOM was present. Such results contrasted COS formation in natural waters with DMS, as described in chapter 3, where COS formation always increased as sunlight exposure increased, indicating that in this case, RIs were less limiting. These conclusions were further supported when the effect of DMS concentration or pH was tested, where similar kinetics were observed. Unlike to cysteine, increasing DOM concentration further increased COS formation which implied the complicating factor of self-quenching was not likely in COS formation with DMS.

Additional tests with isopropanol, the quenching agent of $\bullet\text{OH}$, decreased COS formation which suggested that $\bullet\text{OH}$ was involved in the formation pathways. Additionally, when phenol, trimethylphenol, sorbic acid or O_2 , $^3\text{DOM}^*$ quenching agents, were added to the solutions, COS formation decreased but to a higher degree. For example, with phenol, trimethylphenol, sorbic acid or O_2 , formation dramatically decreased up to 70, 80, 68 and 86%, respectively. These results suggested that $^3\text{DOM}^*$ could be another major contributing RI in forming COS with DMS.

Furthermore, treating the DOM isolates with NaBH₄ to reduce the ketones/aldehydes to their corresponding alcohols, increased COS formation, which implied that the RIs derived from ketones were not involved in COS formation pathways. Additionally, when the net formation from •OH and ³DOM* was compared to the total formation, it was found that these RIs are likely to be the only major contributing RIs in COS formation with DMS, when O₂ was not present. However, these RIs appeared to be different than those for cysteine which implied that the COS formation mechanisms from DMS are likely different than those from cysteine. Given this, further research is required to investigate the RIs involved in COS formation in the presence of O₂ with both organic sulfur precursors.

5.6 References

- (1) Andreae, M. O. Ocean-Atmosphere Interactions in the Global Biogeochemical Sulfur Cycle. *Mar. Chem.* **1990**, *30*, 1–29.
- (2) Erickson III, D. J.; Ghan, S. J.; Penner, J. E. Global Ocean-to-Atmosphere Dimethyl Sulfide Flux. *J. Geophys. Res. Atmos.* **1990**, *95* (D6), 7543–7552.
- (3) Bates, T. S.; Lamb, B. K.; Guenther, A.; Dignon, J.; Stoiber, R. E. Sulfur Emissions to the Atmosphere from Natural Sources. *J. Atmos. Chem.* **1992**, *14* (1), 315–337.
- (4) Modiri Gharehveran, M.; Shah, A. D. Indirect Photochemical Formation of Carbonyl Sulfide and Carbon Disulfide in Natural Waters: Role of Organic Sulfur Precursors, Water Quality Constituents, and Temperature. *Environ. Sci. Technol.* **2018**, *52* (16), 9108–9117.
- (5) Zepp, R. G.; Andreae, M. O. Factors Affecting the Photochemical Production of Carbonyl Sulfide in Seawater. *Geophys. Res. Lett.* **1994**, *21* (25), 2813–2816.
- (6) Vione, D.; Minella, M.; Maurino, V.; Minero, C. Indirect Photochemistry in Sunlit Surface Waters: Photoinduced Production of Reactive Transient Species. *Chem. – A Eur. J.* **2014**, *20* (34), 10590–10606.
- (7) McNeill, K.; Canonica, S. Triplet State Dissolved Organic Matter in Aquatic Photochemistry: Reaction Mechanisms, Substrate Scope, and Photophysical Properties. *Environ. Sci. Process. Impacts* **2016**, *18* (11), 1381–1399.

- (8) Chu, C.; Erickson, P. R.; Lundeen, R. A.; Stamatelatos, D.; Alaimo, P. J.; Latch, D. E.; McNeill, K. Photochemical and Nonphotochemical Transformations of Cysteine with Dissolved Organic Matter. *Environ. Sci. Technol.* **2016**, *50* (12), 6363–6373.
- (9) Huang, J.; Mabury, S. A. Steady-State Concentrations of Carbonate Radicals in Field Waters. *Environ. Toxicol. Chem.* **2009**, *19* (9), 2181–2188.
- (10) McKnight, D. M.; Boyer, E. W.; Westerhoff, P. K.; Doran, P. T.; Kulbe, T.; Andersen, D. T. Spectrofluorometric Characterization of Dissolved Organic Matter for Indication of Precursor Organic Material and Aromaticity. *Limnol. Oceanogr.* **2001**, *46* (1), 38–48.
- (11) Dennis A. Hansell; Carlson, C. A. *Biogeochemistry of Marine Dissolved Organic Matter*; Academic Press: amsterdam, 2002.
- (12) Zhou, H.; Yan, S.; Lian, L.; Song, W. Triplet-State Photochemistry of Dissolved Organic Matter: Triplet-State Energy Distribution and Surface Electric Charge Conditions. *Environ. Sci. Technol.* **2019**.
- (13) Guerard, J. J.; Miller, P. L.; Trouts, T. D.; Chin, Y.-P. The Role of Fulvic Acid Composition in the Photosensitized Degradation of Aquatic Contaminants. *Aquat. Sci.* **2009**, *71* (2), 160–169.
- (14) Bahnmüller, S.; Von Gunten, U.; Canonica, S. Sunlight-Induced Transformation of Sulfadiazine and Sulfamethoxazole in Surface Waters and Wastewater Effluents. *Water Res.* **2014**, *57*, 183–192.
- (15) Guerard, J. J.; Chin, Y.-P.; Mash, H.; Hadad, C. M. Photochemical Fate of Sulfadimethoxine in Aquaculture Waters. *Environ. Sci. Technol.* **2009**, *43* (22), 8587–8592.
- (16) Brugger, A.; Slezak, D.; Obernosterer, I.; Herndl, G. J. Photolysis of Dimethylsulfide in the Northern Adriatic Sea: Dependence on Substrate Concentration, Irradiance and DOC Concentration. *Mar. Chem.* **1998**, *59* (3), 321–331.
- (17) Mopper, K.; Kieber, D. J. Chapter 9 - Photochemistry and the Cycling of Carbon, Sulfur, Nitrogen and Phosphorus; Hansell, D. A., Carlson, C. A. B. T.-B. of M. D. O. M., Eds.; Academic Press: San Diego, 2002; pp 455–507.
- (18) Toole, D. A.; Kieber, D. J.; Kiene, R. P.; White, E. M.; Bisgrove, J.; del Valle, D. A.; Slezak, D. High Dimethylsulfide Photolysis Rates in Nitrate-Rich Antarctic Waters. *Geophys. Res. Lett.* **2004**, *31* (11).

- (19) Vaughan, P. P.; Blough, N. V. Photochemical Formation of Hydroxyl Radical by Constituents of Natural Waters. *Environ. Sci. Technol.* **1998**, *32* (19), 2947–2953.
- (20) Page, S. E.; Arnold, W. A.; McNeill, K. Assessing the Contribution of Free Hydroxyl Radical in Organic Matter-Sensitized Photohydroxylation Reactions. *Environ. Sci. Technol.* **2011**, *45* (7), 2818–2825.
- (21) Brezonik, P. L.; Fulkerson-Brekken, J. Nitrate-Induced Photolysis in Natural Waters: Controls on Concentrations of Hydroxyl Radical Photo-Intermediates by Natural Scavenging Agents. *Environ. Sci. Technol.* **1998**, *32* (19), 3004–3010.
- (22) Zepp, R. G.; Hoigne, J.; Bader, H. Nitrate-Induced Photooxidation of Trace Organic Chemicals in Water. *Environ. Sci. Technol.* **1987**, *21* (5), 443–450.
- (23) Buxton, G.; Greenstock, C.; Helman, W.; Ross, A. Critical Review of Rate Constants for Reactions of Hydrated Electrons, Hydrogen Atoms and Hydroxyl Radicals ($\cdot\text{OH}/\text{O}^{\text{sup}} - ^{\text{sup}}\text{O}^{\text{sup}}\text{H}$) in Aqueous Solution. *J. Phys. Chem. Ref. Data* **2015**, *44* (1), 1.
- (24) Mangalgi, K. P.; Blaney, L. Elucidating the Stimulatory and Inhibitory Effects of Dissolved Organic Matter from Poultry Litter on Photodegradation of Antibiotics. *Environ. Sci. Technol.* **2017**, *51* (21), 12310–12320.
- (25) Wenk, J.; Eustis, S. N.; McNeill, K.; Canonica, S. Quenching of Excited Triplet States by Dissolved Natural Organic Matter. *Environ. Sci. Technol.* **2013**, *47* (22), 12802–12810.
- (26) Larson, R. A.; Zepp, R. G. Reactivity of the Carbonate Radical with Aniline Derivatives. *Environ. Toxicol. Chem.* **1988**, *7* (4), 265–274.
- (27) Canonica, S.; Kohn, T.; Mac, M.; Real, F. J.; Wirz, J.; von Gunten, U. Photosensitizer Method to Determine Rate Constants for the Reaction of Carbonate Radical with Organic Compounds. *Environ. Sci. Technol.* **2005**, *39* (23), 9182–9188.
- (28) Bouillon, R.-C.; Miller, W. L. Photodegradation of Dimethyl Sulfide (DMS) in Natural Waters: Laboratory Assessment of the Nitrate-Photolysis-Induced DMS Oxidation. *Environ. Sci. Technol.* **2005**, *39* (24), 9471–9477.
- (29) Vione, D.; Falletti, G.; Maurino, V.; Minero, C.; Pelizzetti, E.; Malandrino, M.; Ajassa, R.; Olariu, R.-I.; Arsene, C. Sources and Sinks of Hydroxyl Radicals upon Irradiation of Natural Water Samples. *Environ. Sci. Technol.* **2006**, *40* (12), 3775–3781.
- (30) Alegria, A. E.; Ferrer, A.; Sepulveda, E. Photochemistry of Water-Soluble Quinones. Production of a Water-Derived Spin Adduct. *Photochem. Photobiol.* **1997**, *66* (4), 436–442.

- (31) Ronfard-Haret, J.-C.; Bensasson, R. V.; Amouyal, E. Assignment of Transient Species Observed on Laser Flash Photolysis of P-Benzoquinone and Methylated p-Benzoquinones in Aqueous Solution. *J. Chem. Soc. Faraday Trans. 1 Phys. Chem. Condens. Phases* **1980**, *76* (0), 2432–2436.
- (32) Ononye, A. I.; McIntosh, A. R.; Bolton, J. R. Mechanism of the Photochemistry of P-Benzoquinone in Aqueous Solutions. 1. Spin Trapping and Flash Photolysis Electron Paramagnetic Resonance Studies. *J. Phys. Chem.* **1986**, *90* (23), 6266–6270.
- (33) Gan, D.; Jia, M.; Vaughan, P. P.; Falvey, D. E.; Blough, N. V. Aqueous Photochemistry of Methyl-Benzoquinone. *J. Phys. Chem. A* **2008**, *112* (13), 2803–2812.
- (34) Pochon, A.; Vaughan, P. P.; Gan, D.; Vath, P.; Blough, N. V.; Falvey, D. E. Photochemical Oxidation of Water by 2-Methyl-1,4-Benzoquinone: Evidence against the Formation of Free Hydroxyl Radical. *J. Phys. Chem. A* **2002**, *106* (12), 2889–2894.
- (35) Maddigapu, P. R.; Bedini, A.; Minero, C.; Maurino, V.; Vione, D.; Brigante, M.; Mailhot, G.; Sarakha, M. The PH-Dependent Photochemistry of Anthraquinone-2-Sulfonate. *Photochem. Photobiol. Sci.* **2010**, *9* (3), 323–330.
- (36) Maurino, V.; Borghesi, D.; Vione, D.; Minero, C. Transformation of Phenolic Compounds upon UVA Irradiation of Anthraquinone-2-Sulfonate. *Photochem. Photobiol. Sci.* **2008**, *7* (3), 321–327.
- (37) Karsili, T. N. V.; Tuna, D.; Ehrmaier, J.; Domcke, W. Photoinduced Water Splitting via Benzoquinone and Semiquinone Sensitisation. *Phys. Chem. Chem. Phys.* **2015**, *17* (48), 32183–32193.
- (38) Schoeneich, C.; Aced, A.; Asmus, K. D. Mechanism of Oxidation of Aliphatic Thioethers to Sulfoxides by Hydroxyl Radicals. The Importance of Molecular Oxygen. *J. Am. Chem. Soc.* **1993**, *115* (24), 11376–11383.
- (39) Canonica, S.; Jans, U.; Stemmler, K.; Hoigne, J. Transformation Kinetics of Phenols in Water: Photosensitization by Dissolved Natural Organic Material and Aromatic Ketones. *Environ. Sci. Technol.* **1995**, *29* (7), 1822–1831.
- (40) Brimblecombe, P.; Shooter, D. Photo-Oxidation of Dimethylsulphide in Aqueous Solution. *Mar. Chem.* **1986**, *19* (4), 343–353.

- (41) Huang, J.; Mabury, S. A. The Role of Carbonate Radical in Limiting the Persistence of Sulfur-Containing Chemicals in Sunlit Natural Waters. *Chemosphere* **2000**, *41* (11), 1775–1782.
- (42) Maximov, O. B.; Glebko, L. I. Quinoid Groups in Humic Acids. *Geoderma* **1974**, *11* (1), 17–28.
- (43) Stevenson, F. J. *Humus Chemistry, Genesis, Composition, Reactions.*; John Wiley & Sons, Inc.: New York, 1982.

CHAPTER 6. RESEARCH CONTRIBUTION

This study aimed to link how sunlight exposure, various organic precursors/water quality constituents, and temperature affected COS and CS₂ formation. These efforts were made to better elucidate which factors were important and how this could affect their volatilization into the atmosphere and inform global sulfur models. This is a critical issue since these models only use the ocean surface sunlight intensity and UV₃₆₀^{1,2} to predict COS photoproduction rates. While our results further confirmed that DOM and UV₃₆₀ affected COS, other influential factors for COS and CS₂ formation included: (i) length of sunlight exposure, especially for CS₂ which required only a brief period of light to continue formation, (ii) O₂ concentration, which can vary from 4 to 9 mg/L in surface waters depending on salinity and temperature.³ (iii) temperature, which can fluctuate from -1.9°C to 30°C depending on latitude and seasonal variations⁴ and (iv) organic sulfur precursor type. In addition, these findings provided greater mechanistic insights towards the key RIs and other radicals that are involved such as those derived from DOM and quenched by O₂ such as ³DOM*,^{5,6} R*,⁷ and sulfur-centered radicals (e.g. R-S*)⁸.

Further studies with synthetic waters containing DOM alone provided additional insight on the RIs and photochemical mechanisms involved. Interestingly, with DOM alone, only COS was generated whereas CS₂ was not. This finding suggested that RIs generated from other water quality constituents besides those generated from DOM was required to form CS₂. This was further supported when cysteine or DMS was also present in the solutions. One influential factor for COS formation with DOM was the complicating effect of RIs self-quenching by DOM which only happened in the presence of cysteine and not DMS. Also, the contributing RIs in COS formation were found to be different with cysteine and DMS. Specially, •OH, which is an important

environmental oxidant with a lifetime of 5-10 μs ⁹, was not found to be involved in COS formation with cysteine but was involved with DMS. However, ³DOM* was found to be the common contributing RI with both organic sulfur precursor. Overall, these results implied that the COS formation mechanisms from cysteine differs from DMS. Although this study proposed the contribution of certain RIs in COS and CS₂ formation, it is not the complete mechanistic perspective on photochemical formation of COS and CS₂. Especially given the possibility of other RIs playing a role in COS and CS₂ formation which is particularly true in the presence of O₂.

Moreover, given the relatively low yields of COS and CS₂ formation from the organic sulfur precursors tested in this study, it is believed that some group of the important organic sulfur precursors are still missing. One major impedance in linking COS and CS₂ formation to a more robust set of organic sulfur precursors and water quality parameters falls in the inability to quantify total DOS content in natural waters. Recent work has made significant progress in this area but has only estimated upper boundary limits (<0.4) $\mu\text{mol-DOS/L}$ in ocean waters¹⁰. As more exact DOS quantification and characterization methods emerge, we expect that this will aid in more directly linking COS and CS₂ to natural organic sulfur content, which requires future work.

6.1 References

- (1) Lennartz, S. T.; Marandino, C. A.; von Hobe, M.; Cortes, P.; Quack, B.; Simo, R.; Booge, D.; Pozzer, A.; Steinhoff, T.; Arevalo-Martinez, D. L.; et al. Direct Oceanic Emissions Unlikely to Account for the Missing Source of Atmospheric Carbonyl Sulfide. *Atmos. Chem. Phys.* **2017**, *17* (1), 385–402.
- (2) Launois, T.; Belviso, S.; Bopp, L.; Fichot, C. G.; Peylin, P. A New Model for the Global Biogeochemical Cycle of Carbonyl Sulfide – Part 1: Assessment of Direct Marine Emissions with an Oceanic General Circulation and Biogeochemistry Model. *Atmos. Chem. Phys.* **2015**, *15* (5), 2295–2312.

- (3) WOA 2013 Data Access: Statistical mean of oxygen on 1° grid for all decades <https://www.nodc.noaa.gov/cgi-bin/OC5/woa13/woa13oxnu.pl?parameter=o> (accessed Mar 1, 2018).
- (4) Lalli, C. M.; Parsons, T. R. *Biological Oceanography An Introduction*, Second.; Elsevier Butterworth-Heinemann Linacre House, Jordan Hill, Oxford OX2 8DP 30 Corporate Drive, Burlington, MA 01803: University of British Columbia, Vancouver, Canada, 1993.
- (5) McNeill, K.; Canonica, S. Triplet State Dissolved Organic Matter in Aquatic Photochemistry: Reaction Mechanisms, Substrate Scope, and Photophysical Properties. *Environ. Sci. Process. Impacts* **2016**, *18* (11), 1381–1399.
- (6) Parker, K. M.; Pignatello, J. J.; Mitch, W. A. Influence of Ionic Strength on Triplet-State Natural Organic Matter Loss by Energy Transfer and Electron Transfer Pathways. *Environ. Sci. Technol.* **2013**, *47* (19), 10987–10994.
- (7) Wright, J.; Hooman, S.; L., C. L. Stability of Carbon- centered Radicals: Effect of Functional Groups on the Energetics of Addition of Molecular Oxygen. *J. Comput. Chem.* **2008**, *30* (7), 1016–1026.
- (8) Du, Q.; Mu, Y.; Zhang, C.; Liu, J.; Zhang, Y.; Liu, C. Photochemical Production of Carbonyl Sulfide, Carbon Disulfide and Dimethyl Sulfide in a Lake Water. *J. Environ. Sci.* **2016**, *51* (September), 1–11.
- (9) Rosario-Ortiz, F. L.; Canonica, S. Probe Compounds to Assess the Photochemical Activity of Dissolved Organic Matter. *Environ. Sci. Technol.* **2016**, *50* (23), 12532.
- (10) Ksionzek, K. B.; Lechtenfeld, O. J.; Mccallister, S. L.; Schmitt-kopplin, P.; Geuer, J. K.; Geibert, W.; Koch, B. P. Dissolved Organic Sulfur in the Ocean: Biogeochemistry of a Petagram Inventory. *Science*. **2016**, *354* (6311), 456–460.

APPENDIX

Text A1. DOM optical properties

In addition, the regional fluorescence volumes are assessed and represented as: region I (tyrosine-like fluorescence), region II (tryptophan-like fluorescence), region III (fulvic acid-like fluorescence), region IV (soluble microbial product-like fluorescence), and region V (humic acid-like fluorescence), and total fluorescence (Fig. 1 and Table 1). It is found to be correlations between these regions and wastewater signatures.¹

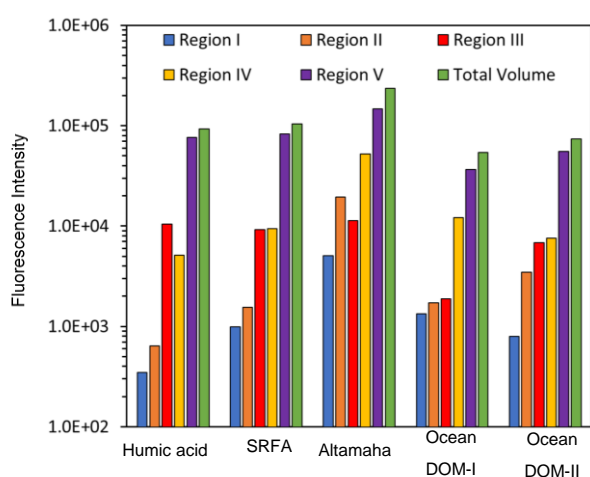


Figure 1. The regional fluorescence volumes of DOM isolates for region I (tyrosine-like fluorescence), region II (tryptophan-like fluorescence), region III (fulvic acid-like fluorescence), region IV (soluble microbial product-like fluorescence), region V (humic acid-like fluorescence), and total fluorescence. Fluorescence intensity is normalized to the Raman shift in water.

For all DOM isolates, the special metrics were also calculated based on previously described methods^{2,3} and are shown in Table 2. The humification index (HI) is calculated as the ratio of the integrated fluorescence intensity for 435-480 nm to that at 300-345 nm for an excitation wavelength of 255 nm. Higher values of HI suggest a lower ratio of hydrogen to carbon and cause the emission spectra of the fluorescing molecules to shift to higher wavelengths.² The HI values

followed the order of humic acid > Altamaha DOM > SRFA > ocean DOM-II > ocean DOM-I, meaning that emission spectra of the fluorescence values happen at higher wavelengths for humic acid. The biological index (BI), is calculated as the ratio of the fluorescence intensity at 380 nm to that at 430 nm for excitation at 310 nm. The BI is commonly used to describe the amount of microbially-derived DOM,² where as expected, the ocean DOM-I had the highest microbial source while humic acid had the lowest value. The ultraviolet absorbance at 254 nm is shown as (UV_{254} , m^{-1}) which is often used as a measure of aromaticity, where humic acid showed the highest aromaticity whereas ocean DOM-II showed the lowest aromaticity. The SUVA at 254 nm ($SUVA_{254}$, $L (mg C)^{-1} m^{-1}$) was calculated by dividing UV_{254} by the DOC concentration. The spectral slopes, $S_{275-295}$ and $S_{350-400}$, were calculated by taking the log regression of the slope of the absorbance from 275-295 nm and 350-400 nm, respectively. The spectral slope ratio, S_R , is defined as the ratio of $S_{275-295}$ and $S_{350-400}$, and is inversely proportional to the molecular weight of the DOM. The $S_{275-295}$, $S_{350-400}$ and S_R suggest similar conclusions to E_2/E_3 regarding DOM isolates.

Table A1. The regional fluorescence volumes of DOM isolates. Fluorescence intensity is normalized to the Raman shift in water.

Sample	Region I	Region II	Region III	Region IV	Region V	Total volume
Humic Acid	347	644	10424	5110	76667	93194
SRFA	794	3460	6814	7553	55138	73760
Altamaha DOM	991	1552	9269	9476	82381	103669
Ocean DOM-I	5060	19491	11397	52133	146808	234889
Ocean DOM-II	1339	1728	1887	12132	36783	53870

Table A2. Spectral metrics of DOM isolates.

Sample	Biological index	Humification index	UV₂₅₄ (m⁻¹)	SUVA₂₅₄ (L m⁻¹ (mg C L⁻¹))	S₂₇₅₋₂₉₅	S₃₅₀₋₄₀₀	S_R
Humic acid	0.39	9.79	68.9	5.3	0.008	0.011	0.73
SRFA	0.67	3.10	24.7	7.06	0.020	0.016	1.24
Altamaha DOM	0.55	3.83	32.5	2.50	0.017	0.017	0.98
Ocean DOM-I	2.20	0.22	20.9	1.64	0.027	0.009	3.08
Ocean DOM-II	0.76	0.42	7.29	0.56	0.036	0.015	2.32

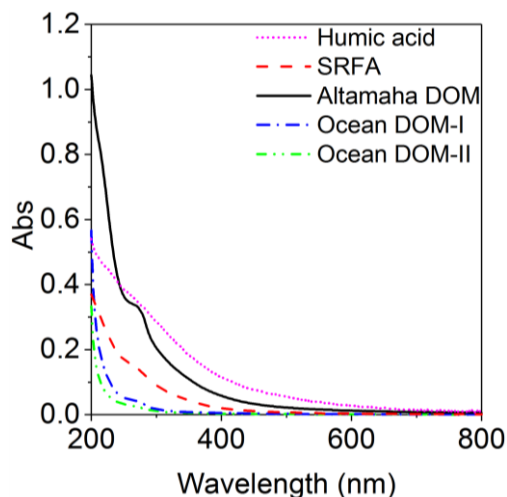


Figure A1. The absorbance spectra of DOM isolates, all at concentration of 5 mg-C/L

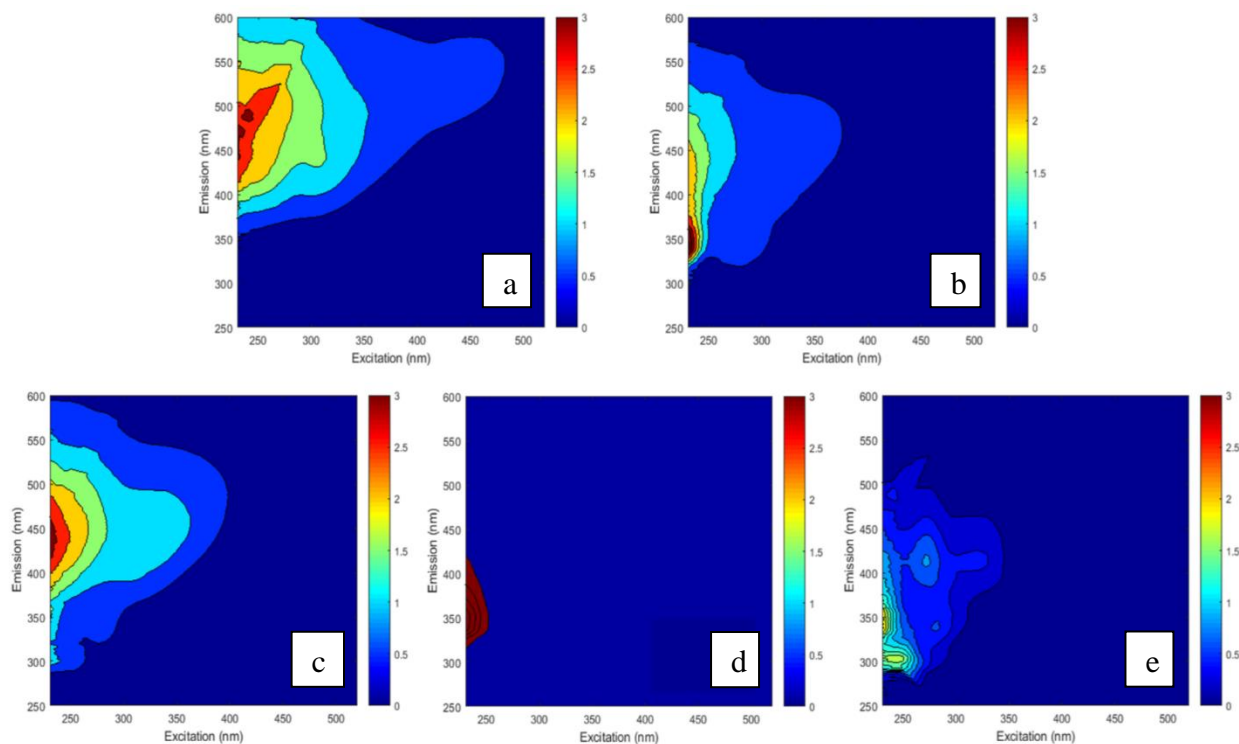


Figure A2. Fluorescence EEMs for: a) humic acid, b) SRFA, c) Altamaha DOM, d) ocean DOM-I, and e) ocean DOM-II. Fluorescence intensity is normalized to the Raman shift in water and plotted on the same scale (0-3) for all samples to highlight overall patterns (graph provided by Dr. Blaney, UMBC).

References:

- (1) Barbosa, M. O.; Ribeiro, A. R.; Ratola, N.; Hain, E.; Homem, V.; Pereira, M. F. R.; Blaney, L.; Silva, A. M. T. Spatial and Seasonal Occurrence of Micropollutants in Four Portuguese Rivers and a Case Study for Fluorescence Excitation-Emission Matrices. *Sci. Total Environ.* **2018**, *644*, 1128–1140.
- (2) Hansen, A. M.; Kraus, T. E. C.; Pellerin, B. A.; Fleck, J. A.; Downing, B. D.; Bergamaschi, B. A. Optical Properties of Dissolved Organic Matter (DOM): Effects of Biological and Photolytic Degradation. *Limnol. Oceanogr.* **2016**, *61* (3), 1015–1032.
- (3) McKnight, D. M.; Boyer, E. W.; Westerhoff, P. K.; Doran, P. T.; Kulbe, T.; Andersen, D. T. Spectrofluorometric Characterization of Dissolved Organic Matter for Indication of Precursor Organic Material and Aromaticity. *Limnol. Oceanogr.* **2001**, *46* (1), 38–48.